ATLAS OCT-ANGIOGRAPHY IN AMD

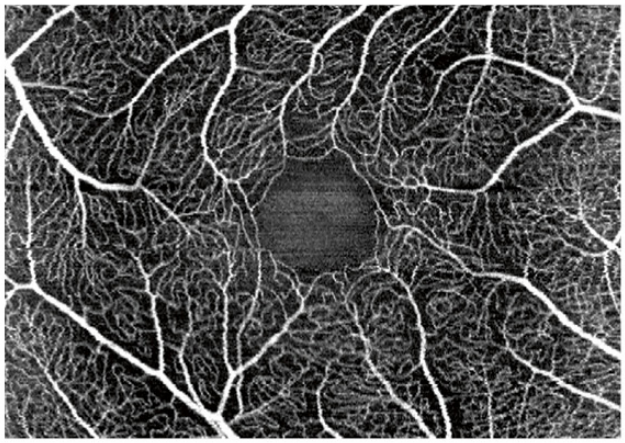

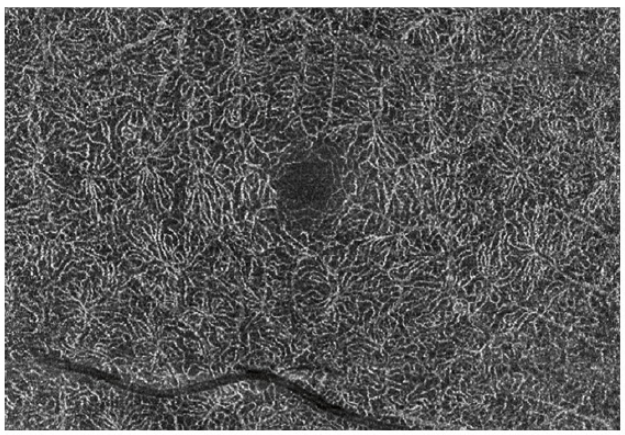

Gabriel Coscas

Marco Lupidi

Florence Coscas

COMPARISON WITH MULTIMODAL IMAGING

ATLAS: OCT-ANGIOGRAPHY IN AMD
COMPARISON WITH MULTIMODAL IMAGING

Published with the generous help of "FONDATION PAULETTE DARTY" - Fondation de France.

This Atlas was achieved with the kind support of HEIDELBERG ENGINEERING, who provided to the authors, under a confidentiality agreement, the SPECTRALIS® OCT-Angiography Prototype.

OPTICAL COHERENCE TOMOGRAPHY ANGIOGRAPHY IN AGE-RELATED MACULAR DEGENERATION

Atlas of OCT-ANGIOGRAPHY in Exudative AMD

Gabriel COSCAS, Marco LUPIDI, Florence COSCAS (Paris, Créteil, Perugia)

AUTHORS

Gabriel COSCAS
Professeur Emérite des Universités
Hôpital de Créteil. Département d'Ophtalmologie de Créteil Université Paris XII, Val de Marne – France
Centre d'Exploration Ophtalmologique de l'Odéon, Paris
Email: gabriel.coscas@gmail.com

Marco LUPIDI
Medical Retina Research Fellow
Centre d'Exploration Ophtalmologique de l'Odéon, Paris
Department of Biomedical and Surgical Sciences, Section of Ophthalmology
"S.Maria della Misericordia" Hospital
University of Perugia, Perugia, Italy
Email: dr.marco.lupidi@gmail.com

Florence COSCAS
Praticien Hospitalier
Hôpital de Créteil. Départementd'Ophtalmologie de Créteil Université Paris XII, Val de Marne – France
Centre d'Exploration Ophtalmologique de l'Odéon, Paris
Email: coscas.f@gmail.com

1 INTRODUCTION

Thanks to a newly released software used for OCT examinations, the retinal and choroidal vasculature can now be imaged without the need for intravenous dye injections.

This new advancement in OCT technology will allow clinicians to easily capture a snapshot of the retinal vessels, retinal capillaries, and choroidal neovascularizations.

This new method of capturing OCT images highlights, together with structural OCT images, lesions of the outer retinal layers and fluid accumulations. It is easy to use, quick, non-invasive, and is very promising, especially in Age-related Macular Degeneration (AMD).

AMD is the main cause of visual impairment in developed countries in individuals over the age of 50.[1,2] Exudative AMD, an advanced type of macular degeneration, is the main cause of vision loss in AMD.[3]

A leading indicator of AMD is the presence of abnormal blood vessels, known as choroidal neovascularization (CNV). CNV originates from the choroid and extends mainly between the Bruch's membrane (BM) and the retinal pigmented epithelium (RPE) [**Type I or sub epithelial or occult CNV**] or in the subretinal space [**Type II or subretinal or classic CNV**].

CNV proliferation can sometimes induce hemorrhages, fluid exudation, and fibrosis, resulting in a severe photo receptor damage and vision loss.[4]

For over 50 years, fluorescein angiography has been the imaging method of choice ("gold standard") for the evaluation of the vascular and capillary bed. This was also the imaging modality that was most used for diagnosis, classification, localization and monitoring of CNV. It recognized and classified CNV as "preepithelial, subepithelial or mixed."

The Indocyanine Green Angiography can be used to identify the extension of the neovascular lesion because of its ability to image sub-RPE structures.[5]

The Optical Coherence Tomography (OCT), and in particular, the Spectral Domain OCT (SD-OCT), has revolutionized the diagnostic approach to AMD.

In 20 years, OCT has become a non-invasive imaging method and a medical diagnostics tool, providing a literal "optical biopsy" of retinal microstructures.

The OCT has helped to highlight several signs of disease activity (hyper-reflective and dense points areas) and changes in the outer retinal layers (ELM and ellipsoid zone), with a high prognostic value for the photoreceptor function.

The SD-OCT is able to define the morphology of the fibrovascular complex and its exudative consequences such as fluid accumulation or retinal thickening, thus providing a marker of therapeutic efficacy that is easy to follow-up and interpret with proven reliability.[6]

The OCT "en face" technique was initially used to detect the hyper-reflective path of choroidal neovascularizations (CNV) in a pigmented epithelium detachment;[7] it is currently used as C-scan reference in OCT-Angiography.

The OCT-Angiography (OCT-A), is a novel revolutionary technique that allows a clear, depth-resolved visualization of the retinal[8] and choroidal microvasculature.

This imaging modality was brilliantly introduced in clinical practice by David Huang, James Fujimoto, and their colleagues from several publications at the occasion of the Imaging Conference that preceded the ARVO meeting in Orlando in 2014.

OCT-A is based on the concept that in a static eye, the only moving structures of the ocular fundus are blood cells flow in the vessels.

By calculating the decorrelation of signal amplitude from repeated consecutive B-scans at the same section, a contrast between static and nonstatic tissue is generated.

This results in a vascular decorrelation signal that enables visualization of three-dimensional retinal and choroidal vasculature of a variable intensity signal according to the speed of blood flow.[9]

OCT-A does not require administration of intravenous dye such as fluorescein or indocyanine-green, thus avoiding the potential risks which can result in rare adverse events.[10,11]

In this atlas, we aimed to show the ability of OCT-A in detecting, defining the type, grading the activity and assisting the treatment decision in cases of exudative AMD.

References

1. **Bressler NM**. Age-related macular degeneration is the leading cause of blindness. *JAMA* 2004; 291(15): 1900-1901.

2. **Wong TY, Wong T, Chakravarthy U et al.** The natural history and prognosis of neovascular age-related macular degeneration: a systematic review of the literature and meta-analysis. *Ophthalmology* 2008; 115(1): 116-126.

3. **Ferris FL III, Fine SL, Hyman L.** Age-related macular degeneration and blindness due to neovascular maculopathy. *Arch Ophthalmol* 1984; 1(02):1640-2.

4. **Ambati J, Ambati BK, Yoo SH et al.** Age-related macular degeneration: etiology, pathogenesis, and therapeutic strategies. *Surv Ophthalmol* 2003; 48:257-93.

5. **Sulzbacher F, Kiss C, Munk M et al.** Diagnostic evaluation of type 2 (classic) choroidal neovascularization: optical coherence tomography, indocyanine green angiography, an fluorescein angiography. *Am J Ophthalmol* 2011; 152(5):799-806 e1.

6. **Coscas G, Coscas F, Vismara S et al.** OCT in AMD (2009). P: 159-166. Springer Medizin Heidelberg.

7. **Coscas F, Coscas G, Querques G, Massamba N, Querques L, Bandello F, Souied EH.** En Face enhanced depth imaging optical coherence tomography of fibro vascular pigment epithelium detachment. *Invest Ophthalmol Vis Sci.* 2012, 28; 53:4147-51.

8. **Spaide RF, Klancnik JM Jr, Cooney MJ.** Retinal vascular layers imaged by fluorescein angiography and optical coherence tomography angiography. *JAMA Ophthalmol.* 2015; 133(1):45-50.

9. **Jia Y, Bailey ST, Wilson DJ et al.** Quantitative optical coherence tomography angiography of choroidal neovascularization in age-related macular degeneration. Ophthalmology 2014; 121(7):1435-44.

10. **Yannuzzi LA, Rohrer KT, Tindel LJ et al.** Fluorescein angiography complication survey. *Ophthalmology* 1986; 93(5): 611-7.

11. **Su Z, Ye P, Teng Y et al.** Adverse reaction in patients with drug allergy history after simultaneous intravenous fundus fluorescein angiography and indocyanine green angiography. *Ocul Pharmacol Ther* 2012; 28(4):410-3.

2 OCT-ANGIOGRAPHY – TECHNICAL ASPECTS

2.1 OCT-Angiography – technical aspects

The OCT-Angiography (OCT-A) is a promising new method to visualize the retinal vasculature and choroidal vascular layers in the macular area.

A key advantage of OCT-A over traditional Fluorescein Angiography (FA) is that it provides depth-resolved functional information of the blood flow in the vessels.

In comparison, FA only provides a two-dimensional (2D) image that superimposes all perfused layers of retinal and choroidal blood vessels.

OCT-A images, in C-scan visualization, often appear similar to FA images, but with additional information. Thus, for a correct interpretation of the images, it is important to understand the differences between the two modalities.

Genesis of OCT-angiograms

The OCT-A is based on the concept that in a static eye, the *only moving structure* in the ocular-fundus is the blood flow in the vessels.

The image is generated by the difference between the moving cells in the vasculature and the static surrounding tissue.

When performing OCT scans of the retina, different factors that contribute to motion should be considered, particularly bulk motion and motion caused by circulating blood. Bulk motion refers to any tissue movement that may be captured by the OCT device, for example motion caused by head movements or eye movements.

If bulk motions are sufficiently compensated, then blood circulation is the predominant source of temporal changes between OCT scans.

OCT scans can then be used to visualize blood flow based on the detection of temporal changes in a sequence of OCT scans.

In order to avoid any artifacts that may arise, a sequence of OCT B-scans has to be taken at the same exact retinal location to detect the blood flow.

Artifacts can arise due to scan positioning errors caused by normal ocular micro-saccades. They commonly occur once every 300 ms (while the typical acquisition time of OCT volume scans with a reasonable resolution and field of view is 2-3 seconds).

Eye-Tracking system

Eye-Tracking (TruTrack™) is a reliable method to acquire OCT volume scans without motion artifacts, and is a method based on simulatenous aquition of fundus and OCT images.

It enables a continuous real-time quality check of the OCT data during the examination and ensures that only accurate OCT-images are stored.

Thus, in routine clinical practice, the physician (and/or the technician or photographer) will not need to schedule a reexamination of the patient due to eye movement or blinking that occurred during the acquisition. The TruTrack™ system significantly helps to improve the signal to noise ratio.

Full spectrum amplitude decorrelation algorithm

The Eye-Tracking system also allows the use of a full spectrum amplitude decorrelation algorithm. This guarantees a clear differentiation between blood flow and static tissue without sacrificing axial resolution (i.e. depth resolution) of the OCT images.

Therefore, **very thin layers** of the vascular network become distinguishable in the C-scan section.

The effect of axial motion (e.g. the patient is moving towards the camera) must be compensated as well. Our approach is to geometrically align the successive B-Scans before performing the analysis of temporal changes. This is done during OCT scan acquisition.

In this case, blood flow can be identified, even if strong bulk motion occurred during acquisition.

Overall, OCT-Angiography with active eye tracking and proper B-scan alignment yields the desired high definition and geometrical accuracy.

To achieve high resolution OCT-angiographies, dense OCT volume scans have to be acquired, and each single B-scan of the volume scan has to be of consistently high quality.

Layer segmentation

En face OCT-Angiography images provide information about the flow detected in a C-scan section. These C-scans can be moved at different depths within an OCT volume scan.

In order to visualize blood flow in the different retinal and choroidal anatomic layers, the layered structures have to be identified and segmented.

The accuracy of layer segmentation is crucial to produce reliable OCT-A images that require high resolution OCT B-scans. This can be achieved through automated or manual layer segmentation.

An automated layer segmentation provides the clinician with an extremely fast way to show the presence of a decorrelation-signal due to perfused vascular structures in any OCT-Angiograms.

This is absolutely useful as a first step analysis, but it could suffer from potential segmentation errors (especially in accentuated macular diseases) and can show coplanarstructures that in fact belong to different layers.

Nevertheless, if segmentation errors occur, the provided software (*SPECTRALIS® Software Version 6.0, Heidelberg Engineering, Heidelberg, Germany*) allows a manual correction of all the boundaries.

Manual segmentation allows a fully customizable analysis, even though it may be more time consuming than the automated one.

Manual segmentation is based both on the possibility of selecting the thickness of the C-scan section and on shaping the section on the most suitable profile (generally ILM, RPE or BM).

Thin sections allow a very selective analysis of specific layers of the retina.

Conclusion

OCT-Angiography is a promising addition to multi-modal retinal imaging, and provides a complementary functional flow information to the structural details seen on conventional OCT. For a comprehensive assessment, OCT-A and conventional OCT scans should be simultaneously monitored in B- and C-scan views.

2.2 Imaging acquisition protocol – OCT-Angiography SPECTRALIS®

SPECTRALIS® OCT-Angiography: how to acquire images

The underlying concept of OCT-A is that in a static eye, the only moving structure in the ocular fundus is the blood that flows through the vessels.

OCT-A generates an image contrast in a full depth-resolved data set by differentiating between moving cells in the vasculature and static surrounding tissue without requiring dye injection. The amplitude of the signal resulting from movement varies rapidly over time.

By calculating the decorrelation of signal amplitude from repeated consecutive B-scans at the same cross-section, a contrast between static and nonstatic tissue is created that generates a vascular decorrelation signal. It facilitates the visualization of three-dimensional retinal and choroidal vasculature.[1-2]

The prototype "SPECTRALIS® OCT2" device (*SPECTRALIS®, Heidelberg Engineering, Heidelberg, Germany*) has been used to acquire the images.

This prototype is able to acquire 70,000 A-scans per second, with a resolution of 7 µm axially and 14 µm laterally, at a scan depth of 1.9 mm in tissue.

The ocular light power exposure was within the *American National Standards Institute safety limit*.[3]

An amplitude decorrelation algorithm developed by Heidelberg Engineering (Heidelberg, Germany) is applicable to a volume scan on a 15 x 5° or 15 x 10° area (4.3 x 1.5 mm or 4.3 x 2.9 mm), which is composed of a variable number of B-scans (ranging from 131 to 261, respectively) at a distance of 11 µm each.

The prototype device, using the **Automatic Real Time** (ART) mode allows the ability to vary the number of frames per scan in order to average the image, to

increase the quality of each single B-scan, and to improve the signal-to-noise ratio.

The B-scan OCT-A is generated by computing the decorrelation between the standard B-scans that are sequentially acquired at the same location. The decorrelation between each acquired B-scan and a second one, taken in the same location, is assessed in order to obtain an OCT B-scan angiogram.

The C-scan ("en-face") visualization of this OCT-A is automatically derived from the OCT B-scan angiograms. The ART mode along with the reduced distance between two consecutive B-scans (11 µm) enables high-resolution C-scan angiograms to be obtained.

Every OCT-A is simultaneously achieved with the corresponding standard OCT B-scan; thus, the visualization of both retinal/choroidal functional and morphological aspects are acquired.

An automated segmentation algorithm for both retinal and choroidal layers is provided with the OCT-A software (HEYEX™ Software Version 1.9.201.0, Heidelberg Engineering, Heidelberg, Germany).

In case of accentuated macular retinal/choroidal lesions, a specific manual segmentation allows the modification of the shape and the location of each C-scan section.

The thickness of every C-scan may also be modified in order to have a constantly thick "slice of tissue" at different retinal or choroidal levels. This approach allows the analysis of all the structures included in a variably thick "slice of tissue" in the "en-face" visualization.

An automatically segmented 30 µm C-scan, shaped on the RPE profile, is manually fine-tuned to be located immediately above the RPE, and then moved progressively deeper in 30 µm steps, up to the choroid-sclera interface.

A transverse section (not aligned with any retinal layer) may also be chosen in order to reduce artifacts due to segmentation errors.

The importance of starting the assessment above the RPE is due to the fact that in normal eyes, no vascular structures exist at this level. Therefore, OCT-A is not expected to identify blood flow (a decorrelation signal) at the depth of the outer retinal layers.

In case a Type II CNV or chorio-retinal anastomosis (CRA) might be present, the 30 µm step OCT-A analysis should be extended to the whole retinal and choroidal thickness, rather than, as usually performed, from the top of the RPE to the choroid-sclera interface.

The co-registered conventional OCT B-scan and C-scans provide useful information, primarily to identify the **specific anatomical level** at which each OCT-A C-scan is analyzed.

This will simultaneously add information about the presence of CNV activity, such as sub-retinal fluid or intraretinal cystoid spaces.

Moreover, they are useful in guiding the detection of certain exudative AMD variants, such as AMD related polyps or CRA.

References

1. **Jia Y, Bailey ST, Wilson DJ et al.** Quantitative optical coherence tomography angiography of choroidal neovascularization in age-related macular degeneration. *Ophthalmology.* 2014 Jul; 121(7):1435-44.

2. **Moult E, Choi W, Waheed NK, Adhi M et al.** Ultrahighspeed swept-source OCT angiography in exudative AMD. *Ophthalmic Surg Lasers Imaging Retina*. 2014 Nov-Dec; 45(6):496-505.

3. **American National Standards for safe use of Lasers**, ANSE Z136. Orlando, FL: laser Institute of America; 2007:1-2007.

2.3 OCT-A screen visualization

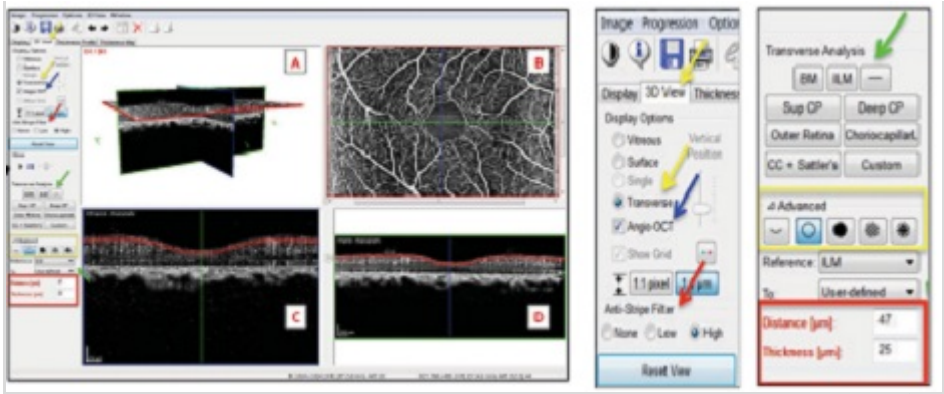

Figure 1: The left image shows the appearance of a SPECTRALIS® OCT Angiogram in Heyex Software (Heyex Software Version 1.9.201.0, Heidelberg Engineering, Heidelberg, Germany). The right images are magnifications of the left image highlighting the menu list.

The 4-picture view can be activated by selecting the “3D View” in the upper bar and then choosing “Transverse” in the display options (yellow arrows).

Image A is a combined visualization of the three other planes (B, C, D) and shows the spatial relationship between them. **Image B** is the “en face” visualization of OCT-A, in this case showing the superficial capillary plexus of a normal subject. The two lines, one horizontal (green) and one vertical (blue), identify the exact position of the two B-scans shown in images C and D.

Images C (orthogonal) and **D** (original) are two B-scan elements of a single volume scan on a 15 x 10° centered in macular area.

To turn on the Angio-OCT mode, select the Angio-OCT box under Display Options (as indicated by the **blue arrow**). If this box is not checked, the resulting image will appear the same as if captured using the traditional OCT mode.

The Anti-Stripe Filter (as indicated by the **red arrow**) is a useful tool to reduce the image noise.

The possibility of selecting an automated segmentation, rather than a manual, is shown by the green arrows. Some C-scan sections (i.e. superficial capillary plexus, outer retinal layers, choriocapillaris) can be provided by automated segmentation. Others can be obtained by the operator in a fully customizable context.

The same thickness of a C-scan and the distance from a given structure (red box) can be selected by the clinician or photographer in order to clearly visualize every element included in a pre-determined B-scan.

Finally, with **the advanced functions** (yellow box), there is also the possibility to modify the contrast of a given C-scan, in order to highlight structures with a high decorrelation signal, or the surrounding hypo-intense ones.

The SPECTRALIS® Software (Heyex Software Version 1.9.201.0, Heidelberg Engineering, Heidelberg, Germany) measures the signal strength using a "Quality Index" (QI) and assigns a number expressed in decibels (dB), ranging from 0 (low quality) to 40 (excellent quality).

This quality index (QI) is influenced by several elements, such as media opacities or the photographer's experience. In this type of examination, mainly qualitative, the closer the QI value is to its maximum, the better the clinician will be able to recognize fine details of the lesion.

3 OCT-ANGIOGRAPHY – SPECTRALIS® IN NORMAL SUBJECTS

Moreover, the angiographies (both FA and ICGA) provided essential dynamic information on the perfusion of different retinal and choroidal vascular layers, including the transit time from the arm to the eye. This resulted in the comprehensive evaluation of all retinal and choroidal vascular diseases that, when added to the morphological data, allowed the clinician to detect diseases and reach the end with the correct diagnosis.

Fluorescein angiography has generally been accepted as the "gold standard" imaging of the fundus, due to the fact that FA is the best, if not the unique, method to visualize the retinal capillary bed, including its dilation or perfusion, particularly in the macular area.

Moreover, FA will allow the clinician to detect and evaluate one main clinical sign: the leakage from abnormal and/or (retinal or choroidal) new-vessels.

Although the fluorescence from the injected dye enabled improved visualization of retinal capillaries, it was also well known that this two-dimensional exam cannot capture all the different layers of the retinal capillary network.

It was reported that fluorescein angiographic images of the retina corresponded to the anatomical arrangement of the superficial retinal vessels, whereas the deeper retinal capillaries were not visualized in the angiogram.[2,3]

Comparable histo-pathological correlations in humans have not been reported. But comparative findings suggest that the deeper capillary network in the retina is not visualized well by fluorescein angiography, possibly due to a light scattering of the retina.[4]

Therefore, even if FA is the gold standard for the visualization of retinal vessels, one of the two major capillary networks do not appear to be imaged well, in spite of the retina being a nearly transparent structure.[5]

Optical coherence tomography angiography (OCT-A) allows a clear, depth-resolved visualization of the retinal[5] and choroidal microvasculature[6], by calculating the decorrelation of the signal between static and nonstatic tissue.

Given that the main moving elements in the ocular fundus are contained in blood vessels, the determining of a vascular decorrelation signal enables the three-dimensional visualization of the retinal and choroidal vascular network.[7]

Moreover, OCT-A does not require administration of intravenous dyes, thus reducing the risk of potential adverse events.[8]

3.1 Retinal and choroidal vascular analysis in healthy subjects

Retinal vascular anatomy

Generally, the blood-supplying artery to the inner retina is the central retinal artery that follows the inferior margin of the optic nerve and enters the eye at the level of the optic nerve head.

The central retinal artery divides into two main branches, and each of these divides again to form the superior nasal and temporal and the inferior nasal and temporal arteries that supply the four quadrants of the retina. The retinal venous vessels are distributed in a similar pattern.

Many anatomical variations in this division and distribution may be observed in the normal fundus. The major arterial and venous branches and the successive divisions of the retinal vasculature are present in the retinal nerve fiber layer (RNFL) close to the internal limiting membrane (ILM).

The retinal arterial circulation is a terminal system with no arterial-venous communication to other arterial systems. Thus, the perfusion of a specific retinal quadrant stems exclusively from a given retinal artery and vein that supply that area (in the most frequent normal distribution of the vessels).

Any impairment or blockage in blood supply therefore causes an ischaemia or infarction. As the large arteries extend within the retina toward the periphery, they divide to form successive level arteries with progressively smaller diameters until they reach the ora serrata.

The retinal arteries branch dichotomously or at right angles to the original vessel.

The arterioles branching from the retinal arteries form an extensive capillary network in the inner retina as far as the external border of the inner nuclear layer (INL), either toward the periphery and/or in the macular area.

Many macular arterioles, branching from the temporal (superior and inferior) retinal arteries, dive into the retina to form the macular capillary bed with two distinct capillary plexus, one in the ganglion cell layer (GCL) (*superficial capillary plexus, SCP*) and the other in the INL (*deep capillary plexus, DCP*).

Generally, no vessels extend deeper than the inner nuclear layer. The outer retinal layers and photo receptors receive their blood supply not from the retinal capillary bed, but from the choriocapillaris.

In less than 20% of all cases, a **cilio-retinal artery**, derived from the short posterior ciliary artery, enters the retina on the temporal side of the optic nerve. It contributes to the retinal vasculature when it reaches the macular area and ends up in the capillary plexus.

3.2 Fluorescein angiography in healthy subjects

Fluorescein angiography images in the current atlas were obtained by the use of a confocal imaging system (SPECTRALIS® HRA2, Heidelberg Engineering, Heidelberg, Germany).

This system captures only light emitted in a predetermined plane and consequently eliminates artifacts (due to reflection and diffraction) and superimposed images.

The macular capillary bed, including the delicate perifoveal anastomotic arcade may be visualized when there is clear media and good contrast.

This arcade will precisely demarcate the central avascular zone.

In some rare cases, fine-tuning the focus could help to identify some differences between *superficial capillary plexus (SCP)* and *deep capillary plexus (DCP*), but imaging them may require a successive focusing.

Fine structures, including pathologic conditions such as a neovascularization, are clearly visualized.

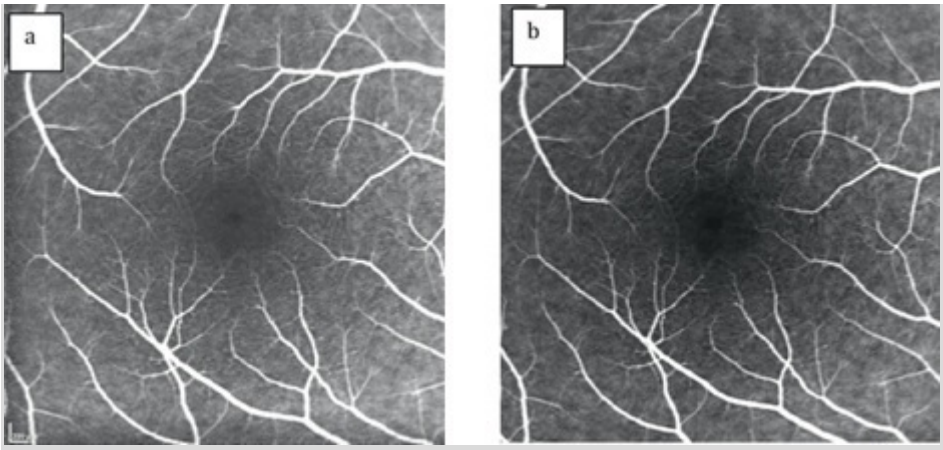

Figure 2: (a) Fluorescein angiography in the early artero-venous phase. Retinal veins, arteries, and macular branches are fully perfused with no evidence of any filling impairment. Clear visualization of the *superficial capillary plexus* occurs mainly in the perifoveal area. The perifoveal arcade is not completely visible on 360°. **(b) Fluorescein angiography in the early arterial-venous phase** focused deeper than in **(a)** to obtain information about the deep retinal vessels. Despite the focusing process, the *deep capillary plexus* is visible, but not very clear because of retinal light scattering.

3.3 Retinal OCT-Angiography in healthy subjects

All the OCT-A examinations were performed using a SPECTRALIS® OCT2 Angiograph prototype (Heidelberg Engineering, Heidelberg, Germany) that was able to acquire 70,000 A-scans per second with a resolution of 7 µm axially and 14 µm laterally at an imaging depth of 1.9 mm in tissue. The ocular light power exposure was within the limits of the American National Standards for safe use of Lasers.[9]

The C-scan shows arteries clearly distinguishable from veins by the presence of the surrounding hypo-intense halo. This is due to the absence of efferent vessels directly coming out from the walls.

The **superficial capillary plexus (SCP)** appears as a fine capillary network with an intense signal. The perifoveal arcade is clearly visible on 360° (**figure 3).**

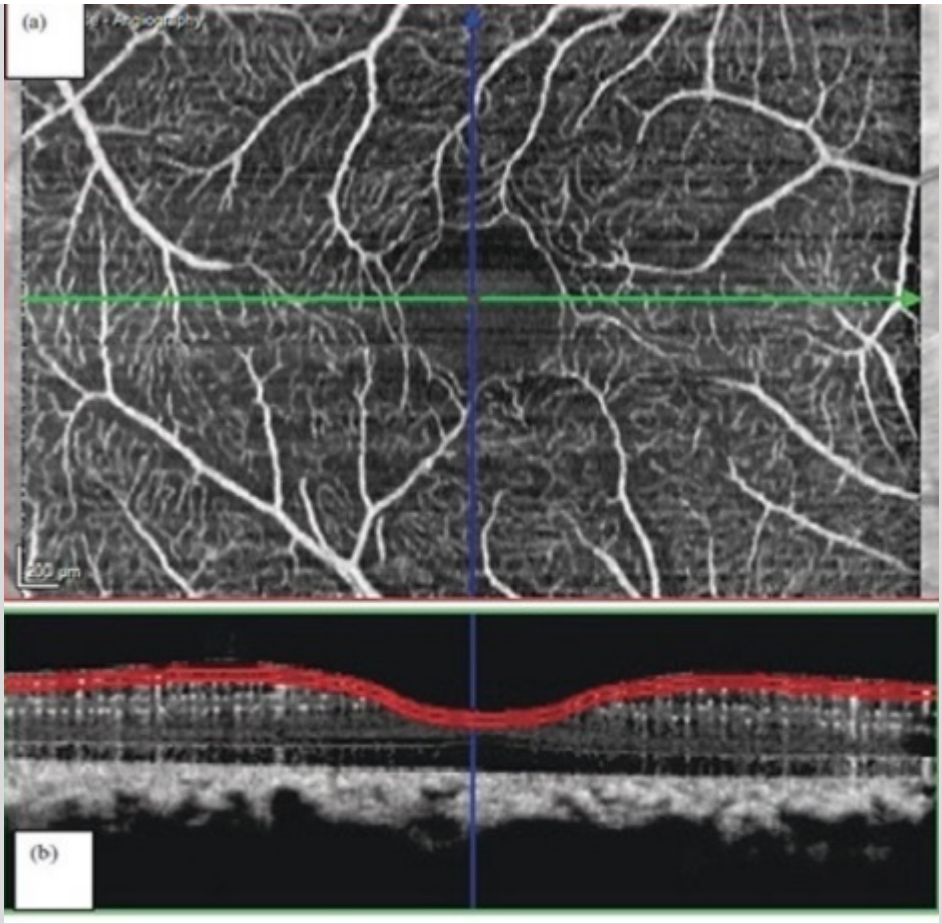

Figure 3: Superficial capillary plexus (SCP). (a) 25-µm-thickness OCT-A C-scan, shaped on the inner limiting membrane (ILM) profile. The C-scan is taken at the level of the ganglion cell layer (GCL), 40 µm below the ILM [as shown with the red line in **(b)**]. Arteries are clearly distinguishable from veins by the presence of the surrounding hypo-intense halo due to the absence of efferent vessels directly coming out from the walls. It is shown as a fine capillary network, which corresponds to the *superficial capillary plexus* (SCP). The perifoveal arcade is clearly visible on 360°.

The **deep capillary plexus** is shown in the C-scan (see **figure 4**) taken at the level of the inner nuclear layer (INL), 130 µm below the ILM (as shown with the red line in **figure 4 b**). A dense capillary network, different from the superficial one, becomes clearly visible developing all around the perifoveal area.

This is the first in-vivo examination that could allow a detailed visualization of the deep capillary plexus (DCP), very dense, regularly anastomosed, with sinuous arborization, and without visibility of arterioles and venules.

The corresponding B-scans show regularly aligned hyperintense dots stratified in two main lines (deep and superficial) and an intermediate one, corresponding to the interconnections between the two plexa.

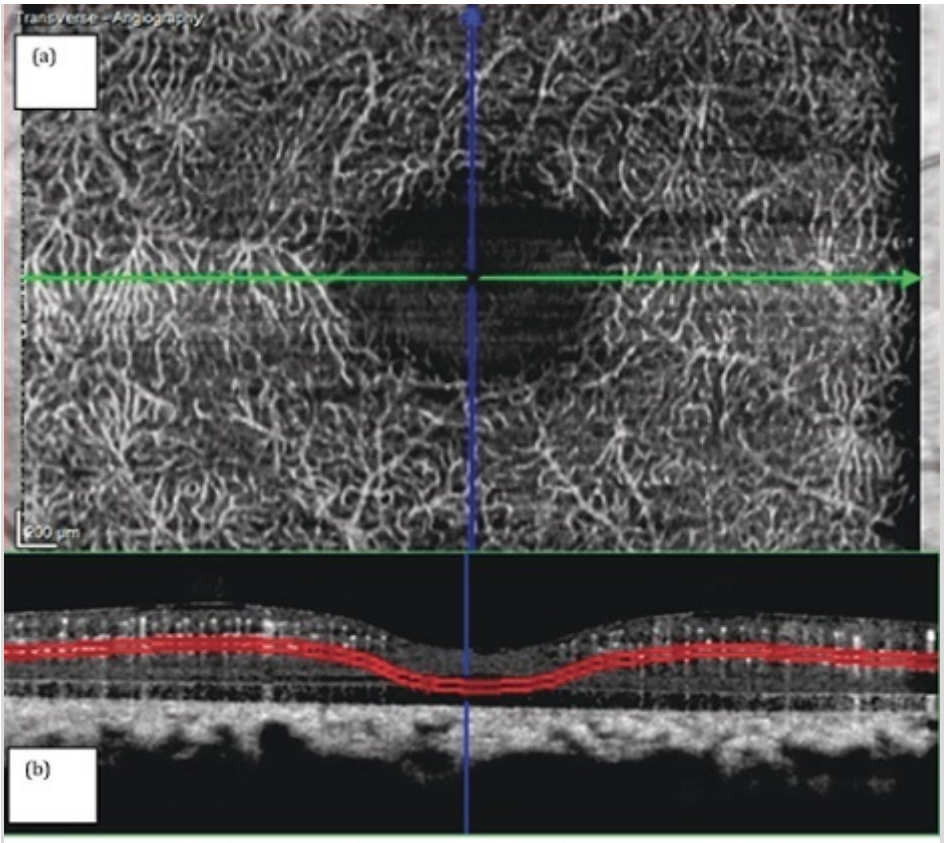

Figure 4: Deep capillary plexus (DCP). (a) 25-µm-thickness OCT-A C-scan, shaped on the inner limiting membrane (ILM) profile. The C-scan is taken at the level of the inner nuclear layer (INL), 130 µm below the ILM [as shown with the red line in **(b)**]. Clearly distinguishable, a dense capillary network is present all around the perifoveal area, corresponding to the deep capillary plexus (DCP). This is the first in-vivo examination that allows a detailed visualization of the DCP.

Traditional fluorescein angiography and OCT-A should not be directly compared. This is mainly due to the two-dimensional (2D) aspect of the FA, in which all the vascular structures that are included in the whole retinal thickness are simultaneously seen. Therefore, this type of imaging suffers from some limitations due to the superimposition of the different layers and light scattering.

The OCT-Angiography (OCT-A), for the same nature of a depth-resolved examination, provides a clear visualization of the different structures (as seen

in **figures 5 and 6**), and enables the clinician to evaluate layer by layer all retinal and choroidal tissues for a detailed vascular analysis.

In a limited but useful area (in this case 15 x 10°), a substantial difference is evident between the traditional FA (on the background) and the OCT-A (in the foreground). In the external areas belonging to the FA, in which the images are not overlapped, there is no possibility to clearly visualize SCP (**figure 5a**) nor the DCP (**figure 5b**), unlike on OCT-A.

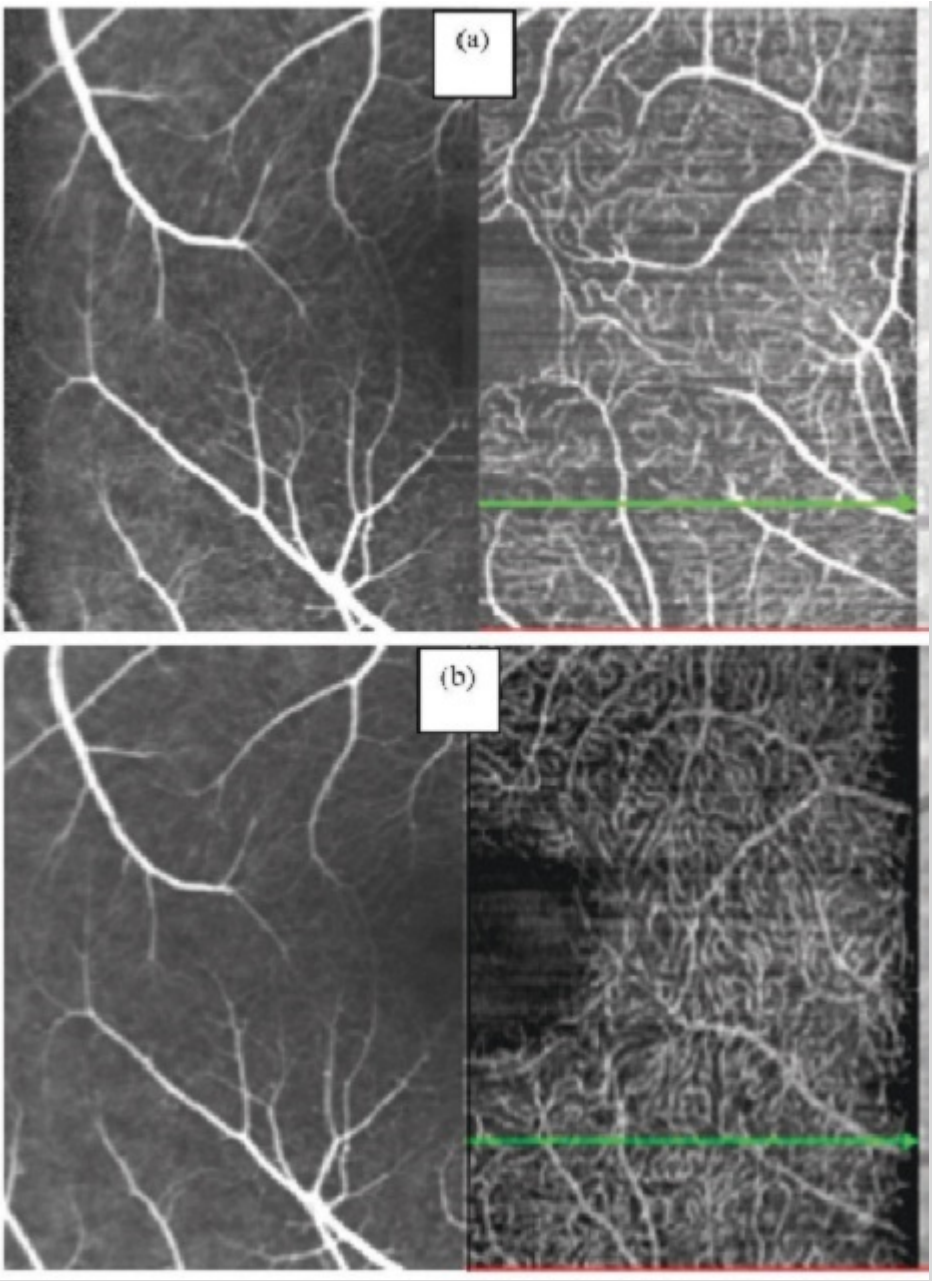

Figure 5: Comparison between traditional fluorescein angiography (left) and OCT-angiography (right). (a) *Superficial capillary plexus (SCP).* **(b)** *Deep capillary plexus (DCP).*

3.4 Choroidal vascular anatomy

A large part of the blood supply of the eye comes from the choroid, which originates from the ophthalmic arteries. The left and right ophthalmic arteries in the widest part of the individuals arise as the first major branch of the internal carotid, usually where the latter breaks through the dura mater to exit the cavernous sinus.

The posterior ciliary arteries, which form the blood supply to the choroid, and the central retinal artery, enters the eye via the optic nerve, are branches of the ophthalmic artery. Other branches of the ophthalmic artery supply the lacrimal gland, extra-ocular muscles, and lids.

The choroid is vascularized by two arterial systems: the short posterior ciliary arteries, which supply the posterior choroid, and the long posterior ciliary arteries, which supply the anterior portion of the choroid (as well as the iris and ciliary body).

Short posterior ciliary arteries (approximately 16–20) penetrate the sclera in a circular pattern surrounding the optic nerve. The distance between these vessels and the nasal side of the nerve is closer than that on the temporal side.

The circle of Zinn, an annular artery surrounding the optic nerve, is formed by the anastomoses of these arteries within the sclera. The branches from the circle of Zinn contribute to the pial circulation, the optic nerve at the level of the lamina cribrosa, and the nerve fiber layer of the optic disk.

The short posterior ciliary (other branches originating from the circle of Zinn) enter the choroid to provide the arterial blood supply to the posterior uvea. These arteries divide rapidly to terminate in the **choriocapillaris**, an exceptionally dense capillary bed that nourishes the posterior choroid up to the level of the equator of the eye.

The two long posterior ciliary arteries penetrate the sclera on either side of the optic nerve. The long posterior ciliary arteries begin to branch just anterior to the equator and contribute to the circulation of the iris and the ciliary body. Just anterior to the equator, some branches of these vessels course down into the choroid and branch to terminate in the choriocapillaris from the ora serrata back to the equator of the eye.

Choriocapillaris layer

These arteries continue to branch and ultimately form the extensive choriocapillaris layer adjacent to the acellular Bruch's membrane. This layer is located on the basal side of the RPE with a lumen diameter of nearly 20 µm in the macular region and 18–50 µm in the periphery.

Venous collecting vessels from the choriocapillaris emerge that ultimately exit the eye through the vortex veins (approximately 4–7). In addition to the choroid, the vortex veins also drain the ciliary body and iris circulation.

The vortex veins usually exit the sclera at the equator or up to 6 mm posterior to this location after forming an ampulla near the internal sclera. The vortex veins drain into the superior and inferior ophthalmic veins, which leave the orbit and enter the cavernous sinus.

3.5 Indocyanine green angiography in healthy subjects

Indocyanine Green Angiography (ICGA) has dramatically advanced our understanding and interpretation of choroidal imaging in ophthalmology.

A normal angiogram is difficult to define because of the many changes that can occur with aging or that may be related to differences in pigmentation.

Anatomical variants are common in the arrangement and distribution of choroidal blood vessels and regarding the circulatory dynamics filling and drainage.

Arteries may emerge from different sites, usually perimacular and peripapillary, at variable intervals (**figure 6**).

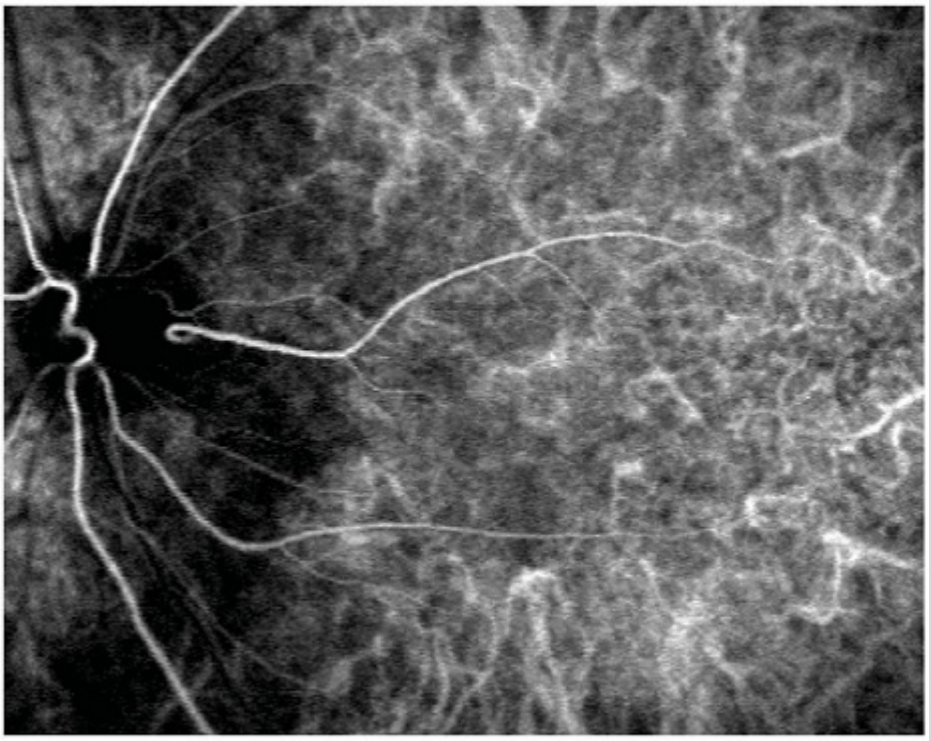

Figure 6: The dye is first seen in choroidal arteries with their initial distinctive loop and their oblique path towards the periphery. Note the simultaneous filling of a cilio-retinal artery.

Veins present unusual paths even more frequently, sometimes draining into the posterior pole (**figures 7 and 8**).

However, vascular branches are usually no longer visible over their entire length due to the undulating nature of their pathways, the layered distribution, and the variable caliber of vessels within choroidal tissue. Therefore, imaging them may require successive focusing.

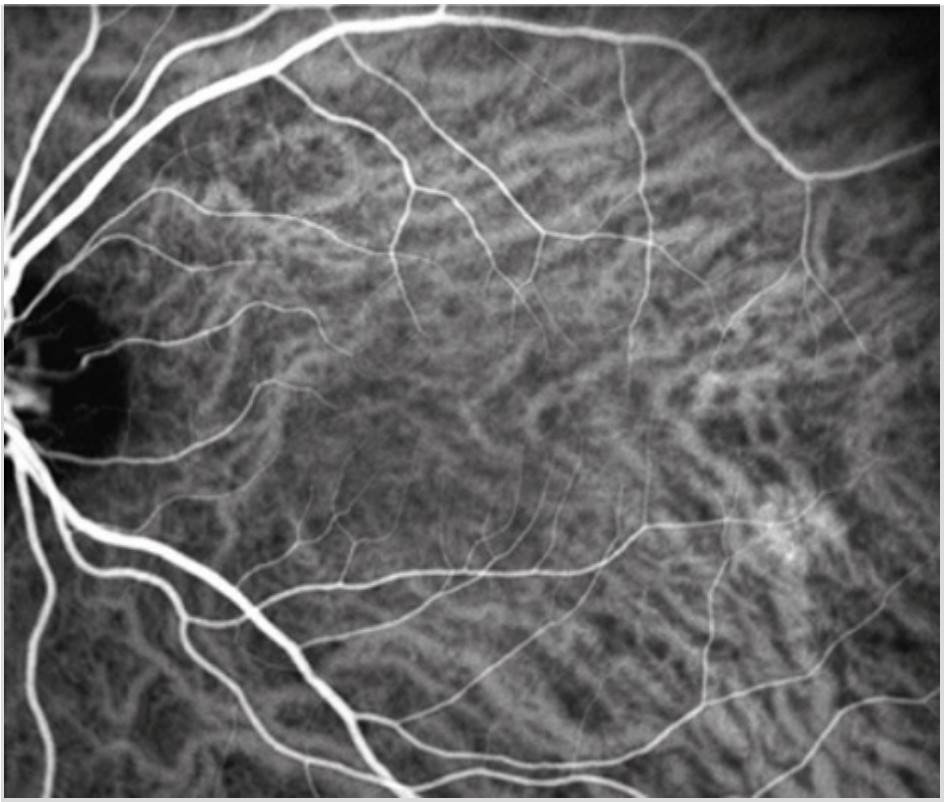

Figure 7: Early venous phase of ICGA without significant changes in large vessels choroidal network. There is a clear predominance of the venous network, and there are difficulties in distinguishing the arterial pattern. There is an asymmetrical arrangement of venous drainage, which is mainly directed towards the superior and inferior temporal periphery.

Figure 8: Mid venous phase of ICGA. The choroidal vessels are faintly visible.

3.6 Choroidal OCT-Angiography in healthy subjects

OCT-A, in addition to the depth-resolved information about retinal vessels, may provide further insight into the choroidal blood flow.

Choriocapillaris

In fact, the information given by segmentation slides at different levels deeper than Bruch's membrane is still relatively limited and still not fully understood. From the Bruch's membrane to 20 µm below the BM, different C-scans shaped on the BM profile will show a relatively homogenous grayish image.

This image depicts numerous tiny hyper-or hypo-intense dots, with a few that are moderately bigger.

This homogenous pattern could correspond to the very richly anastomosed vascular layer of the choriocapillaris.

No vascular channels are clearly detectable at this level (**figure 9**).

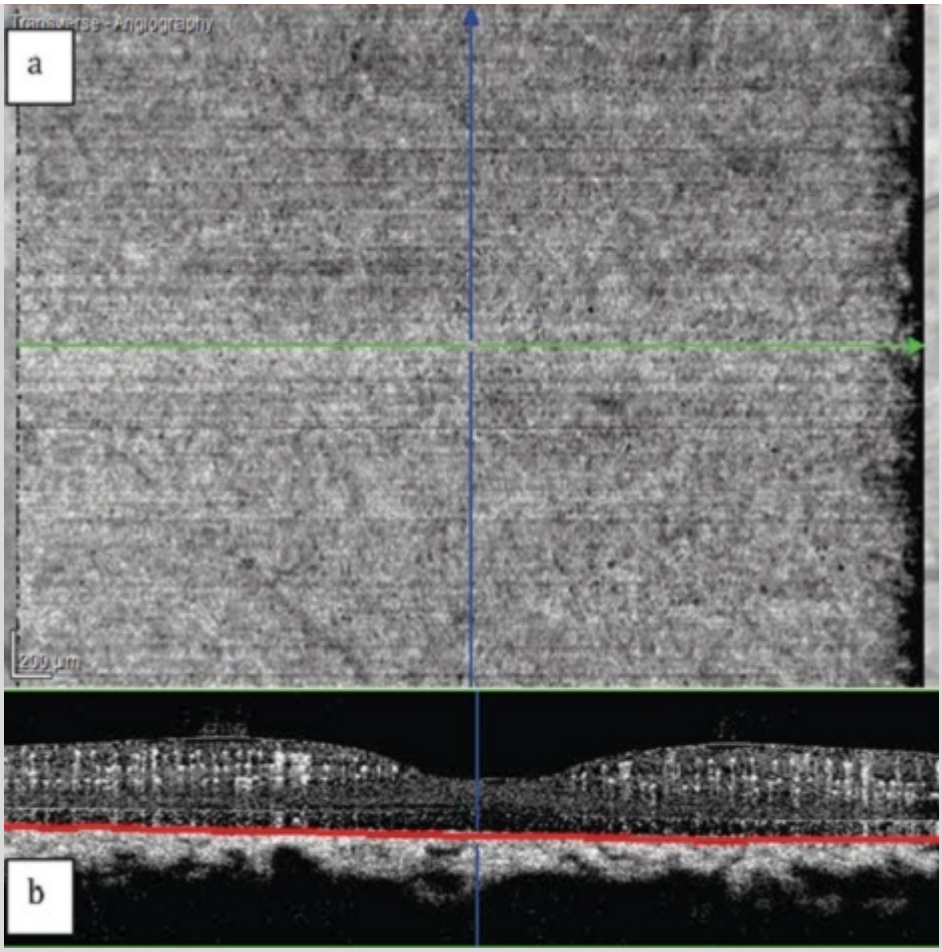

Figure 9: Choriocapillaris. (a) At the level of the choriocapillaris, 10-µm-thickness OCT-A C-scan shaped on the Bruch's membrane (BM) profile. The C-scan is taken at 10 µm below the BM [as shown in **(b)**]. Diffuse hyper-intense signal without a fine capillary network appreciable. Relatively homogenous grayish image depicts numerous tiny hyper-or hypo-intense dots. This pattern could correspond to the very richly anastomosed vascular layer of the choriocapillaris.

Choroid (Sattler's layer)

Different C-scans of 30-um in thickness (each), below the choriocapillaris, will allow for the evaluation of the Sattler's layer (medum choroidal vessels layer).

This layer is clearly visible on the Angio B-scan with continuous hyper-intense signal which is mixed with some hypo-intense structures.

The corresponding C-scan shows many linear (tubular) entities resembling the medium vessels network in an almost continuous hyper-intense grayish background (**figure 10**).

The reason why we are not able to distinguish a fine vascular network, may be due to the attenuation of the signal induced by the structures above or to the diffusion of the same signal from the choriocapillaris.

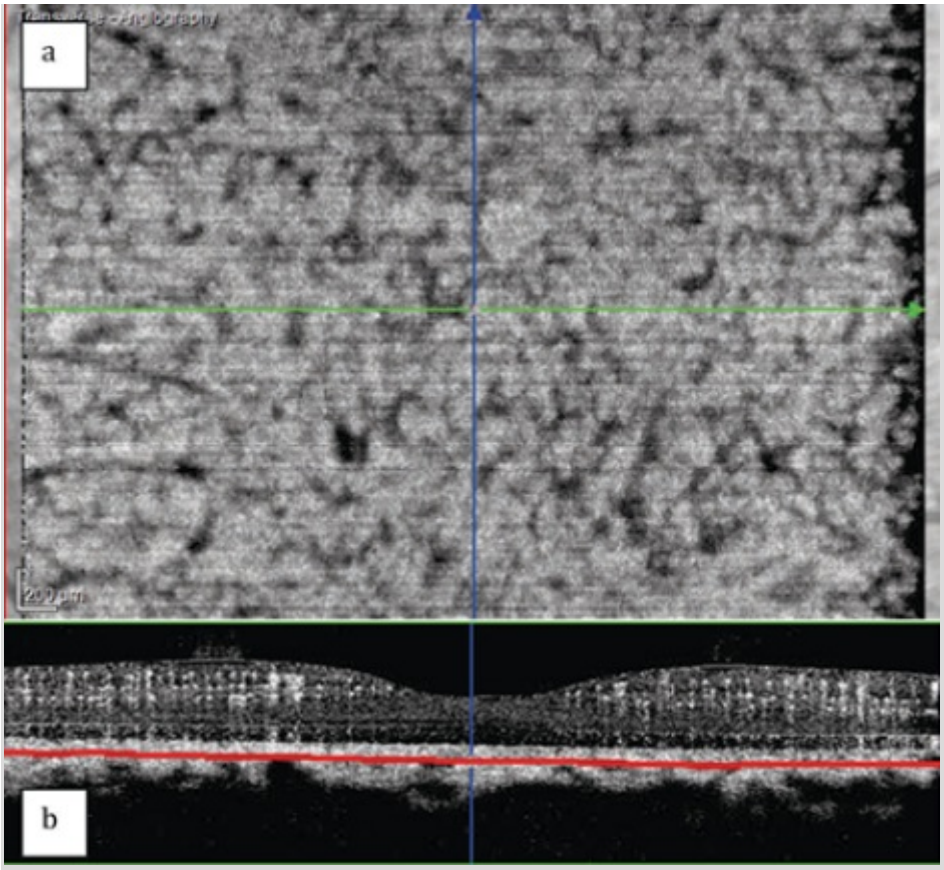

Figure 10: Sattler's layer. (a) At the level of the Sattler's layer (medium choroidal vessels), 10-µm-thickness OCT-A C-scan shaped on the Bruch's membrane (BM) profile. The C-scan is taken at 70 µm below the BM [as shown in **(b)**]. The diffuse hyper-intense signal due to the choriocapillaris does not allow a clear visualization of the medium choroidal vessels. Several hypo-intense linear structures are appreciable in this C-scan section, probably representing the choroidal vessels at this level and partially masked by the signal absorbed/diffused by the structures above.

Choroid (Haller's layer)

Going even deeper, C-scan segmentation will allow the visualization of the large choroidal vessels (so called Haller's layer).

The B-scan section shows alternative areas of hypo- and hyper-intense signals corresponding to these vessels, whose caliber is much larger than the Sattler's layer (**figure 11**).

The C-scan shows that the signal in this layer is discontinuous with multiple interruptions. This may be due to either the different speed of the blood and/or the sinuous trajectory of the vessels and/or the attenuation or diffusion of the signal induced by the structures above (mainly the choriocapillaris).

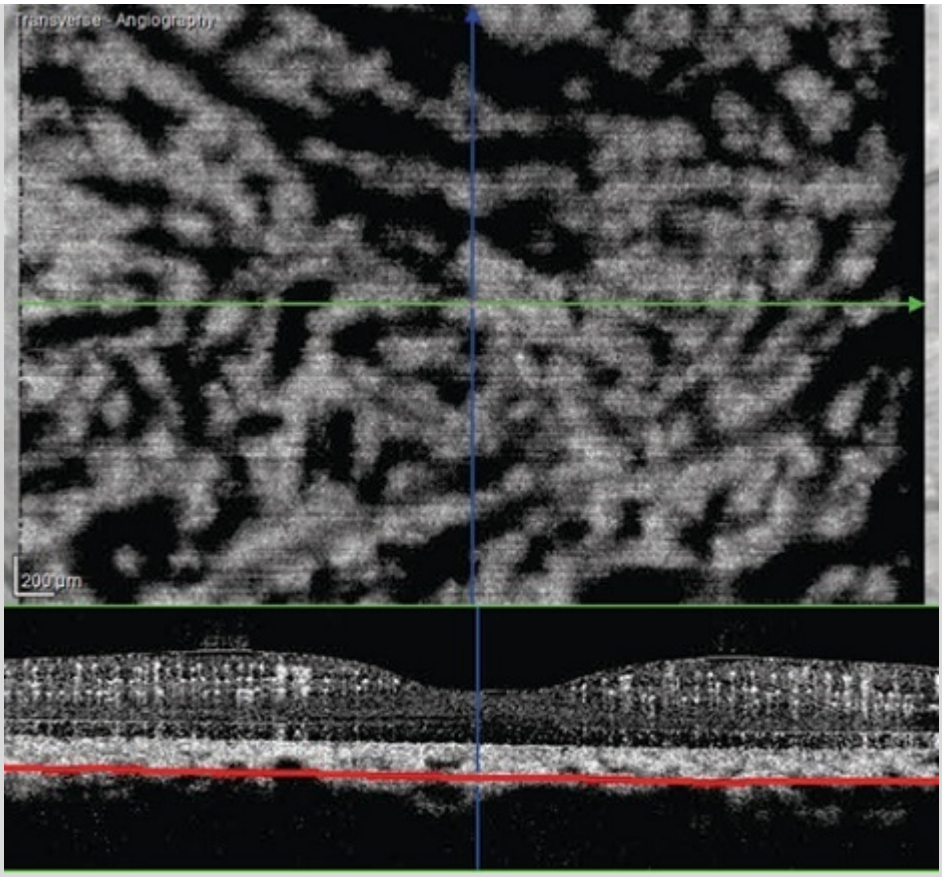

Figure 11: Haller's layer. (a) At the level of the Haller's layer (large choroidal vessels), 10-µm-thickness OCT-A C-scan shaped on the Bruch's membrane (BM) profile. The C-scan is taken at 140 µm below the BM [as shown in **(b)**]. Numerous hypo-intense linear structures are evident. These could be related to large choroidal vessels present at this level. As for the Sattler's layer, the decorrelation signal in these vessels is masked by the absorption of the structures above.

3.7 References

1. **Sulzbacher F, Kiss C, Munk M et al.** Diagnostic evaluation of type 2 (classic) choroidal neovascularization: optical coherence tomography, indocyanine green angiography, an fluorescein angiography. *Am J Ophthalmol.* 2011; 152(5):799-806 e1.

2. **Snodderly DM, Weinhaus RS, Choi JC.** Neural-vascular relationships in central retina of macaque monkeys (Macacafascicularis). *J Neurosci.* 1992; 12(4):1169-1193.

3. **Weinhaus RS, Burke JM, Delori FC, Snodderly DM.** Comparison of fluorescein angiography with microvascular anatomy of macaque retina. *Exp Eye Res.* 1995; 61(1):1-16.

4. **Mendis KR, Balaratnasingam C, Yu P et al.** Correlation of histologic and clinical images to determine the diagnostic value of fluorescein angio graphy for studying capillary detail. *Invest Ophthalmol Vis Sci.* 2010; 51(11):5864-5859.

5. **Spaide RF, Klancnik JM Jr, Cooney MJ.** Retinal vascular layers imaged by fluorescein angiography and optical coherence tomography angiography. *JAMA Ophthalmol.* 2015; 133(1):45-50.

6. **Moult E, Choi W, Waheed NK et al.** Ultrahighspeed swept-source OCT angiography in exudative AMD. *Ophthalmic Surg Lasers Imaging Retina.* 2014; 45(6):496-505.

7. **Jia Y, Bailey ST, Wilson DJ et al.** Quantitative optical coherence tomography angiography of choroidal neovascularization in age-related macular degeneration. *Ophthalmology* 2014; 121(7):1435-44.

8. **Yannuzzi LA, Rohrer KT, Tindel LJ et al.** Fluorescein angiography complication survey. *Ophthalmology.* 1986; 93(5):611-7.

9. **American National Standard for Safe Use of Lasers**, ANSI Z136. Orlando, FL: Laser Institute of America; 2007:1–2007.

4 OCT-ANGIOGRAPHY IMAGE ANALYSIS: HOW TO INTERPRET IMAGES IN AMD

4.1 SPECTRALIS® OCT-Angiography: how to interpret images in AMD

OCT-Angiography (OCT-A) is an emerging imaging technique, which provides a clear visualization of blood flow in both retinal and choroidal tissue.

The ability of OCT-A in detecting a vascular network where normally absent (i.e. in between the retinal pigmented epithelium (RPE) and the Bruch's membrane) allows the clinician to have a real image of the neovascularization and to assess its changes during the follow-up after treatment.

This evaluation is particularly important and useful in areas, where there are normally no vessels: in the space between RPE and Bruch's membrane, as well as in the subretinal space and the outer retinal layers.

The traditional dye angiographies (FA and ICGA) provide two-dimensional images, showing all the vascular and avascular structures coplanar. This can cause evident artifacts due to the phenomenon of superimposition.

However, OCT-A is able to obtain depth resolved images of a given retinal or choroidal tissue and therefore to have a layer-by-layer visualization of the entire CNV.

Well-known criteria, such as leakage, pooling and staining are regularly used to have a precise and qualitative description of a neovascular network.

On OCT-A, other criteria are indispensable to account for the absence of these dynamic phenomena.

Innovative criteria became necessary to evaluate the activity and degree of proliferation, the persistence and/or recurrence, or conversely the stabilization and wound healing, comprising vessels that become "mature".

These criteria are particularly important during the spontaneous evolution and even more after the treatment, in order to guide the decision of extending or interrupting the IVT injections.

These criteria are based on elements that are easy to recognize, such as: "shape", "branching pattern", "anastomosis", "vessel termini aspect" ("anastomotic arcade" or "dead tree") and finally, the existence of a perilesional halo.

4.2 OCT-A features of choroidal neovascularization

The following description, based on five different criteria, could not only provide a morphological assessment that is useful to identify the lesion, but also a functional one, since some of the features could be related to an active pattern, rather to a quiescent one.

Still active forms requiring treatment and quiescent ones, that justify only a monitoring will thus be recognized and distinguished.

These OCT-A criteria were selected after considering previously reported findings based on histopathology,[1,2] FA[3] and ICGA angiography,[4] OCT[5] and the recently introduced OCT-A.[6,7]

1. **Shape:** A well-defined (tortuous vessels, *lacy-wheel* or *sea-fan shaped*) CNV lesion in contrast to one with *long filamentous linear vessels*.

2. **Branching pattern:** *Numerous tiny capillaries* in contrast *large mature vessels*.

3. **Anastomoses:** *Presence* or *absence* of anastomoses and loops.

4. **Morphology of the vessel termini:** Presence of a *peripheral arcade* in contrast to a *"dead tree" appearance*.

5. **Perilesional Halo:** Presence of a perilesional hypo-intense halo, considered as regions of *choriocapillaris alteration*, either corresponding to flow impairment and/or localized atrophy.[6,7]

All the previously reported criteria, in the opinion of the authors, allow a specific description of the most relevant morphologic features of a neovascular lesion.

Studies (in progress) will bring quantitative and statistical confirmations, using blood flow and its variations as an index of response before and after treatment.

Therefore the possibility to identify specific features of a neovascular network can be useful: changes in vascular pattern may be a direct sign of how a CNV varies with time and how it responds to the therapy itself.

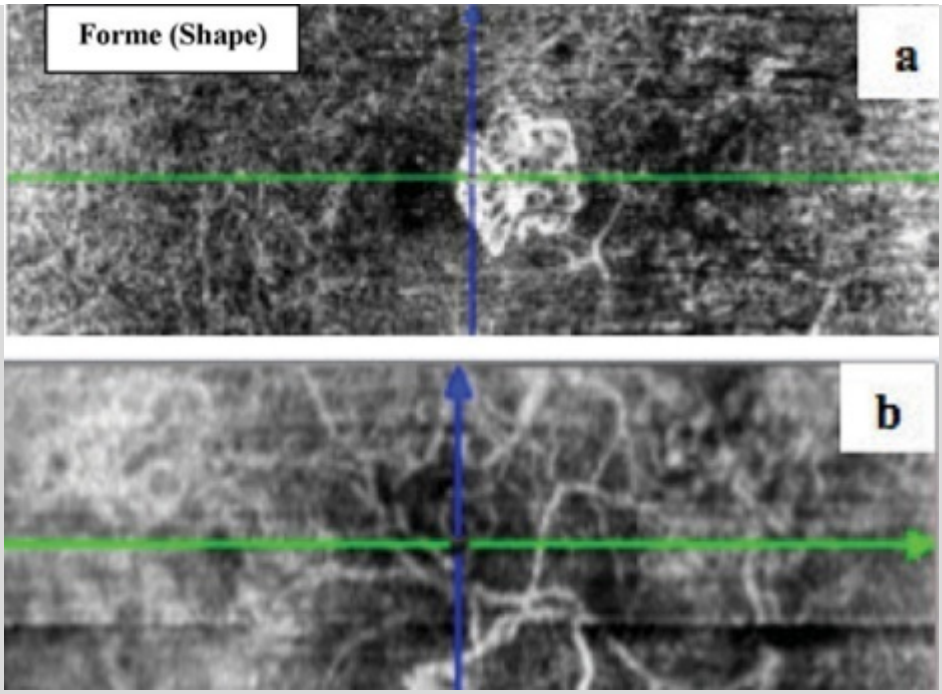

Figure 12: **OCT-A criteria for CNV analysis – shape. (a)** Typical *lacy-wheel shape* in contrast to **(b)** *long filamentous linear vessels*.

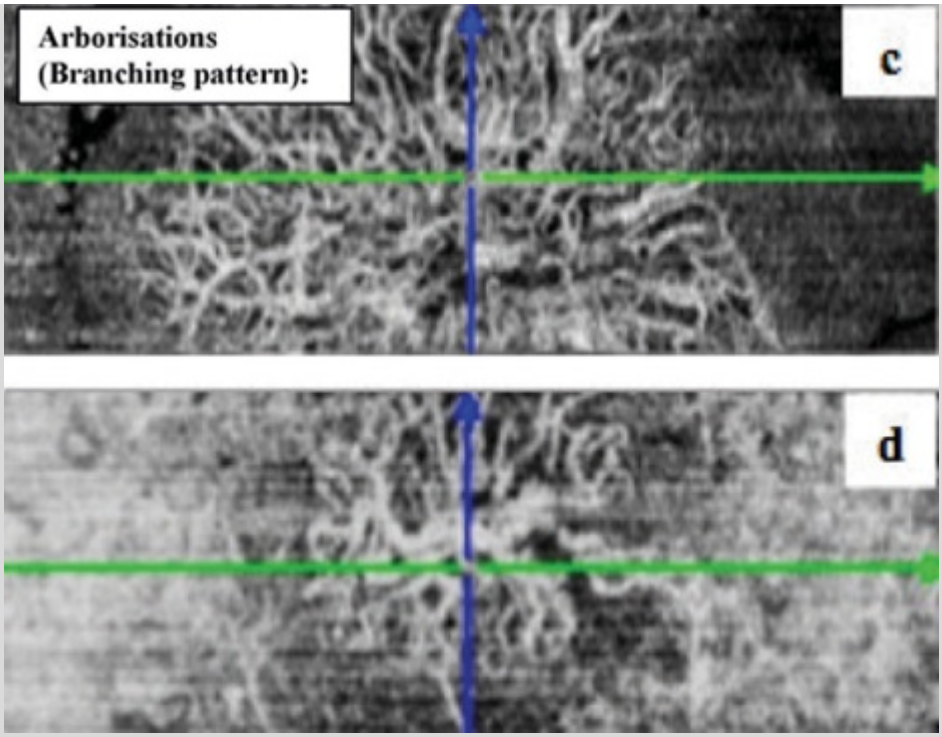

Figure 12 cont1: OCT-A criteria for CNV analysis – branching pattern. © *Numerous tiny capillaries* versus **(d)** *large mature vessels.*

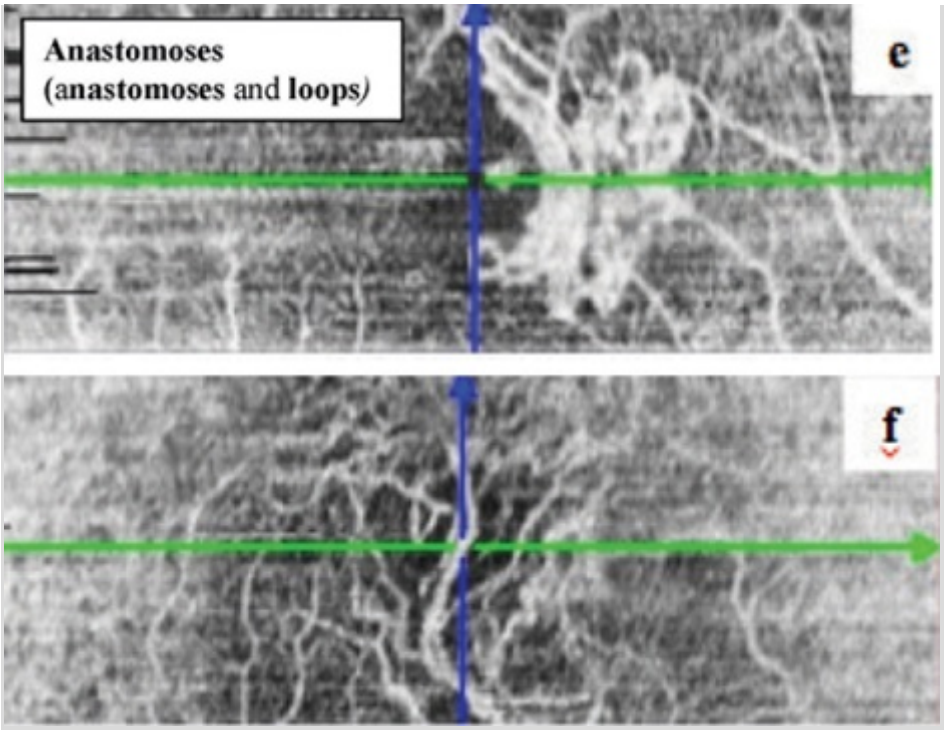

Figure 12 cont2: OCT-A criteria for CNV analysis – anastomoses. (e) *Widely anastomosed network* in contrast to **(f)** a *rarely anastomosed network.*

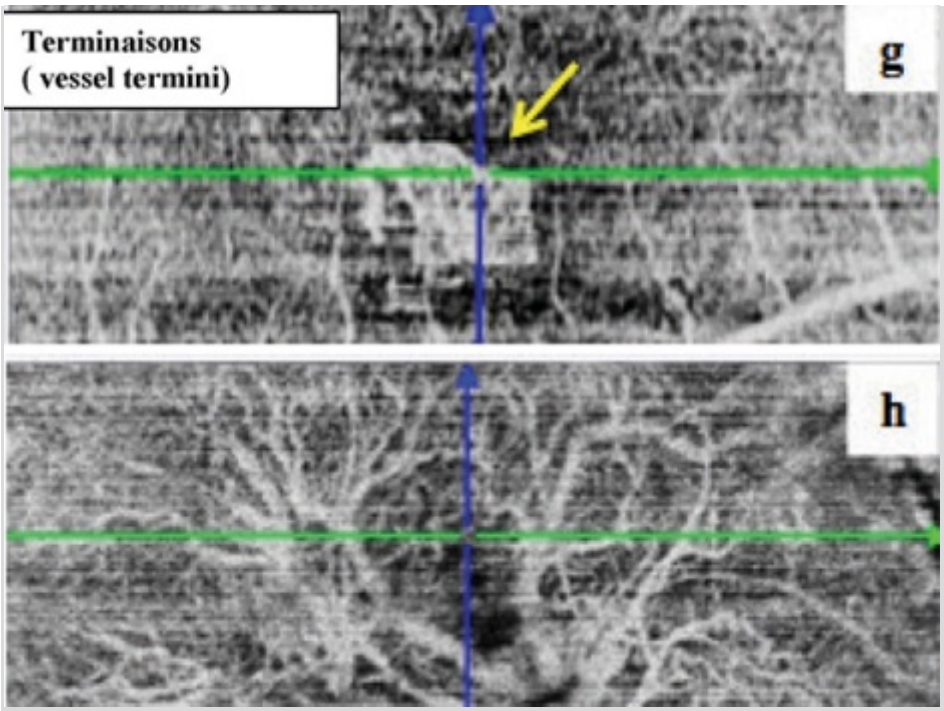

Figure 12 cont3: OCT-A criteria for CNV analysis – vessel termini. (g) *Peripheral arcade* versus **(h)** *"dead tree aspect".*

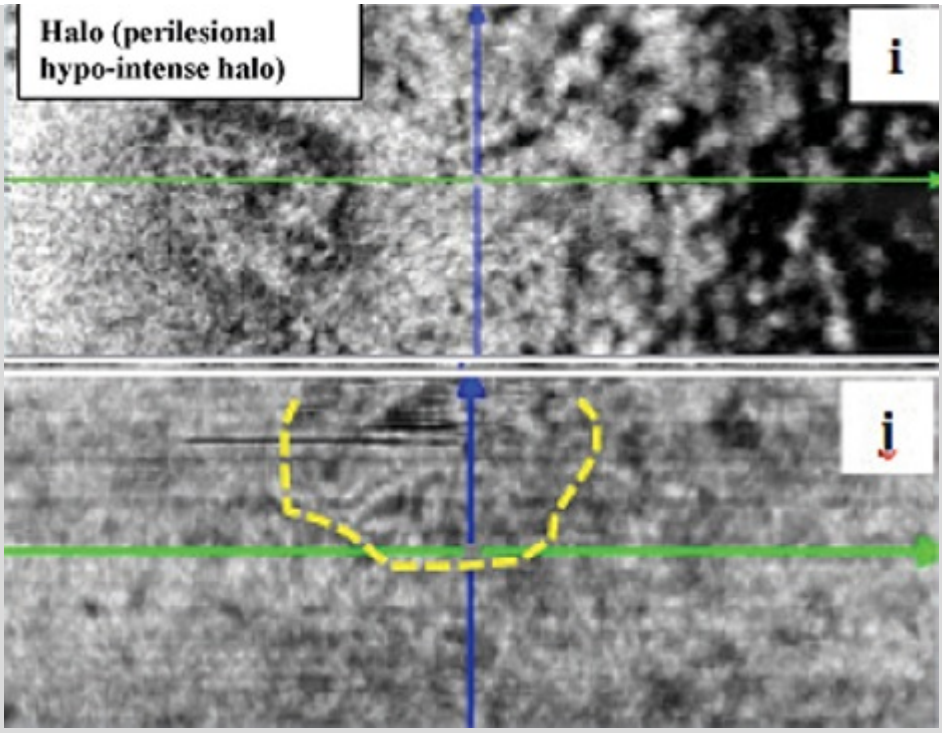

Figure 12 cont4: OCT-A criteria for CNV analysis – perilesional halo. [i] Evidence rather than absence **(j)** of *perilesional hypo-intense halo.*

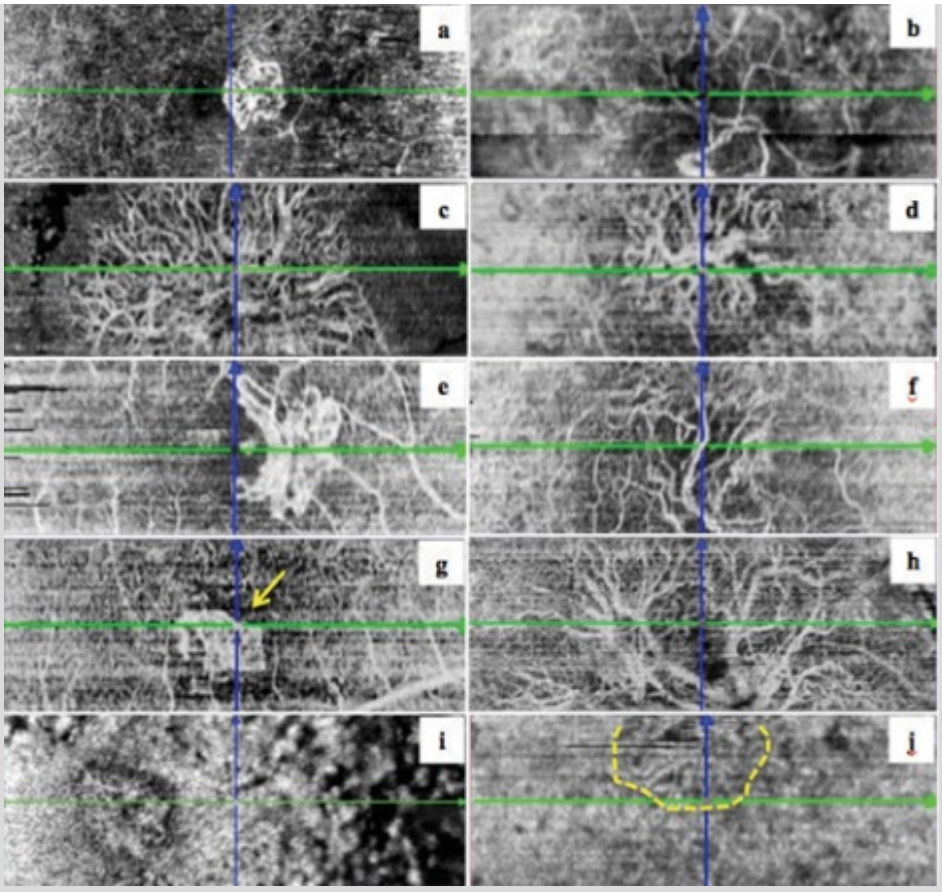

Figure 12 cont5: OCT-A criteria for CNV analysis – overview. All the images reported (a–h) were from a single 30 µm OCT-A C-scan section passing between the RPE and the Bruch's membrane. The two C-scans, (i & j), were taken immediately below the Bruch's membrane, at the level of the

choriocapillaris layer. Fur further description of the visualized structures: see the description of the different parts of figure 12 above.

4.3 References

1. **Ohkuma H, Ryan SJ.** Vascular casts of experimental subretinal neovascularization in monkeys. Invest Ophthalmol Vis Sci. 1983; 24(4): 481-90.

2. **Ohkuma H, Ryan SJ.** Experimental subretinal neovascularization in the monkey. Permeability of new vessel. Arch Ophthalmol. 1983; 101(7): 1102-10.

3. **Gass JD.** Pathogenesis of disciform of the neuroepithelium. Am J Ophthalmol. 1967; 63(3): Suppl:1-139.

4. **Hyvärinen L, Flower RW.** Indocyanine green fluorescence angiography. Acta Ophthalmol. (Copenh). 1980; 58(4):528-38.

5. **Lawman GA, Rosenfeld PJ, Fung AE et al.** A variable-dosing regimen with intravitreal ranibizumab for neovascular age-related macular degeneration: year 2 of the PrONTO Study. Am J Ophthalmol. 2009; 148 (1): 43-58.e1.

6. **Jia Y, Bailey ST, Wilson DJ et al.** Quantitative optical coherence tomography angiography of choroidal neovascularization in age-related macular degeneration. Ophthalmology 2014; 121(7): 1435-44.

7. **Moult E, Choi W, Waheed NK et al.** Ultrahighspeed swept-source OCT angiography in exudative fluorescence angiography. Acta Ophthalmol AMD. Ophthalmic Surg Lasers Imaging Retina. 2014 Nov-Dec; 45(6): 496-505.

5 Clinical Case No. 1: CNV Mixed-Type – Type I + Type II Minimally Classic

5.1 Introduction

OCT examinations have entered **clinical routine** over the last several years as an essential component of follow-up procedures after treatment.

These tests can directly demonstrate the efficacy of treatment, based essentially on the regression or persistence of exudation resulting from the abnormal permeability of the new vessels, with simple measurements such as macular thickness or the presence of intra or sub-retinal fluid accumulation.

The alterations in the outer retinal layers can be evaluated to determine the impact on the photoreceptors or to confirm the presence of new vessels, either under the RPE (occult – Type I) or more rarely, above the RPE (classic – Type II). Consequently, OCT examinations rapidly established their preeminent place among the different diagnostic strategies that have been used to confirm therapeutic indications and guide the follow-up after treatment.

In spite of the apparent simplicity of image acquisition and its safety, OCT cannot replace all the examinations used to evaluate various ophthalmological diseases.

Functional and morphological correlations are obviously essential for diagnosing and guiding treatment strategy, taking into account the importance of objective measurements such as central vision and the imaging features.

Fluorescein angiography (in case of preepithelial neovascularization) and *indocyanine green angiography* (for occult new vessels) remain essential for the accurate diagnosis of the various clinical forms of neovascularization.

These various information gathered by the ophthalmologist and evaluated as a whole will help in establishing the indications, timing and duration of intravitreal injections and the terms of clinical monitoring adopted in the case of AMD.

However, conventional OCT does not allow the visualization of new vessels or the degree of perfusion or their exact location and route, but only provides indirect signs, even though these are particularly valuable and informative.

New OCT techniques

OCT-Angiography (OCT-A) is a revolutionary new technique without dye injection, which enables the visualization of well-defined 3D-images of the choroidal and retinal microvasculature.

The OCT-A is based on a new concept: in a fixed eye, when analyzed by a very fast imaging protocol, the only moving structures in the ocular fundus are blood cells circulating in the vessels.

By calculating the amplitude **"decorrelation" signal** from repeated and consecutive B-scans in the same section, a contrast is generated; this contrast is useful to differentiate moving cells from static surrounding tissue.

A signal of variable intensity makes the retinal and choroidal vascular layers visible in three dimensions. This signal is hyper- or hypo-intense depending on the speed of the circulatory flow.

This has an important role in AMD, allowing the visualization of the blood moving inside the normal and new vessels. In addition, a conventional OCT scan may be simultaneously obtained.

These new OCT techniques provide both morphological and functional data. Such data are essential to help decide, if the treatment is to be extended or interrupted.

These examination methods and strategies are essentially adapted to wet AMD. However, they can also be used in atrophic age-related macular forms to help the early detection of possible new vessels.

Clinically, the detailed analysis and comparison between traditional multimodal imaging and **OCT-Angiography** images constitute the essential element of the clinical case chapters that follow, to sequentially describe each of the main clinical forms of AMD.

Examples of clinical cases will help to understand the contribution of OCT-A in comparison with dye angiographies and functional tests.

OCT-A will help to guide the diagnosis and treatment decision, currently based on intravitreal injections of anti-VEGF generally.

Neovascular AMD forms

Despite recent progress, AMD remains in all countries with a high standard of living as the major cause of visual impairment; its adverse impact appears to be increasing probably due to increased life expectancy and improved screening.

Neovascular AMD represents about 50 % to 65 % of the severe forms of AMD. The remaining is attributed to atrophic forms without neovascularization.

Risk factors comprise of arteriosclerosis (arterial hypertension and lipids) as well as environmental and lifestyle factors.

It appears that genetic predisposition, recently individualized, also plays a very important role.

A macular functional syndrome is usually present in the case of a wet AMD.

This syndrome rapidly evolves in case of visible, preepithelial CNV. However, in the case of occult new vessels (or subepithelial or vascularized PED) the functional signs progress over a long period of time.

Ocular fundus imaging currently appears to play a major role in the early detection and accurate diagnosis of neovascular AMD.

Monochromatic and color photographs as well as autofluorescence helped to identify fixed anatomic landmarks to subsequently recognize the presence of signs or complications of AMD.

However until now, only angiography allowed the visualization of the new vessels.

OCT enables the non-invasive demonstration of the indirect signs of AMD such as abnormal fluid accumulation.

Subepithelial CNV is the most common form of wet AMD representing more than 80 % to 85 % of the clinical forms of neovascular proliferations in AMD. They are often called “occult“, because they are poorly visible subepithelial or even undefined on fluorescein angiography.

OCT examinations, compared with angiographic studies, showed that such subepithelial choroidal new vessels always lead to the detachment of the RPE from the Bruch’s membrane.

The preepithelial CNV or visible or “classic“ CNV are significantly less frequent and rarely seen alone.

This is most often due to progressive and advanced forms of occult CNV, which seem to have broken through the retinal pigment epithelium.

Such evolution could be very limited (minimally classic), or sometimes more extensive (predominantly classic).

A separate form can be seen in 7–10 % of cases: chorioretinal anastomoses (CRA). These CRAs combine, within a PED, CNV (visible in SLO-ICG) and anastomoses with a macular artery and / or venule.

Modern techniques of SD-OCT allow us to directly analyze the impact of CNV on the outer retinal layers.

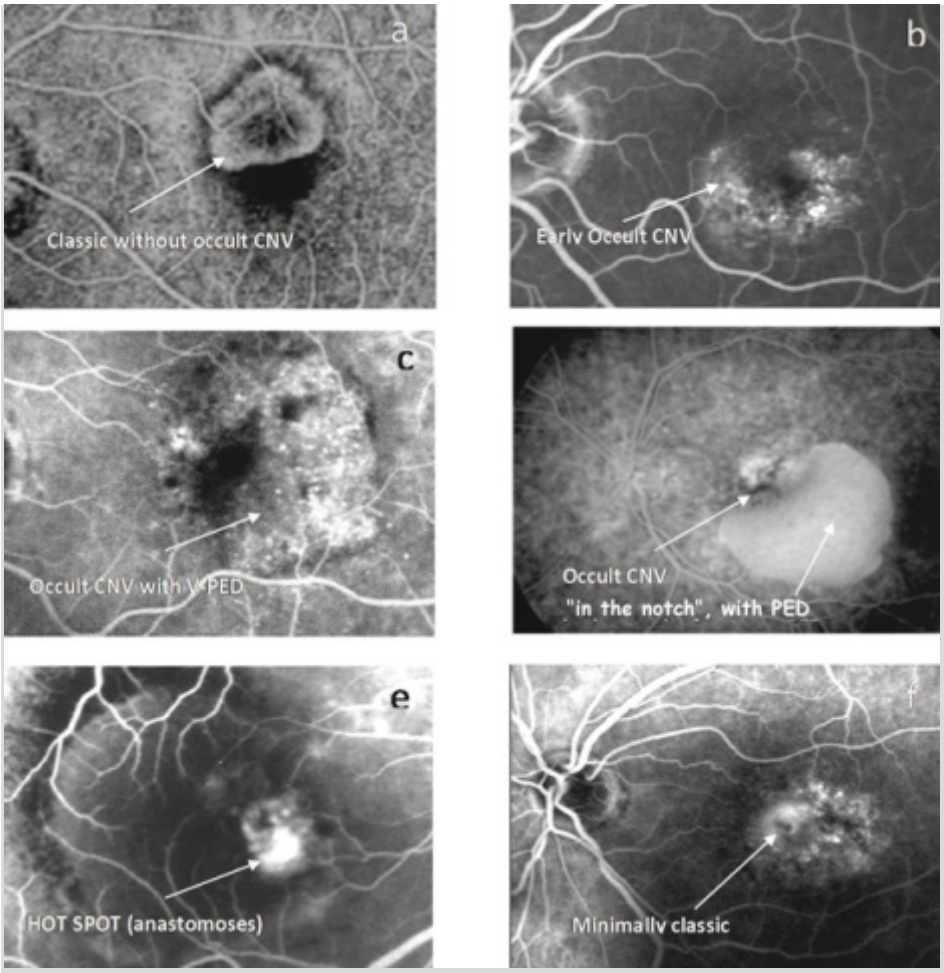

Figure 13: Principal types of choroidal neovascularization – main types of choroidal new vessels on fluorescein angiography. (a) Preepithelial or visible or "classical" neovascularization. **(b)** Occult or subepithelial neovascularization: tiny lesion. **(c)** Occult or subepithelial neovascularization: extensive lesion associated with a PED. **(d)** Occult or subepithelial neovascularization: in the notch of a sero-bullous PED. **(e)** Hot spot in a serous PED: choroidal-retinal anastomosis. **(f)** Mixed neovascularization with a small bouquet of visible vessels within a wide occult lesion *(minimally classic).*

5.2 Clinical and biomicroscopic signs

A 78-year-old woman presented with gradual loss of vision and metamorphopsia, mainly in the right eye, for several months prior to examination.

- BCVA- RE: 20/63
- BCVA- LE: 20/40

Biomicroscopic examination revealed several small and medium-sized drusen in the posterior pole, associated with sub-retinal fluid (SRF) accumulation in the foveal area. The entire macular lesion appeared to measure about two Disc Diameters (DD).

5.3 Traditional multimodal imaging

Autofluorescence (figure 14)

Images show the presence of a circular foveal lesion located over the xanthophyll pigment with an irregular mottled halo that is hypo- and hyper-fluorescent.

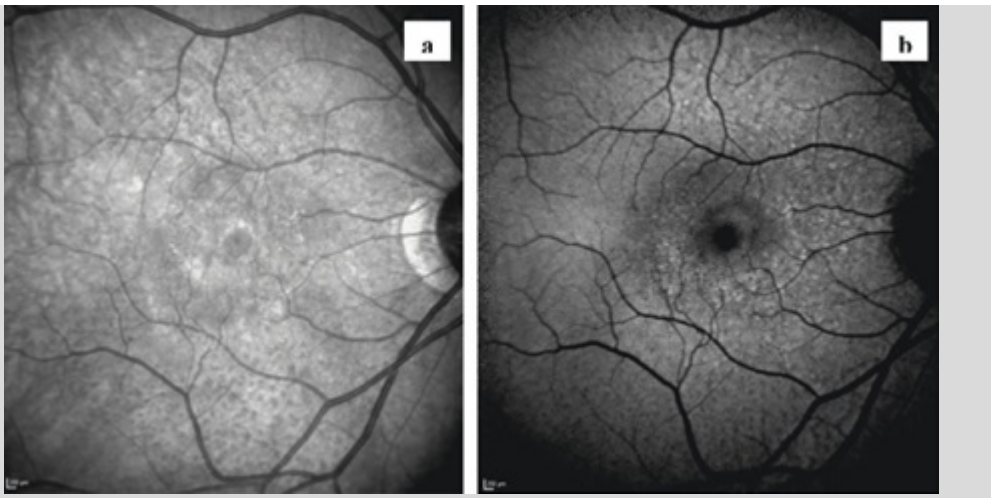

Figure 14 (a): **Infrared.** Large macular lesion of about 2 DD with numerous drusen in the posterior pole. **(b) Autofluorescence.** Circular foveal lesion with an irregular halo of hypo- and hyper-fluorescence.

Fluorescein angiography, FA **(figure 15)**

Fluorescein angiography in the arterio-venous phase shows a well-demarcated, hyper-fluorescent foveal lesion with well-defined irregular borders and a fine hypo-fluorescent halo (Type I CNV).

The lesion is partially circumscribed, mainly in the inferior-temporal area, by an irregular hyper-fluorescent area, probably resembling a wide fibrovascular pigment epithelium detachment (PED). The late phase of FA shows marked hyper-fluorescence of this zone, associated with intense fluorescein leakage.

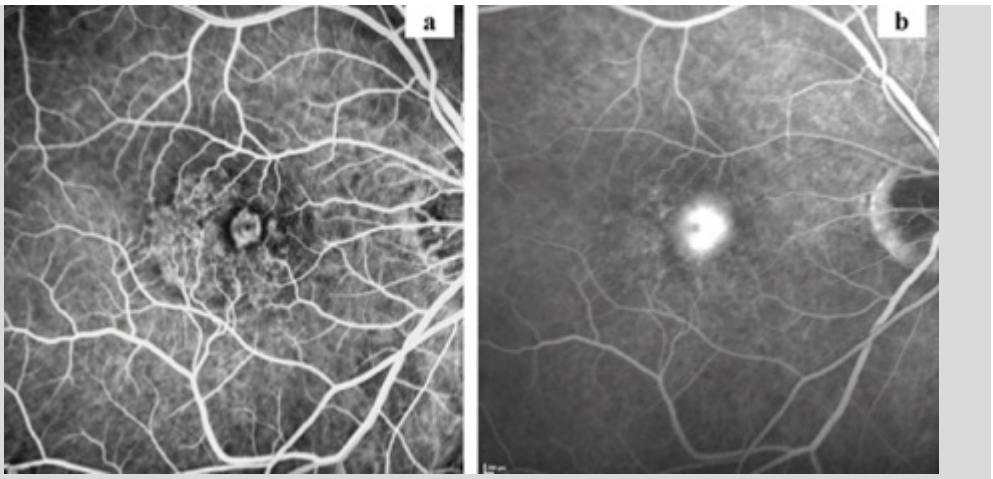

Figure 15 (a): Fluorescein angiography (arterio-venous phase). Well-demarcated early lesion in the centre (Type II *classic),* associated with a intense hypo-fluorescent halo. This lesion is circumscribed by an extensive hyper-fluorescent lesion, with mottled hyper-fluorescence and a well-defined irregular borders (Type I *subepithelial*). **(b) Fluorescein angiography (late phase).** Marked hyper-fluorescent, intense fluorescein leakage of the central

lesion (Type II component), associated with limited hyper-fluorescence of the surrounding neovascular network within the border of the dark PED (Type I component, *subepithelial/occult* CNV).

Indocyanine Green Angiography, ICGA **(figure 16)**

The small area of Type II (preepithelial / classic) choroidal neovascularization (CNV) was rapidly stained and surrounded by a dark border, with rapid wash-out in the later phase.

A wide Type I (*subepithelial / occult*) CNV was observed from the early arterio-venous phase, forming a poorly defined hyper fluorescent neovascular network within the dark PED and partially surrounding the Type II component. In the very late phase (inversion phase), a large neovascular plaque is seen almost involving the entire macular area.

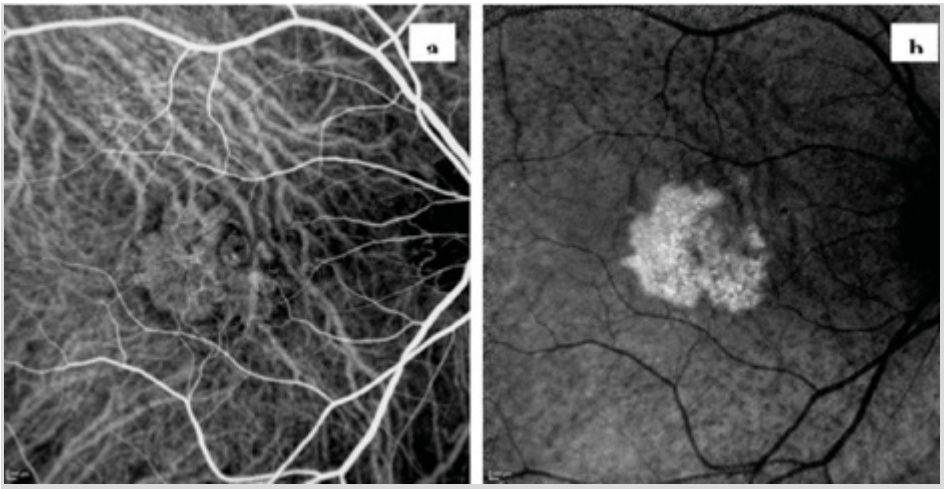

Figure 16 (a): **ICGA (arterio-venous phase).** The small Type II (*preepithelial / classic*) CNV is rapidly stained and surrounded by a dark halo, separated from the large CNV network of Type I CNV. **(b) ICGA (late phase).** In the inversion phase, a large neovascular plaque is visible almost involving the entire macular area.

Optical Coherence Tomography, SD-OCT **(figure 17)**

The neurosensory retina is thickened with sub-retinal fluid accumulation (subfoveal hypo-reflective space) and partial impairment of the foveal depression.

A flat, irregular PED extends temporally to the fovea and allows a clear visualization of the Bruch's membrane.

A tiny subretinal hyper-reflective lesion with a well-defined, dome-shaped appearance is located in the subfoveal area immediately contiguous with the previously described PED.

In particular, it causes disorganization of the outer retinal layers with evident ellipsoid zone swelling and partial disruption of the external limiting membrane. It probably represents the Type II (*preepithelial / classic*) component of an extensive mixed CNV.

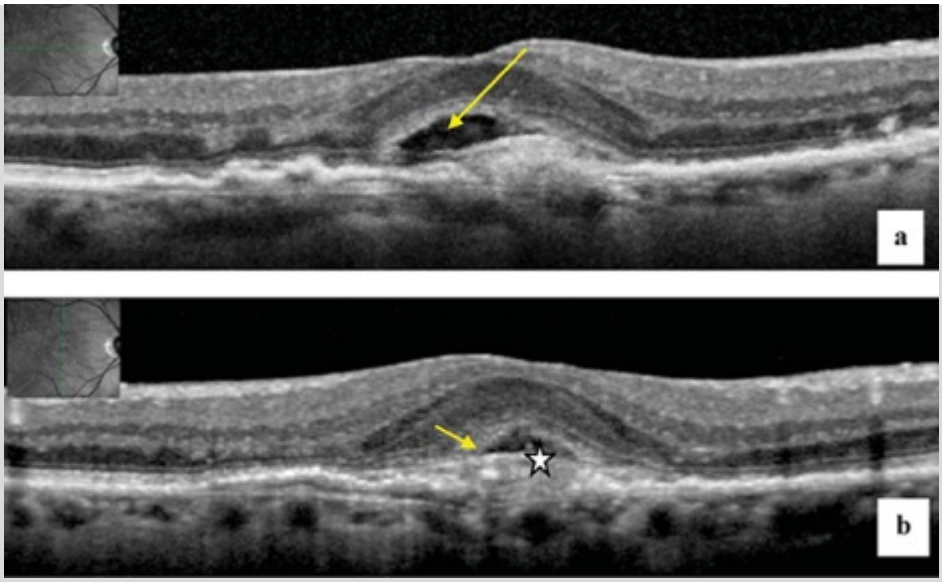

Figure 17: SD-OCT. The neurosensory retina is thickened with subretinal fluid accumulation (subfoveal hypo-reflective space*, arrow*) and partial impairment of the foveal depression. A flat, irregular PED extends temporally to the fovea and allows a clear visualization of the Bruch's membrane *(small arrow*). A tiny sub-retinal hyper-reflective lesion is located in the subfoveal area with a well-defined, dome-shaped appearance, probably representing a Type II (*preepithelial / classic*) component (marked by the *star*) of an extensive mixed CNV. A clear disorganization of the outer retinal layers is seen, with swelling of the EZ and partial disruption of the ELM.

Suggested multimodal imaging diagnosis:

Extensive mixed Type I-II neovascular lesion composed by a wide Type I (occult) CNV, associated with a small area of Type II (classic) neovascularization (minimally classic).

5.4 OCT-Angiography

One "well-selected" single C-scan section will show, in many cases, a very striking and suggestive image of the CNV network (**figure 18**).

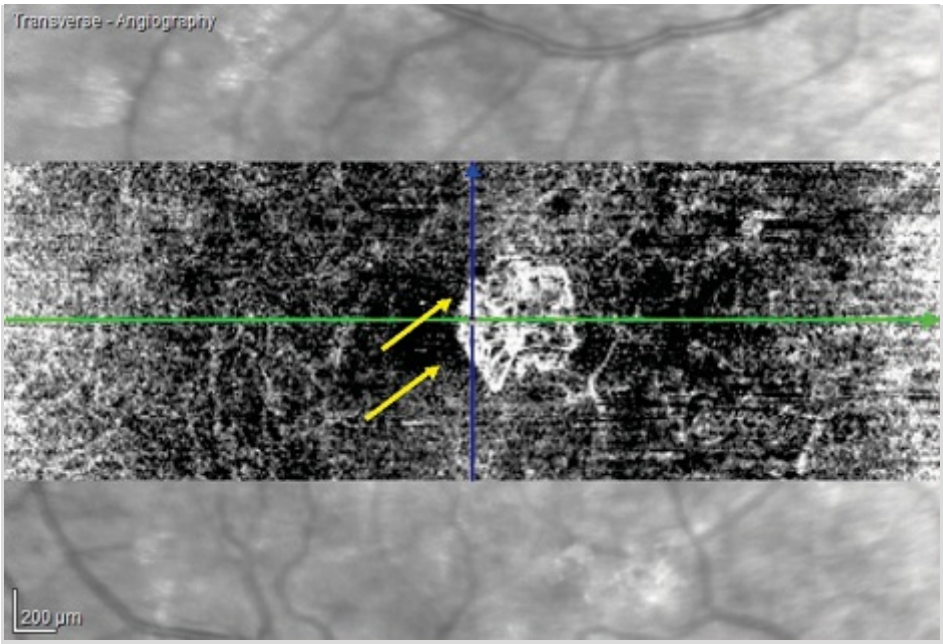

Figure 18: Detection and presence of a typical CNV network. Well circumscribed, "lacy-wheel"-shaped lesion, with a well-demarcated, hyper-intense signal. The network is organized with numerous finely anastamosed branches that are located inside the lesion at this level. No other clear hyper-intense structures appear at this level in the OCT-angiogram.

This will be due to the very dense and intense signal related to the active flow in the neovascularized lesion and will contrast with the surrounding tissue, immediately above the RPE, which has no significant decorrelation signal or vessels.

Nevertheless, additional information is needed. This must be achieved by obtaining multiple C-scan sections **at successive levels**.

Each C-scan must be associated with the *corresponding B-scan* (both in Standard-mode and Angio-mode) to be able to accurately localize the lesion in relation to the RPE and to the Bruch's membrane.

OCT angiogram imaging technique

The OCT angiogram is initially obtained from a volume scan of 151 B-scans in Angio-mode. A simultaneous acquisition of a standard OCT B-scan is also possible (**figure 19).**

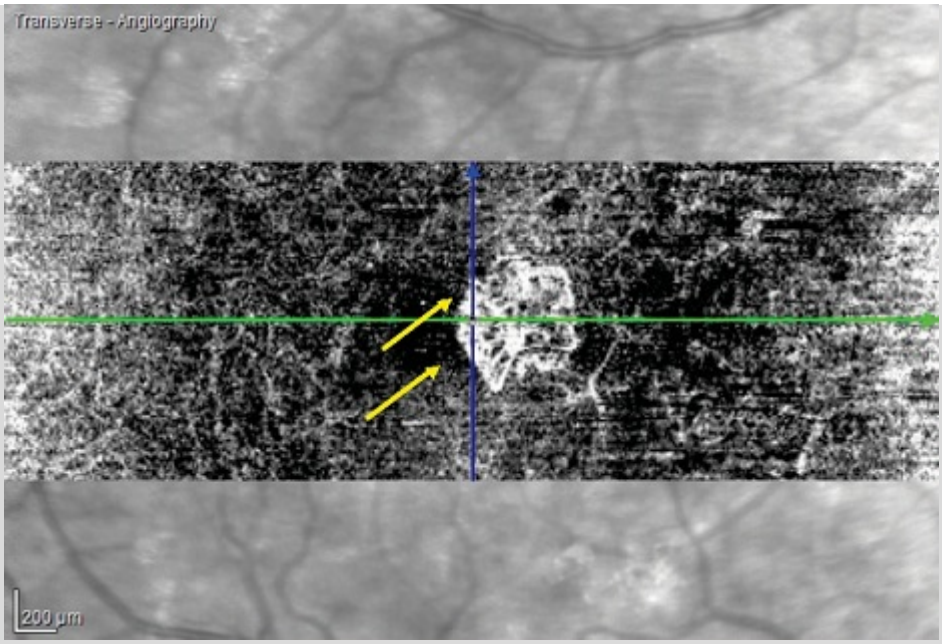

Figure 19: (a) OCT-Angio-mode C-scan (30 µm above the RPE). Well circumscribed, “lacy-wheel”-shaped lesion with a clear hyper-intense signal. There are numerous finely anastomosed vessels inside the lesion at this level, with a well-defined and well-delimited peripheral arcade. No other clear hyper-intense structures appear at this level in the OCT-angiogram: *Type II lesion* (*arrow*). **(b) OCT-Angio-mode B-scan.** An evident decorrelation signal is visible with multiple microdots in the retina (superficial and deep retinal capillary plexus). White signals from the choroidal vasculature (choriocapillaris and from Sattler and Haller layers. Moreover, a pathologic hyper-intense signal is also present in the lesion area *(yellow star)*, immediately above the RPE: *Type II lesion.* **(c) Conventional OCT B-scan (30 µm above the RPE).** Same pattern as evident from the corresponding Angio-mode B-scan (figure **b**). Moreover, conventional OCT is useful to identify the exact location (*yellow star*) of the lesion (above the RPE) and the presence of subretinal fluid accumulation (*small arrow*).

Two red lines indicating the thickness of the section (usually manually selected as 30 µm) will appear on both the conventional and Angio-mode B-scans. These lines are initially aligned on the Bruch’s membrane profile. **The level of the section** is indicated by these lines and could be manually shifted upward or downward to successively explore the entire thickness of the lesion from the preepithelial space to the subepithelial and towards the choroid (a*utomated segmentation* is also possible to allow rapid detection of the lesion).

The C-scan is obtained from the entire volume of B-scans and evaluated with multiple 30-µm-thickness images, starting 30 µm above the RPE to the choroidal-scleral interface. The 30-µm-step outer retinal / choroidal analysis allows the complete imaging of the entire lesion by highlighting different decorrelation signals, but only if they belong to coplanar structures.

Clinical case

On the C-scan obtained at 30 µm above the RPE, a well circumscribed, “lacy-wheel”-shaped lesion with a clear hyper-intense signal is immediately evident, with finely anastomosed vessels inside the lesion at this level: *Type II, classic lesion*.

No other clear hyper-intense structures appear at this section level in the OCT-angiogram **(figure 19)**.

The next C-scan section is placed **at the back surface of the RPE** and therefore, where the PED is present, in between the RPE and the Bruch's membrane **(figure 20)**.

At this level the Type II lesion is still visible, but less contrasted, while *another lesion* becomes evident*: a "U" shaped vessel* **(Figure 20, yellow arrow)**, probably draining or feeding and arriving from a deeper level to reach the preepithelial component of the CNV.

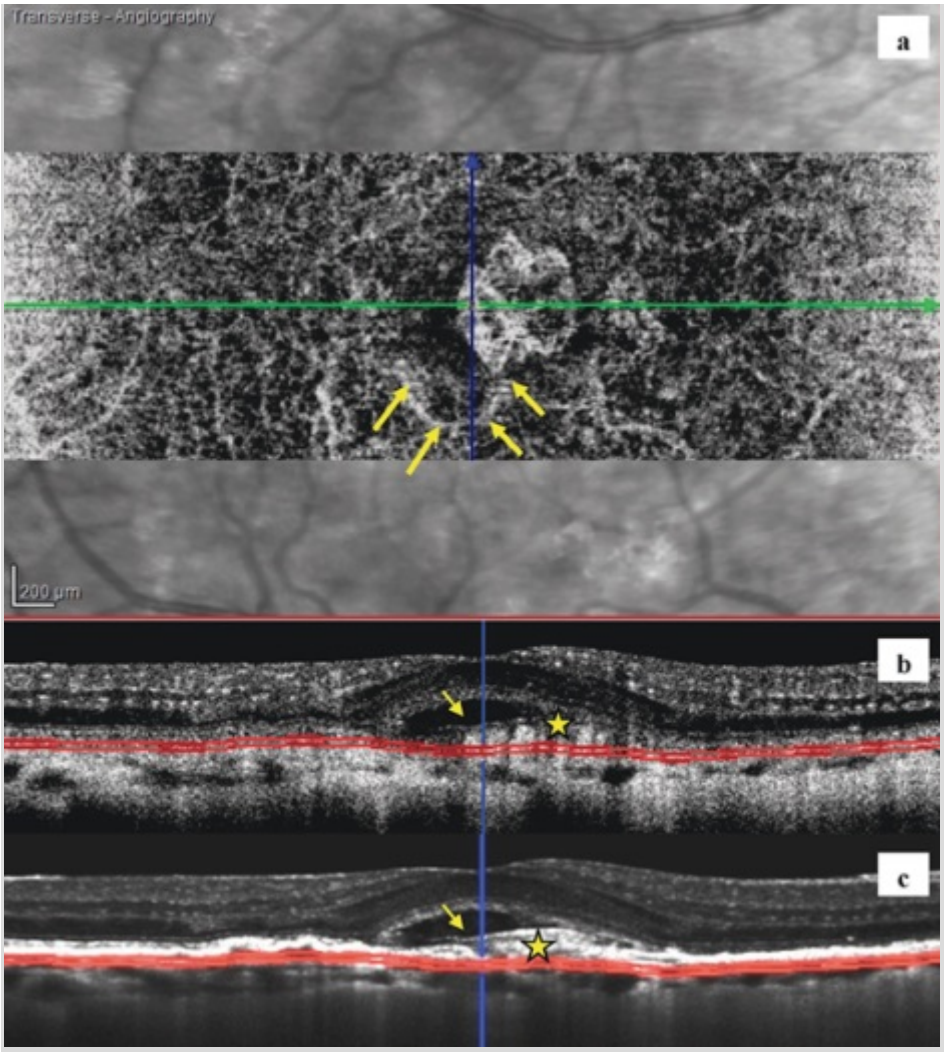

Figure 20: (a) OCT-A C-scan (back surface of the RPE). The 30-µm C-scan section is positioned at the back surface of the RPE (see **(b)** and **(c)**) and, where a PED is present, in between the RPE and the Bruch's membrane. Here, only a slight shadow of the Type II lesion is seen, while a "*U"-shaped draining / feeding vessel* is evident, coming from a deeper level and reaching the preepithelial component of the CNV *(multiple yellow arrows)*. **(b) OCT-A B-scan (back surface of the RPE).** The OCT B-scan (both in Angio-mode and in conventional mode) shows the position of the previous C-scan; in this case at the back surface of the RPE and clearly below the Type II CNV lesion. **(c) Conventional OCT B-scan.** Same pattern like before, the scan is useful to identify the exact location of the lesion *(yellow star)* at the back surface of the RPE and the presence of subretinal fluid accumulation *(small arrow)*.

The following C-scan **(figure 21)**, **deeper inside the CNV (above the BM)**, detects an additional Type I (*subepithelial / occult*) network. The presence of this large neovascular network is highlighted on the C-scan *(yellow dashed line circle*), finely anastomosed and with numerous tiny radiating vessels branching from the centre to the periphery.

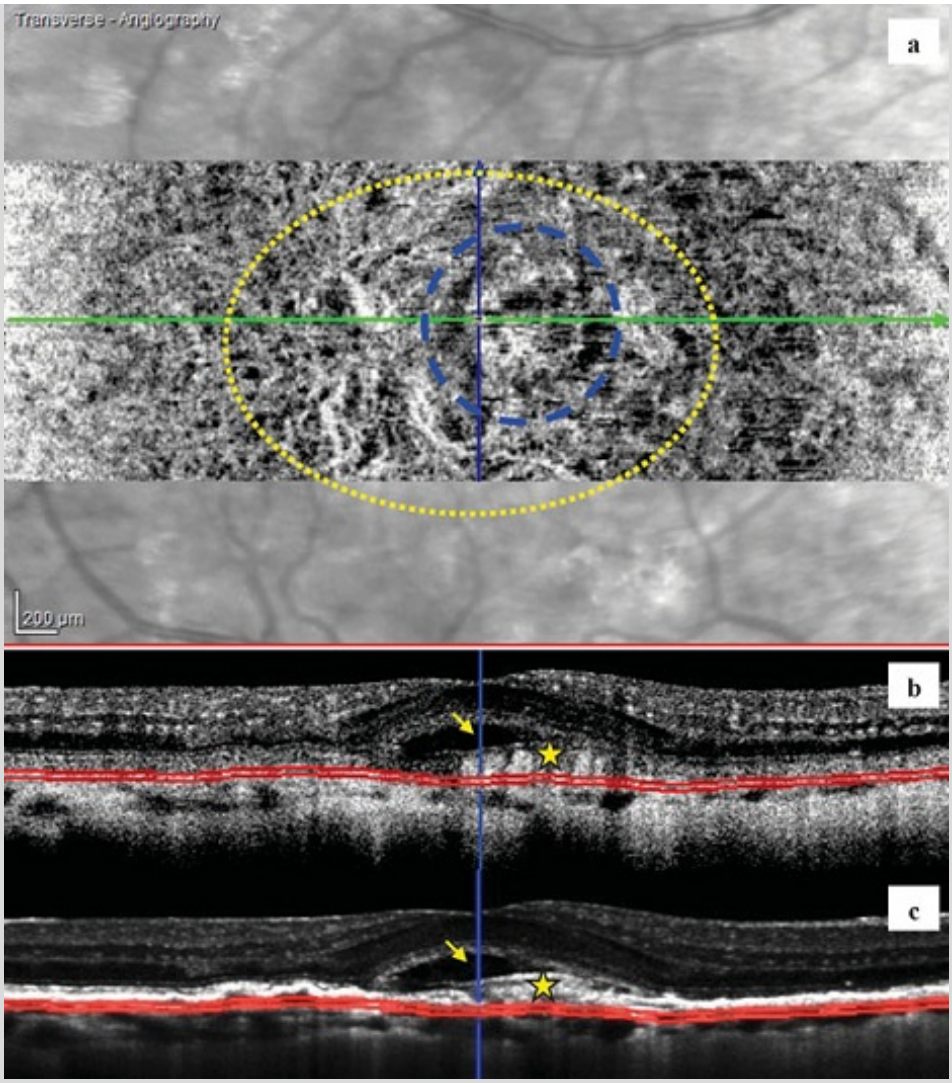

Figure 21: (a) OCT-A C-scan (above the Bruch's membrane). The 30 µm C-scan section is positioned immediately above the Bruch's membrane (see **(b)** and **(c)**) and therefore deeper in the PED. Here, a large neovascular network is evident, finely anastomosed, and with numerous tiny branching vessels radiating from the centre to the periphery *(dashed yellow line)*. **(b) OCT-A B-scan (above the Bruch's membrane).** The OCT B-scan, (both in Angio- and in conventional mode) shows the position of the previous C-scan, in this case deeper inside the flat PED (above the Bruch's membrane). **(c) Conventional OCT B-scan.** Same pattern like before, the scan is useful to identify the exact location of the lesion *(yellow star)* above the Bruch's membrane and the presence of subretinal fluid accumulation *(small arrow)*.

Below the Bruch's membrane (figure 22) and directly inside the choroid, some large choroidal vessels are visible. We also see a diffuse hyper-intense signal (*yellow ring*), probably due to the remnants of the choriocapillaris and the Sattler's layer.

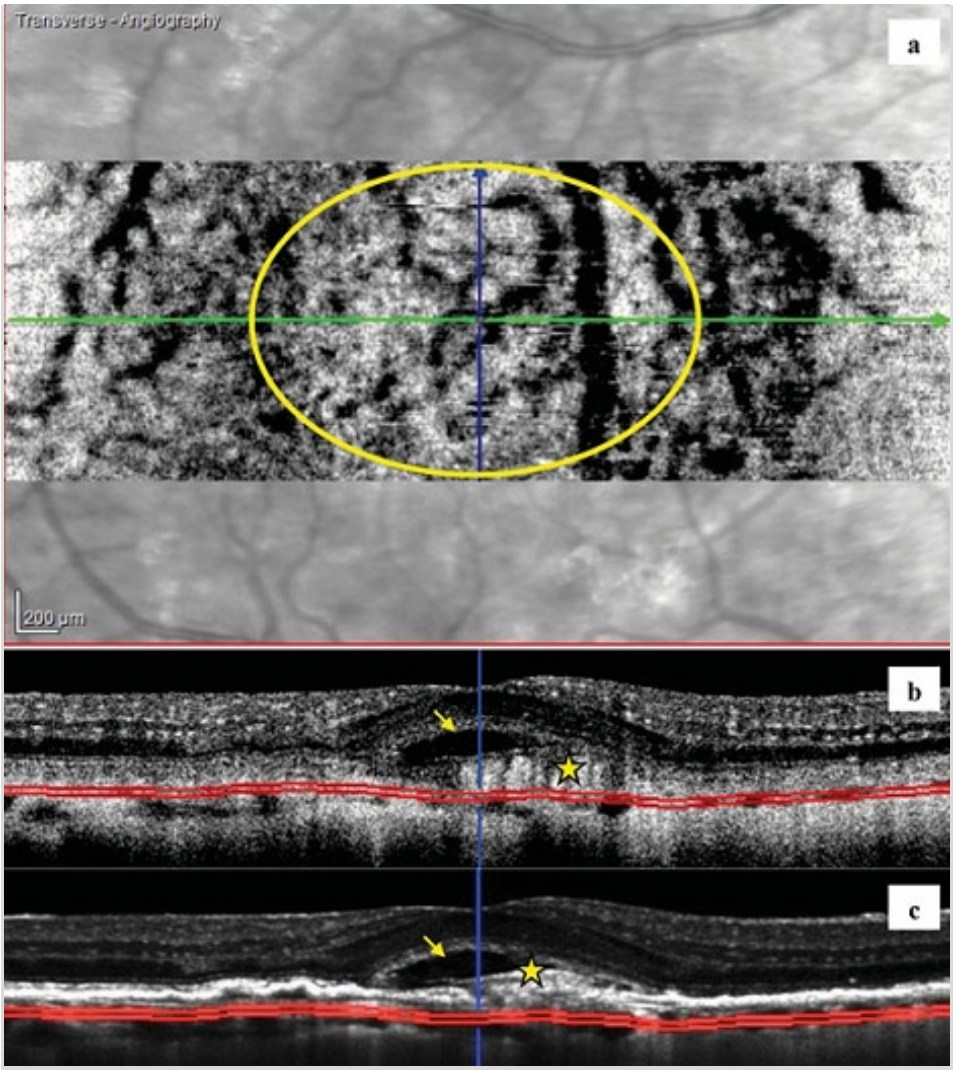

Figure 22: (a) OCT-A C-scan (below the Bruch's membrane). The 30 µm C-scan section is positioned below the Bruch's membrane (see **(b)** and **(c)**) and therefore deep in the substantially thinned choroid, as usual in the case of AMD. Some large choroidal vessels are visible. A diffuse hyper-intense signal is also seen, probably due to remnants of the choriocapillaris and the Sattler's layer. A hypo-intense tubular structure is present. This could be due to the presence of a highly hyper-intense signal from the structures above (i.e. choriocapillaris), which can hide the decorrelation signal coming from the large choroidal vessels layer. **(b) OCT-A B-scan (above the Bruch's membrane).** The OCT B-scan, (both in Angio- and in conventional mode) shows the position of the previous C-scan, in this case deep inside the choroidal tissue (below the Bruch's membrane). **(c) Conventional OCT B-scan.** Same pattern like before, the scan is useful to identify the exact location of the lesion *(yellow star)* above the Bruch's membrane and the presence of subretinal fluid accumulation *(small arrow)*.

Suggested OCT-A diagnosis:

Moderately large Type I (occult) CNV, complicated by a small juxtafoveal and subfoveal zone of Type II (classic) CNV.

The "lacy-wheel"-shape of both Type I and Type II CNV, with finely branching pattern, richly anastomosed and with a well-defined peripheral arcade suggests the diagnosis of an active lesion.

5.4 Synthesis

The compliation of the different results is shown in **figure 23.**

Fluorescein angiography shows a well demarcated hyper fluorescent foveal lesion (*yellow arrow*). The lesion is partially circumscribed in the inferior-temporal area by a hyper-fluorescent area (fibrovascular PED) (*dashed line).*

ICGA shows a wide Type I (subepithelial / occult) CNV, forming a poorly defined hyper-fluorescent neovascular network *(dashed green line)*, partially surrounding the Type II component (*dashed yellow line*).

OCT-A shows a **"lacy-wheel"-shaped lesion** with a clear hyper-intense signal (*yellow arrow)* and finely anastomosed vessels inside the lesion. No other CNV signal is seen at this level.

At a deeper level, OCT-A shows a large neovascular network on the C-scan (*dashed yellow line*), finely anastomosed, and with numerous **tiny radiating vessels** (*yellow circle*) branching from the centre to the periphery.

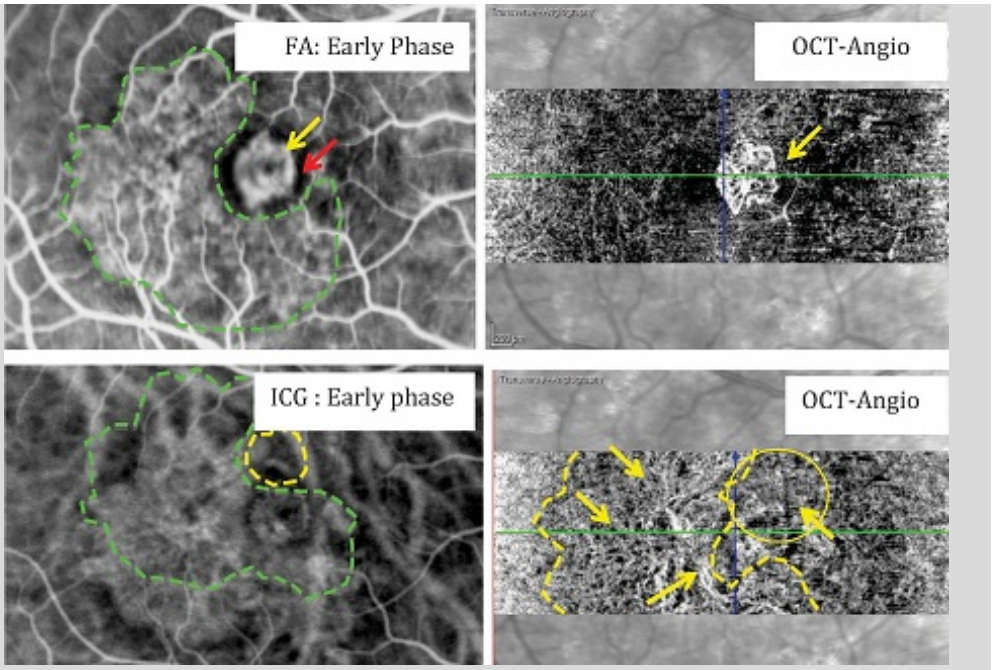

Figure 23: The FA and the ICGA (left) and the OCT-Angiography (right) clearly show a **CNV mixed Type I + Type II (minimally classic)**.

This is a "mixed lesion", with a preepithelial (classic or Type II) neovascular network in the centre and a peripheral subepithelial (occult or Type I) neovascular network with connective vessels.

Both are active, suggesting an indication for (re-)treatment.

6 CLINICAL CASE NO. 2: ACTIVE TYPE I CNV (SUBEPITHELIAL OR OCCULT) – RECURRENT

6.1 Clinical and biomicroscopic signs

An 82-year-old man presented with declining visual acuity and metamorphopsia in the right eye.

Previous diagnosis of exudative AMD, treated by multiple anti-VEGF intravitreous injections on a PRN scheme after the loading phase during the last 24 months.

- BCVA- RE: 20/63
- BCVA- LE: 20/25

Biomicroscopic examination revealed an extensive macular lesion of about two Disc Diameters (DD). There are also several hard drusen appreciable, mainly in the macular area. No haemorrhage, no lipids.

6.2 Traditional multimodal imaging

Autofluorescence (figure 24)

The image shows the presence of a large irregular hypo-fluorescent lesion in the macular area, surrounded by an intense hyper-fluorescent halo. This halo, associated to hypo-fluorescent dots, seems to extend nasally and superiorly with an irregular shape.

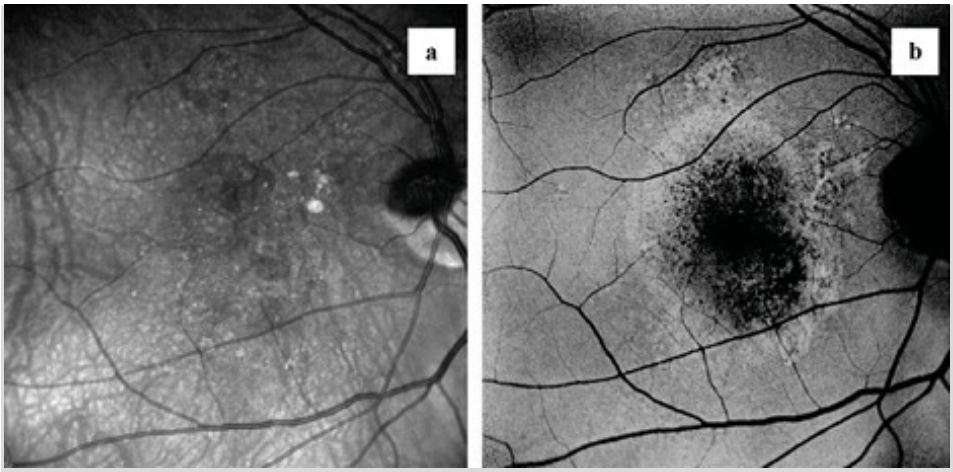

Figure 24: (a) Infrared. Extensive macular lesion of about 2/3 Disc Diameters

(DD). There are also several hard drusen, appreciable mainly in the macular area. **(b) Autofluorescence.** Large irregular hypo-fluorescent lesion in the macular area, surrounded by an intense hyper-fluorescent halo. This halo, associated with hypo-fluorescent dots, seems to extend nasally and superiorly with an irregular shape.

Fluorescein angiography, FA **(figure 25)**

Fluorescein angiography in early arterial-venous phase shows an irregular hyper-fluorescence with pinpoints in the macular area and with poorly defined irregular borders.

The late phase of FA highlights a well-defined hyper-fluorescent area due to staining phenomena mainly in the centre of the CNV and a moderate fluorescein leakage at the border of the lesion.

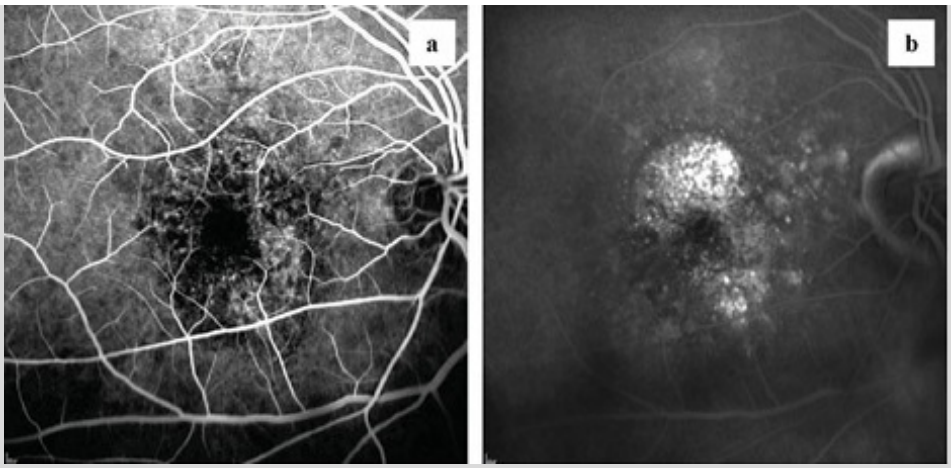

Figure 25: (a) Fluorescein angiography (arterial-venous phase). In the early arterial-venous phase, an irregular hyper-fluorescence is evident with pinpoints in the macular area, and with poorly defined irregular borders. **(b) Fluorescein angiography (late phase).** Well-defined hyper fluorescent area due to staining phenomena mainly in the centre of the CNV lesion and some fluorescein leakage at the border of the lesion.

Indocyanine Green Angiography, ICGA **(figure 26)**

A large Type I (subepithelial / occult) CNV is visible since the early arterial-venous phase, forming a well-defined neovascular network within the PED. There are several definite, well-defined vessels radiating from the periphery towards the nasal centre of the lesion. The drainage of the lesion seems to have a clear prevalence towards the nasal and inferior part of the lesion.

In the late venous phase, the borders of the neovascular lesion are less defined with hypo-fluorescent areas suggesting RPE impairment.

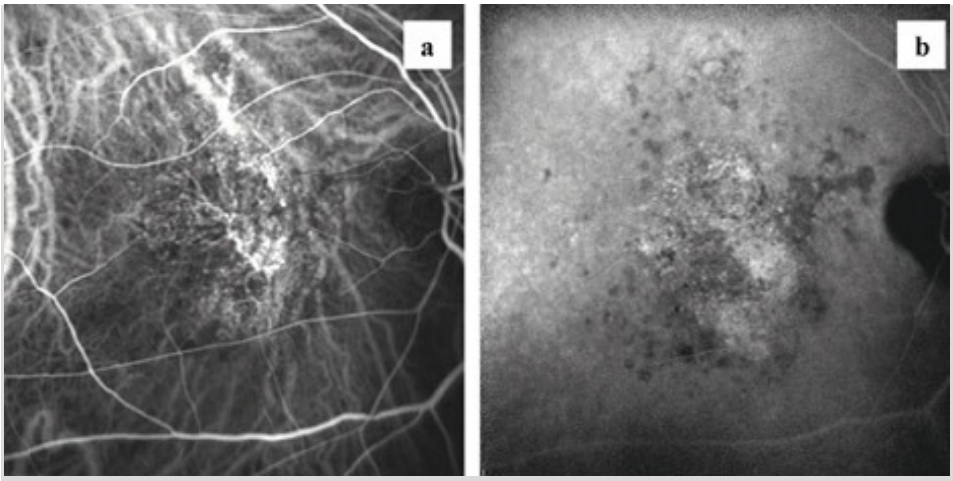

Figure 26: (a) ICG angiography (arterial-venous phase). A large Type I (subepithelial / occult) CNV is visible since the early arterial-venous phase, forming a well-defined neovascular network within the PED. There are several definite, well-defined vessels radiating from the periphery towards the nasal centre of the lesion. The drainage of the lesion seems to have a clear prevalence from the superior and the inferior quadrant of the macula. **(b) ICG angiography (late venous phase).** In the late venous phase, the borders of the neovascular lesion are less defined with hypo-fluorescent areas suggesting RPE impairment.

Optical Coherence Tomography, SD-OCT **(figure 27)**

The foveal depression is substantially maintained with limited subretinal fluid accumulation (subfoveal hypo-reflective space). The outer retinal layers, and mainly the outer nuclear layer, are thinned or not detectable in the whole 30° linear scan. There are appreciable interruptions of the external limiting membrane and the swelling of the ellipsoid zone.

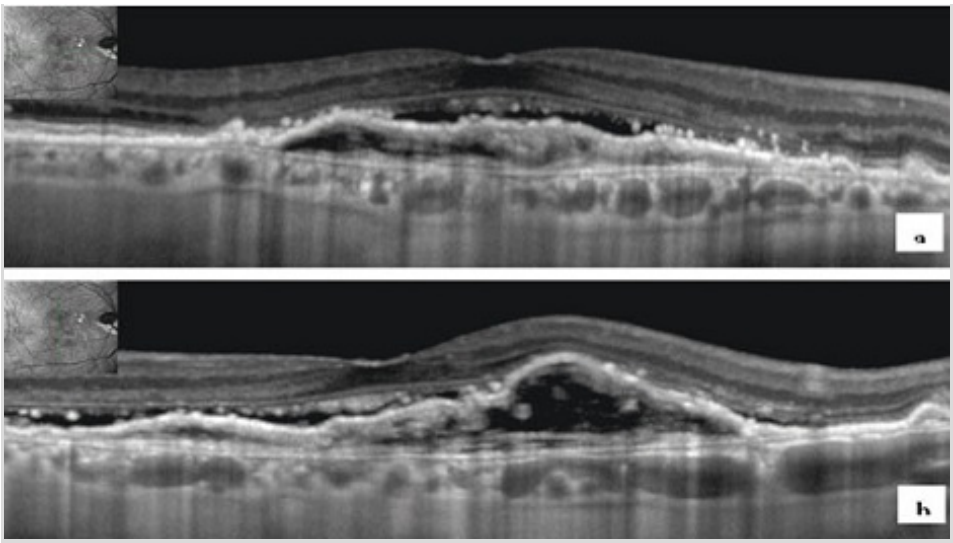

Figure 27: SD-OCT. (a) The foveal depression is substantially maintained with limited subretinal fluid accumulation (subfoveal hypo-reflective space). The outer retinal layers are thinned or not detectable in the whole 30° linear scan. Note the interruption of the ELM and EZ swelling and multiple hyper-reflective dots. **(b)** A large, fibrovascular PED, involving almost the entire macular area, and presenting some hyper-reflective structures and several hypo-reflective spaces, therefore showing a non-homogeneous pattern. A clearly visible Bruch's membrane divides the fibrovascular PED from a thin choroid, which is mainly represented by large choroidal vessels (Haller's layer).

A large, fibrovascular PED is present, involving almost the entire macular area, with some hyper-reflective structures and several hypo-reflective spaces, showing therefore a non-homogeneous pattern and multiple hyper-reflective dots.

A clearly visible Bruch's membrane divides the fibrovascular PED from a thin choroid, which is mainly represented by large choroidal vessels (Haller's layer).

Suggested multimodal imaging diagnosis:

Still active, large, Type I neovascular lesion.

6.3 OCT-Angiography

The OCT angiogram is evaluated with multiple 30-µm-thickness transverse C-scans, starting 30 µm above the RPE to the choroidal-scleral interface. The 30-µm-step outer retinal/choroidal analysis allowed a complete imaging of the entire lesion by highlighting different decorrelation signals, but only if belonging to coplanar structures.

Above the RPE (figure 28)

In the 30-µm-thickness C-scan, just above the RPE, there is no evidence of a clear decorrelation signal that could be attributed to choroidal neovascularization.

Some slightly hyper-intense signals are due to "pseudo-images" of the retinal vessels, caused by the reflectivity of the RPE or by the proximity of some intensely perfused structures (choriocapillaris).

The highly hypo-intense areas are due to subretinal fluid accumulation.

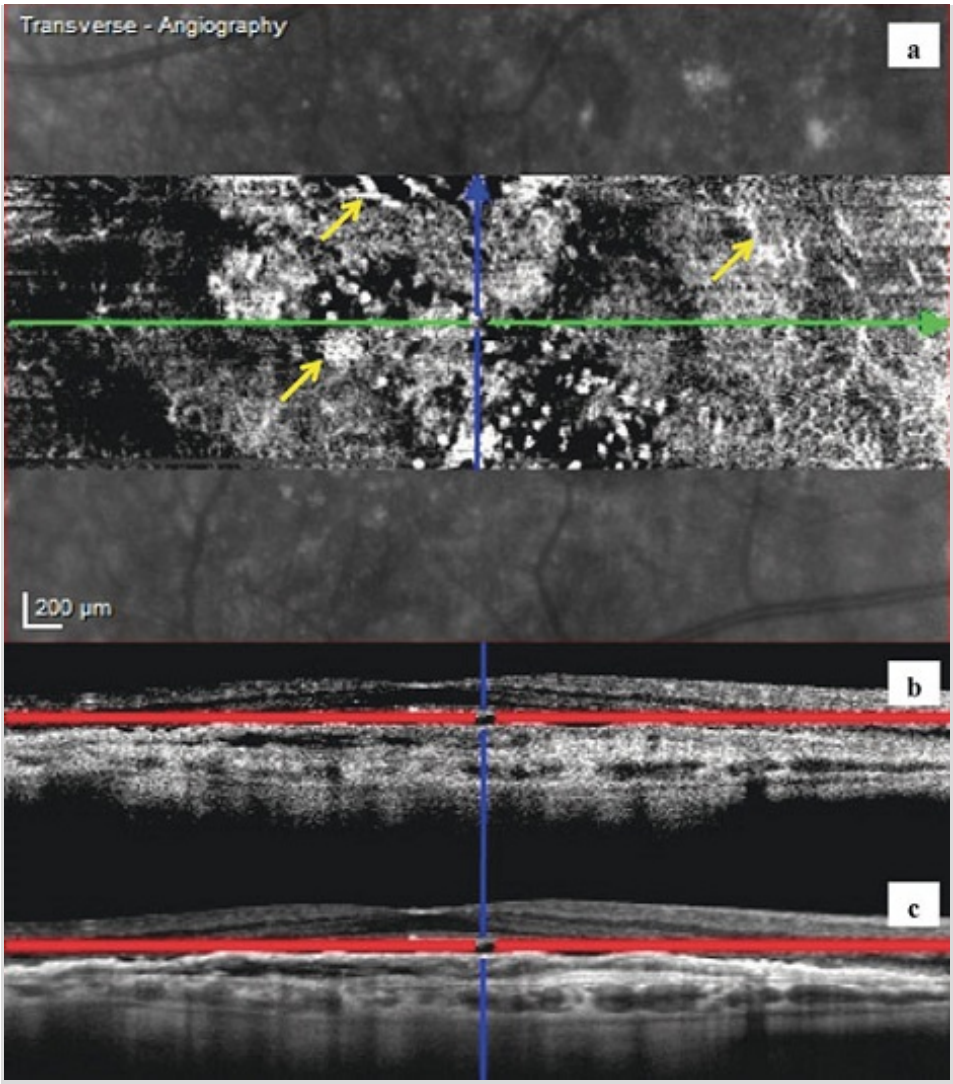

Figure 28: (a) OCT-A C-scan (30 µm above the RPE). No evidence of a clear decorrelation signal that could be attributed to choroidal neovascularization. The highly hypo-intense areas are caused by *subretinal fluid accumulation. So*me slightly hyper-intense signals are due to "pseudo-images" of the retinal vessels (*yellow arrows),* caused by reflection of the RPE or by the proximity of some intensely perfused structures (choriocapillaris). **(b) OCT-Angio B-scan (30 µm above the RPE).** An evident decorrelation signal is appreciable, both from normal retinal and choroidal vasculature. Moreover, a pathologic hyper-intense signal is also present below the scanned area inside the PED (as also evident from the corresponding conventional B-scan). **(c) Conventional OCT B-scan (30 µm above the RPE).** The conventional OCT is useful to identify the exact location of the lesion (above the RPE) and the presence of subretinal fluid accumulation. *The red lines indicate the thickness of the section (selected as 30 µm, aligned on the BM profile).*

At the back surface of RPE (figure 29)

The 30-µm C-scan section is positioned at the back surface of the RPE and therefore inside the PED.

Most of the vessels are large and "mature" vessels with few ramifications, but some branche into smaller ones and origin a localized, fine anastomotic network with numerous tiny vessels, richly anastomosed, and a fine peripheral arcade.

This area is mainly visible at the inferior nasal periphery with an initial visualization of a “sea-fan”-shaped CNV (*yellow dashed line*).

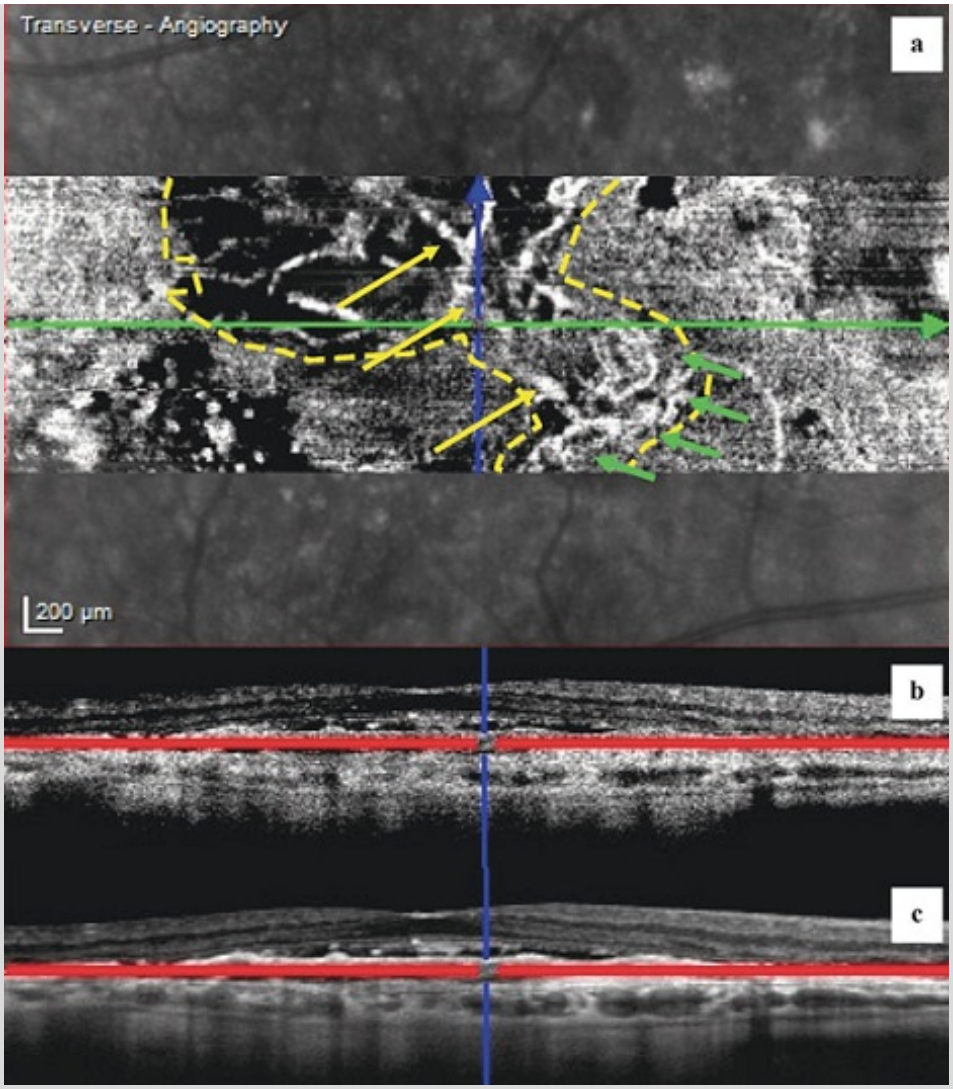

Figure 29: (a) OCT-A C-scan (back surface of the RPE). The 30-µm C-scan section is positioned at the back surface of the RPE (see **(b)** and **(c)**) inside the PED. Most of the vessels are large and “mature“ with few ramifications (*yellow arrows*), but some vassels branche into smaller ones and origin a localized, fine network with numerous tiny vessels, richly anastomosed and a fine peripheral arcade (*green arrows*). This area is mainly visible at the inferior nasal periphery with an initial visualization of a “sea-fan”-shaped CNV (*yellow dashed line*). **(b) OCT-Angio B-scan (back surface of the RPE).** The OCT-Angio B-scan shows the position of the C-scan *(red lines)*, in this case at the back surface of the RPE. (**c) Conventional OCT B-scan (back surface of the RPE).** The conventional OCT B-scan shows the position of the C-scan (*red lines*), in this case at the back surface of the RPE.

Above the Bruch’s membrane (figure 30)

The following 30-µm C-scan deeper inside the PED shows almost the whole extension of the neovascular network (*yellow dashed line*).

This part of the lesion is mainly made by large mature vessels with a “dead-tree” aspect. Some tiny ones form peripheral anastomotic arcades (*green arrow*). This pattern could be an index of a very localized activity or a recurrence of this part of the lesion.

The OCT-Angio B-scan shows the position of the C-scan (*red lines*) deeper inside the PED above BM. The conventional OCT B-scan also shows the position of the C-scan (*red lines*), deeper inside the flat PED and the subretinal fluid accumulation.

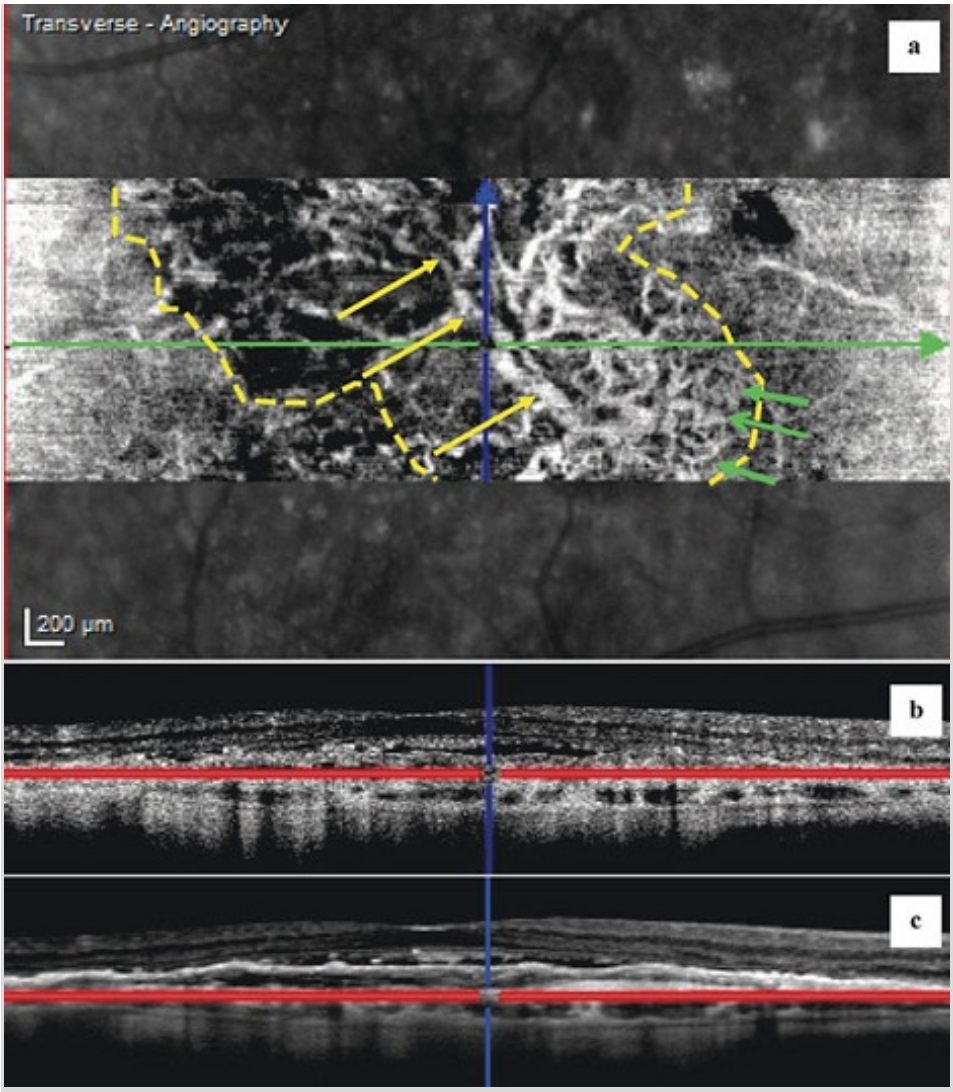

Figure 30: (a) OCT-A C-scan (above the Bruch's membrane). The following 30 µm C-scan deeper inside the PED shows almost the whole extension of the neovascular network (*yellow dashed line*). This part of the lesion is mainly made by large mature vessels with a "dead-tree" aspect. Some tiny ones form loops, anastomoses and peripheral anastomotic arcades (*green arrows*). This could be an index of a very localized activity or a recurrence of this part of the lesion. **(b) OCT-Angio B-scan (above the Bruch's membrane).** The OCT-Angio B-scan shows the position of the C-scan *(red lines)*, in this case deeper inside the PED (above the Bruch's membrane). **(c) Conventional OCT B-scan (above the Bruch's membrane).** The conventional OCT B-scan shows the position of the C-scan (*red lines*), i.e. deeper inside the flat PED (above the BM), and the subretinal fluid accumulation.

Below the Bruch's membrane (Figure 31)

The 30-µm C-scan section is positioned directly inside the choroid with a diffuse hyper-intense signal, probably due to remnants of the choriocapillaris and the Sattler's layer.

Some large choroidal vessels (*green arrows*) are also visible as hypo-intense tubular structure. This could be due to the presence of highly hyper-intense signals from the structures above (i.e. choriocapillaris or CNV) that are able to hide the decorrelation signal coming from the large choroidal vessels layer.

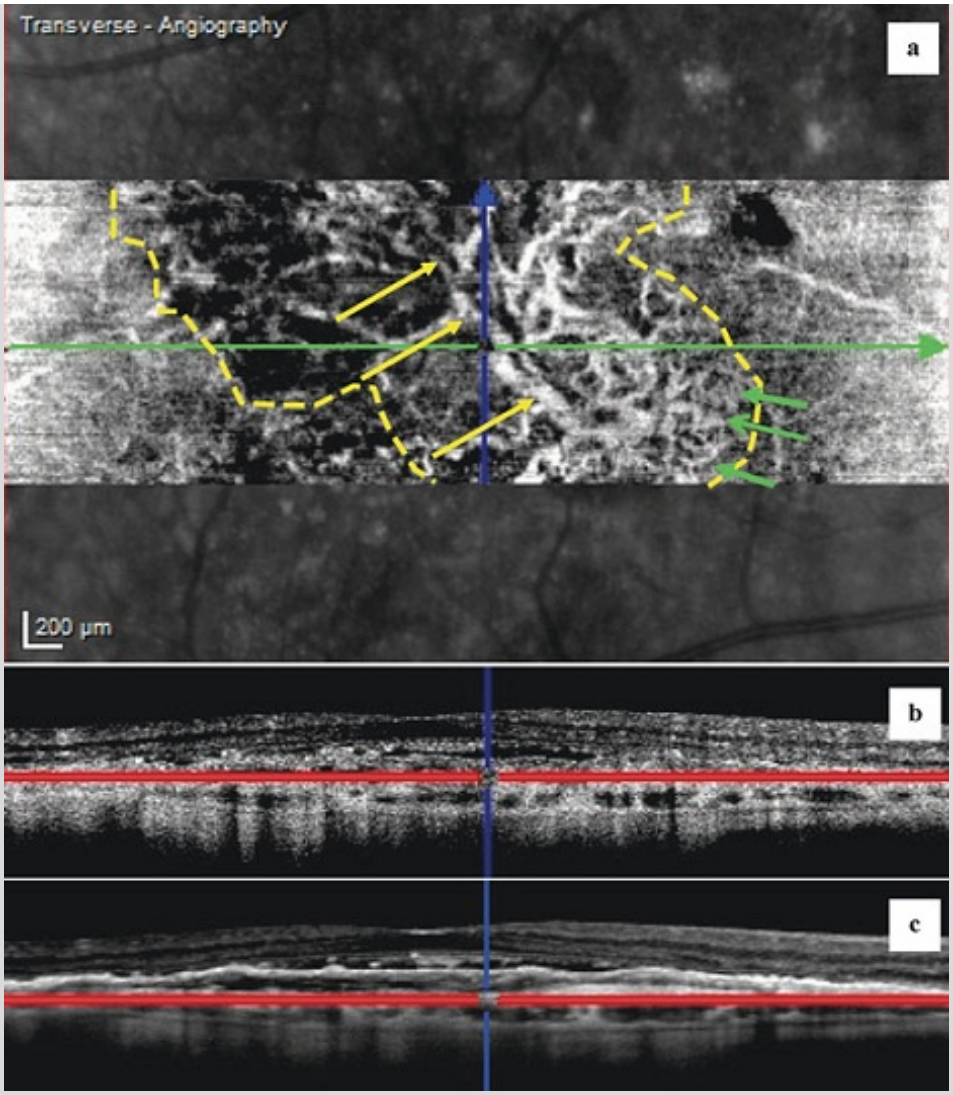

Figure 31: (a) OCT-A C-scan (below the Bruch's membrane). The 30 µm C-scan section is positioned directly inside the choroid with a diffuse hyper-intense signal, probably due to remnants of the choriocapillaris and the Sattler's layer. Some large choroidal vessels (*green arrows*) are also visible as hypo-intense tubular structure. This could be due to the presence of highly hyper-intense signals from the structures above (i.e. choriocapillaris or CNV), that are able to hide the decorrelation signal coming from the large choroidal vessels layer. **(b) OCT-Angio B-scan (below the Bruch's membrane).** The OCT-Angio B-scan shows the position of the C-scan (*red lines*), i.e. deep inside the choroid below the Bruch's membrane. **(c) Conventional OCT B-scan (below the Bruch's membrane).** The conventional OCT B-scan shows the flat PED above the BM, and the subretinal fluid accumulation and position of the C-scan (*red lines*), in this case deep inside the choroid (below the Bruch's Membrane).

Suggested OCT-A diagnosis:

Extensive Type I neovascular lesion, partially stabilized in the upper part, but still at the periphery of lesion.

6.4 Synthesis

The compliation of the different results is shown in **figure 32.**

ICGA shows the presence of:

- **large, mature vessels** radiating towards the centre (*yellow arrow*), within a poorly defined PED
- **small peripheral vessels** (*green arrows*) are appreciable although difficult, on the left and inferior part of the lesion

OCT-A allows a clear visualization of almost the **entire neovascular network**. **In the centre**, large **"mature"** vessels are present that are long and linear with only a few branches (*yellow arrow*).

But at the periphery of the lesion, the OCT-A shows the development of a typical "**sea fan"-shaped CNV** branch with **fine tiny vessels, anastomoses and loops** and a peripheral arcade, mainly in the inferior and nasal part (*green arrows)*.

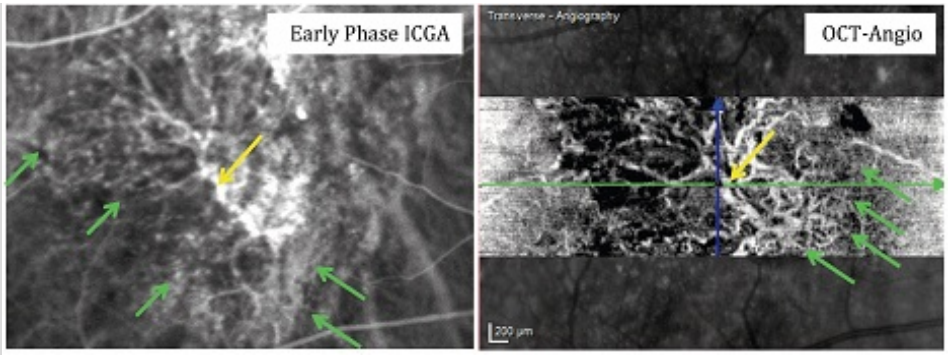

Figure 32: Both the ICGA (left) and the OCT-Angiography (right) clearly pinpoint a subepithelial (occult or Type I) neovascular network.

Both ICGA (left) and OCT-Angiography (right) clearly pinpoint a subepithelial (occult or Type I) neovascular network.

This is a "mixed lesion", with a centre already stabilized and a peripheral part that is again active, suggesting a recurrence and the indication for (re) treatment.

7 CLINICAL CASE NO. 3: ACTIVE TYPE I CNV (SUBEPITHELIAL OR OCCULT) – PERSISTENT

7.1 Clinical and biomicroscopic signs

A 73-year-old woman presented with gradual loss of vision and metamorphopsia in her left eye.

She had been treated with anti-VEGF injections for exudative AMD in both eyes.

- BCVA RE: 20/100
- BCVA LE 20/40

Biomicroscopic examination revealed an extensive macular lesion of about 2 to 3 Disc Diameters (DD). There are also numerous hard drusen were present especially in the macular area.

7.2 Traditional multimodal imaging

Autofluorescence (figure 33)

The image shows the presence of irregular hypo-fluorescent macular lesions surrounded by an intense oval-shaped *hyper-fluorescent halo*, extending beyond the borders of the macular area.

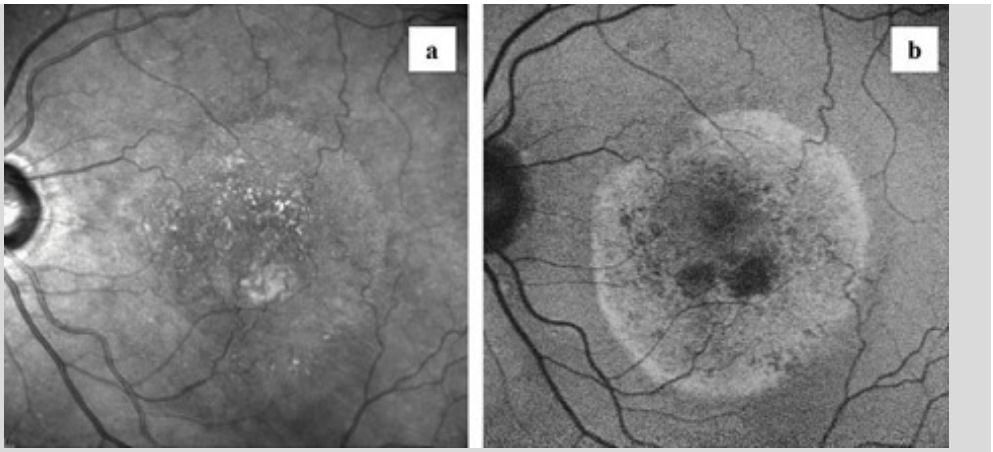

Figure 33: (a) Infrared. Extensive macular lesion of about 2 to 3 Disc Diameters (DD) and several hard drusen. **(b) Autofluorescence.** Presence of irregular hypo-fluorescent macular lesions surrounded by an intense oval-

shaped hyper-fluorescent halo, extending beyond the borders of the macular area.

Fluorescein angiography, FA **(figure 34)**

FA in the early arterio-venous phase shows an irregular hyper-fluorescence with pinpoints in the macular area, and poorly defined irregular borders. Macular lesion is almost surrounded by a slightly hypo-fluorescent halo.

The late phase of FA shows the presence of hyper-fluorescent areas due to the staining phenomena, mainly in the centre of the CNV and a slight fluorescein leakage at the border of the lesion.

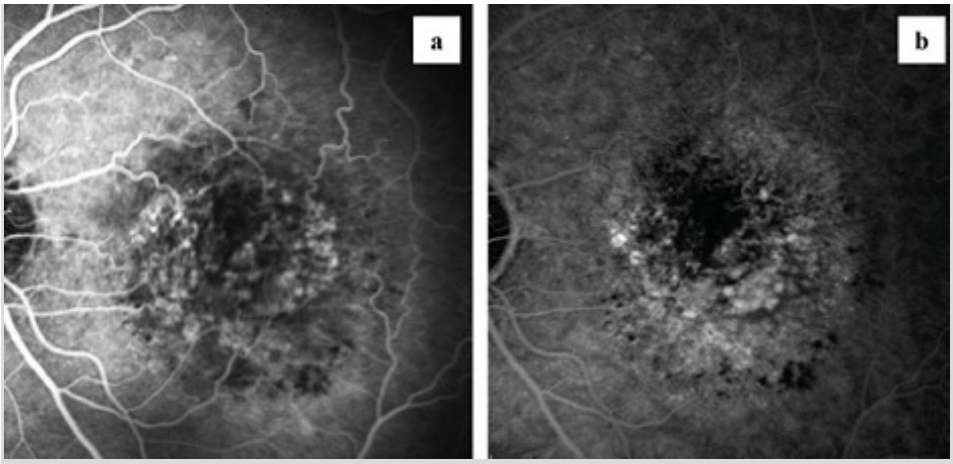

Figure 34: (a) Fluorescein angiography (arterial-venous phase). Irregular hyper-fluorescence with pinpoints in the macular area. The borders are poorly defined and irregular with a hypo-fluorescent halo. **(b) Fluorescein angiography (late phase).** Hyper-fluorescent areas due to the staining phenomena mainly in the centre of the CNV, and a slight fluorescein leakage at the border of the lesion.

Indocyanine Green Angiography, ICGA **(figure 35)**

A large Type I (subepithelial/occult) CNV is observed from the early arterio-venous phase, forming a poorly defined neovascular network within the PED. The drainage of the lesion appears to be prevalent into the infero-temporal quadrant of the choroid.

In the late venous phase, the borders of the neovascular lesion are clearly hyper-fluorescent, showing the entire network. A hypo-fluorescent halo almost surrounds the whole CNV.

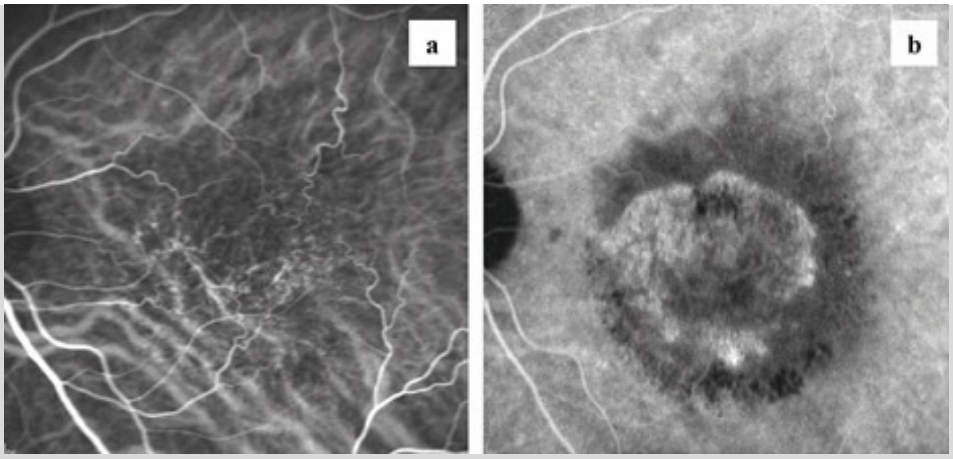

Figure 35: (a) ICG angiography (arterio-venous phase). A large Type I subepithelial / occult) CNV is observed, forming a poorly defined neovascular network within the PED. The drainage of the lesion seems to be prevalent into the inferior-temporal quadrant of the choroid. **(b) ICG angiography (late phase).** The borders of the neovascular lesion are clearly hyper-fluorescent and prevalent inside the entire network; a hypo-fluorescent halo surrounds almost the whole CNV.

Optical Coherence Tomography, SD-OCT **(figure 36)**

The foveal depression is partially maintained, but tiny intra-retinal cystoid spaces are visible, suggesting a persistent exudation. There are interruptions in the external limiting membrane and a swelling of the ellipsoid zone. A large **fibrovascular PED**, almost involving the entire macular area with a heterogeneous pattern (some hyper-reflective structures and several hypo-reflective spaces), has resulted in an upward dislocation of the neurosensory retina and a downward dislocation of the Bruch's membrane; the latter is seen to be detached from the RPE layer.

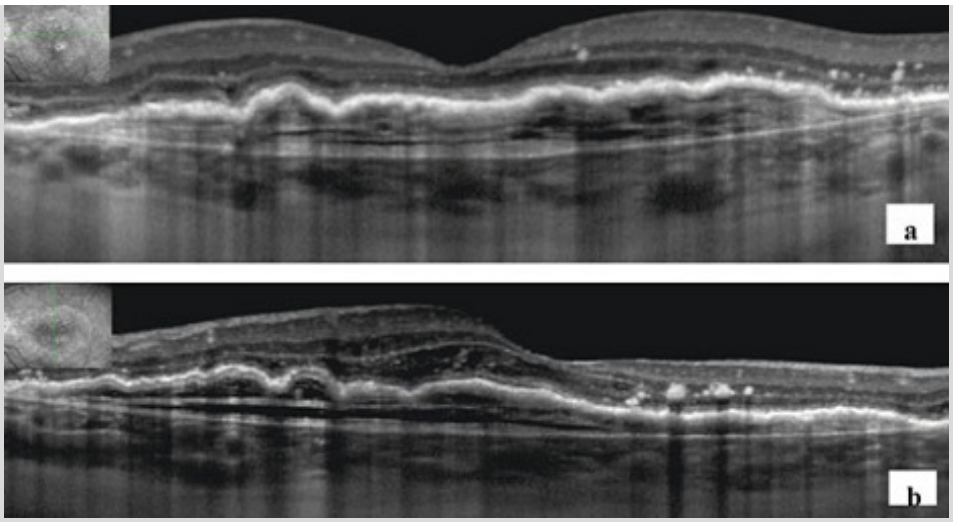

Figure 36: SD-OCT. (a) The foveal depression is partially maintained, but tiny intra-retinal cystoid spaces are visible, suggesting persistent exudation. There are interruptions in the ELM and EZ swelling. **(b)** A large, fibrovascular PED, almost involving the entire macular area, with a heterogeneous pattern (some hyper-reflective structures and several hypo-reflective spaces), has resulted in an upward dislocation of the neurosensory retina and a downward one of the Bruch's membrane; the latter is seen to be detached from the RPE layer.

Suggested multimodal imaging diagnosis:

Still active, large, Type I neovascular lesion.

Indication for prolongation of treatment.

7.3 OCT-Angiography

The OCT angiogram is evaluated with multiple 30-µm-thickness C-scans, shaped on the RPE profile, starting 30 µm above the RPE and ending at the choroidal-scleral interface. The 30-µm-step outer retinal/choroidal analysis allows a complete imaging of the entire lesion by highlighting different decorrelation signals, but only if they belong to coplanar structures.

Just above the RPE (figure 37)

In the 30-µm-thickness C-scan, there is no evidence of a clear decorrelation signal that could be attributed to a choroidal neovascularization.

Some slightly hyper-intense signals are due to “pseudo-images” of the retinal vessels caused by the reflectivity of the RPE or by the proximity of some intensely perfused (choriocapillaris).

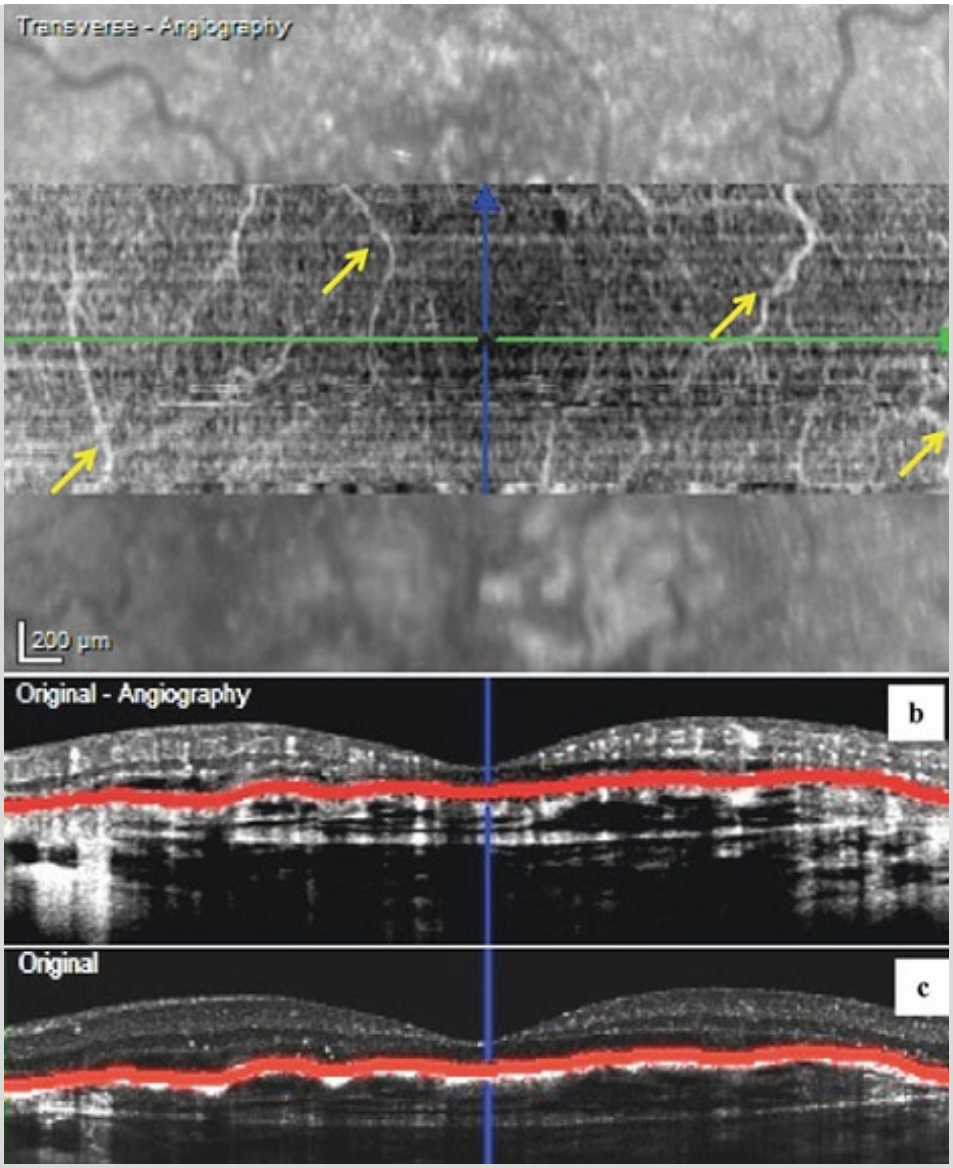

Figure 37: (a) OCT-A C-scan (30 µm above the RPE). No evidence of a clear decorrelation signal that could be attributed to choroidal neovascularization. Some slightly hyper-intense signals are due to "*pseudo-images"* of *retinal vessels* (*yellow arrows)* that are caused by the reflectivity of the RPE or by the proximity of some intensely perfused structures (choriocapillaris). **(b) OCT-Angio B-scan (30 µm above the RPE).** An evident decorrelation signal is appreciable from both retinal and choroidal vasculature. A pathologic hyper-intense signal is also present below the scanned area, in between the RPE and the Bruch's membrane. **(c) Conventional OCT B-scan (30 µm above the RPE).** The conventional OCT is useful to identify the exact location of the C-scan section.

At the back surface of the RPE (figure 38)

The next C-scan section is therefore placed *inside the PED*. Here, a broad neovascular network mainly composed of numerous finely anastomosed, sinuous vessels can be clearly seen.

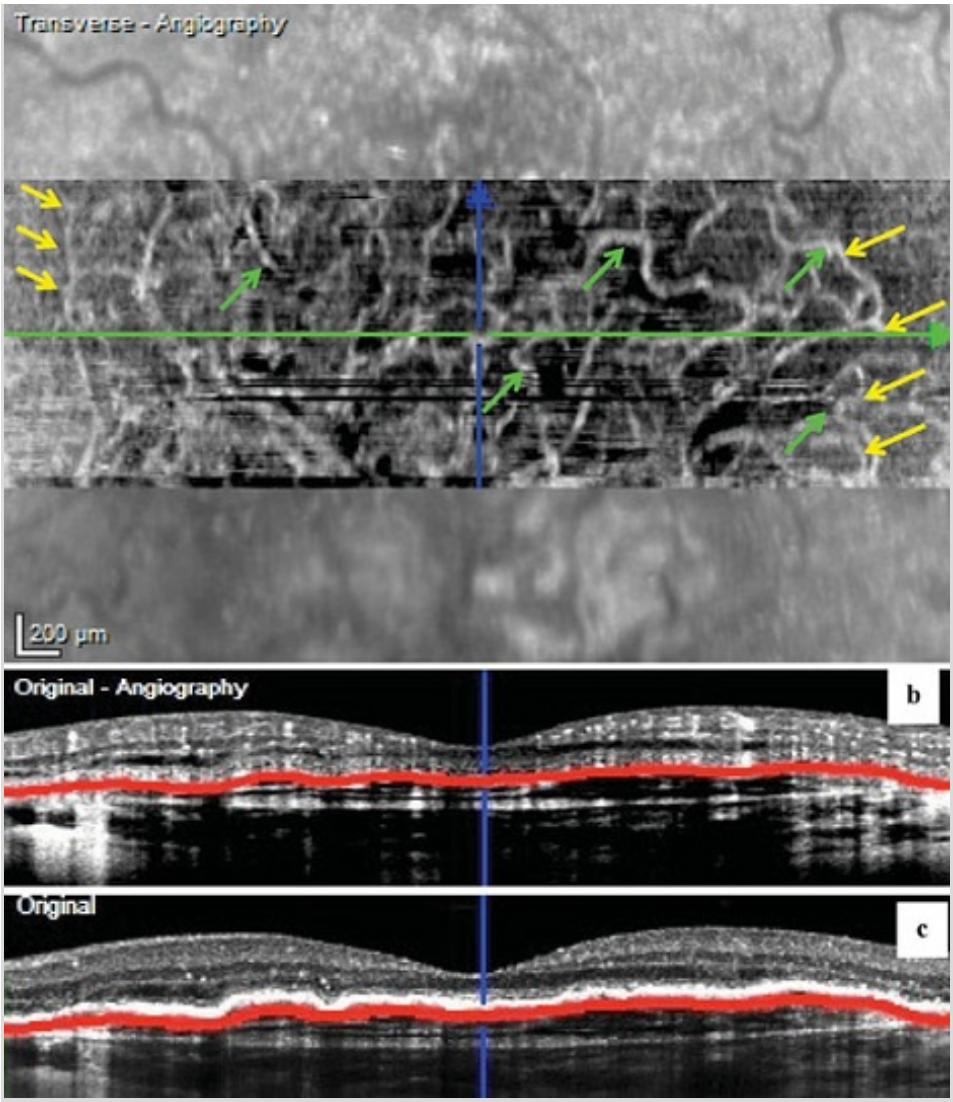

Figure 38: (a) OCT-A C-scan (back surface of the RPE). The 30 µm C-scan section is positioned at the back surface of the RPE and therefore inside the PED. Neovascular network, mainly composed of numerous finely anastomosed sinuous vessels (*green arrows*) with a peripheral arcade (*yellow arrows*) are clearly seen. **(b) OCT-Angio B-scan (back surface of the RPE).** The OCT-Angio B-scan shows the position of the C-scan (*red lines*), in this case at the back surface of the RPE. (**c) Conventional OCT B-scan (back surface of the RPE).** The conventional OCT B-scan shows the position of the C-scan *(red lines)*, in this case at the back surface of the RPE.

Deeper inside the PED (figure 39)

The following C-scan shows a different plane of the lesion, in which some tiny branching vessels forming peripheral arcades can be seen.

This could be an index of activity in this part of the lesion.

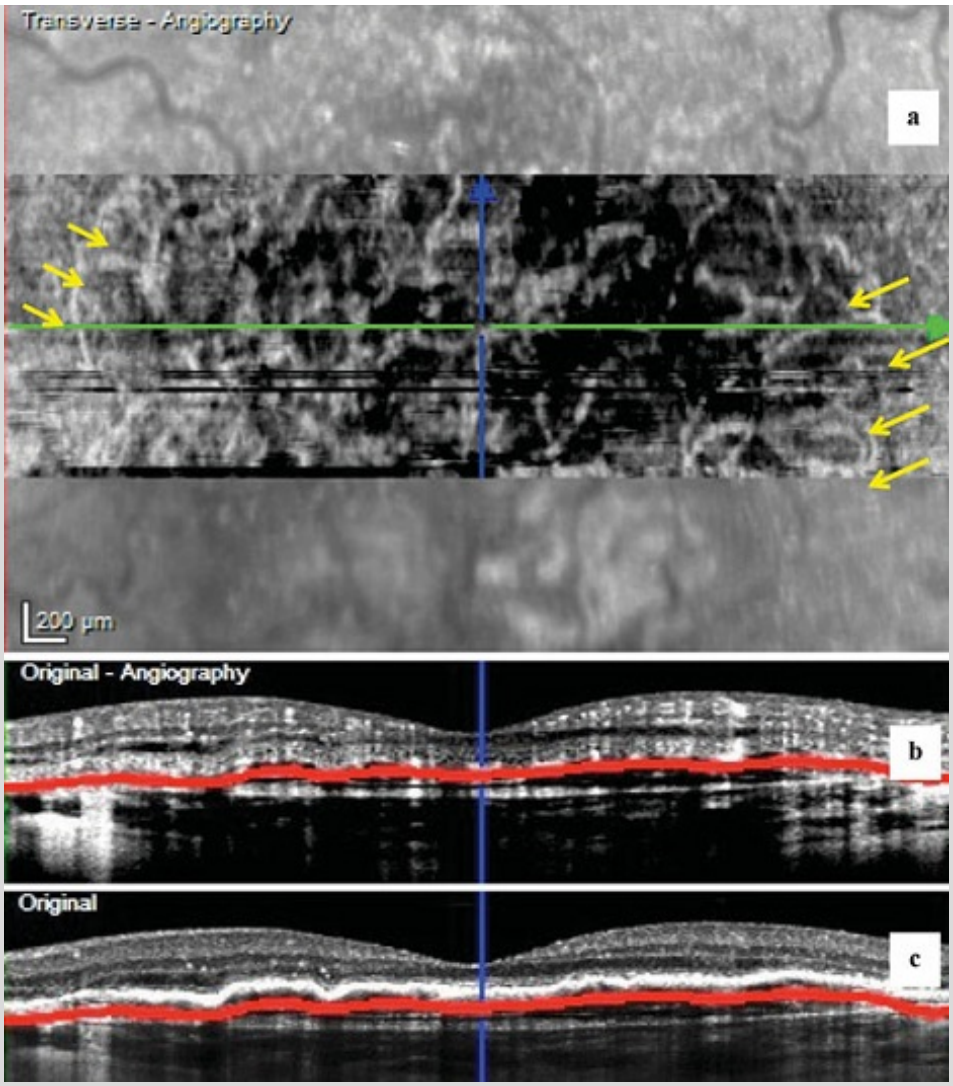

Figure 39: (a) OCT-A C-scan (above the Bruch's membrane). The following C-scan, deeper inside the PED, shows a different level of the lesion, in which some tiny branching vessels forming peripheral arcades (*yellow arrows*) are seen. **(b) OCT-Angio B-scan (above the Bruch's membrane).** The OCT-Angio B-scan shows the position of the C-scan (*red lines*), in this case deeper inside the PED (above the Bruch's membrane). **(c) Conventional OCT B-scan (above the Bruch's membrane).** The conventional OCT B-scan shows the position of the C-scan (*red lines*), in this case deeper inside the PED (above the BM).

Below the Bruch's membrane (figure 40)

Directly inside the choroid, we can see some areas of hyper-intense signals, while several confluent large choroidal vessels are also visible as hypo-intense structures.

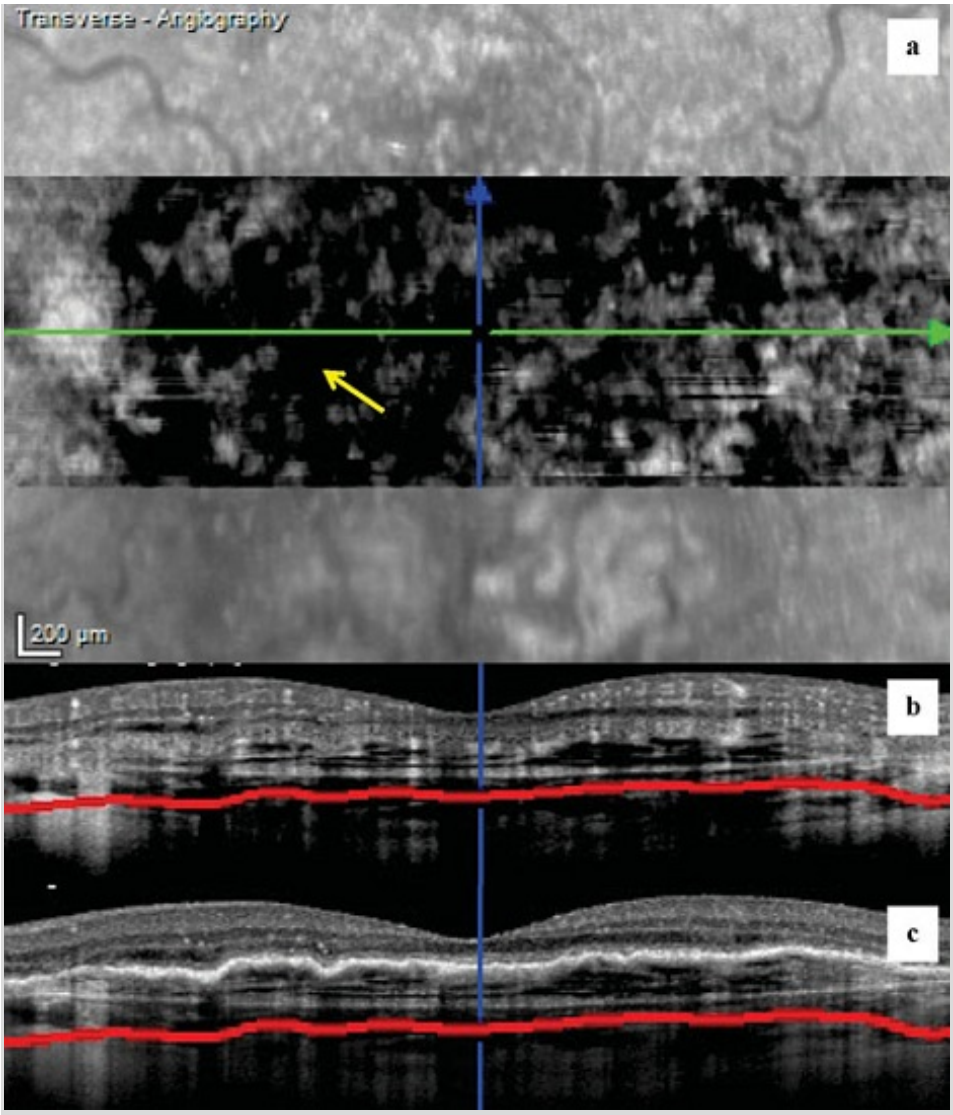

Figure 40: (a) OCT-A C-scan (below the Bruch's membrane). The 30-µm C-scan section is positioned directly inside the choroid. We appreciate some areas of hyper-intense signals, while several confluent large choroidal vessels are also visible as hypo-intense structures (*yellow arrow*). **(b) OCT-Angio B-scan (below the Bruch's membrane).** The OCT-Angio B-scan shows the position of the C-scan (*red lines*), in this case deep inside the choroid (below the Bruch's membrane). **(c) Conventional OCT B-scan (below the Bruch's membrane).** The conventional OCT B-scan shows the position of the C-scan (*red lines*), in this case deep inside the choroid (below the Bruch's membrane).

Suggested OCT-A diagnosis:

Extensive Type I neovascular lesion, active at the periphery.

Indication for prolonging the treatment.

7.4 Synthesis

The compliation of the different results is shown in **figure 41.**

ICGA shows a large Type I (subepithelial / occult) CNV, forming a **poorly defined neovascular network within the PED.**

A few large mature vessels are visible with large mature vessels in the centre of the lesion and tiny anastomotic vessels at the periphery.

OCT-A shows a broad neovascular network, mainly composed of numerous, finely anastomosed, sinuous vessels *(yellow arrows)* and a peripheral arcade.

The large mature vessels in the centre of the lesion are not visible, because it is much deeper.

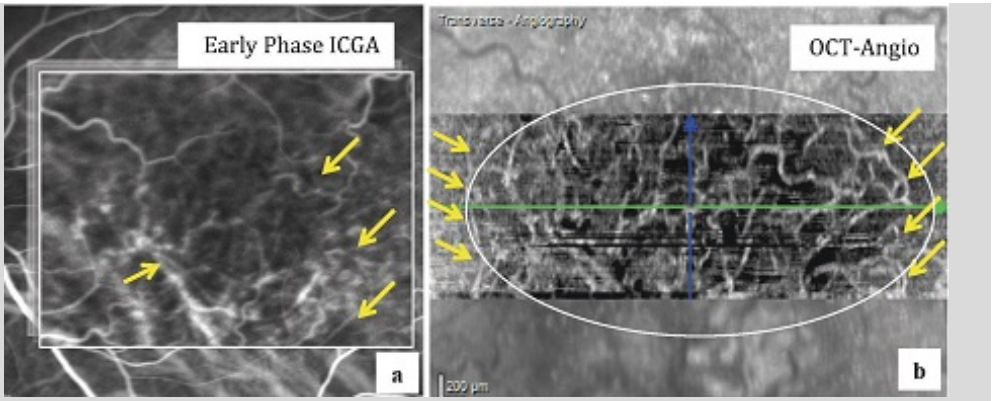

Figure 41: Both the ICGA (left) and the OCT-Angiography (right) clearly pinpoint a subepithelial (occult or Type I) neovascular network.

Both ICGA (left) and OCT-Angiography (right) clearly show a subepithelial (occult or Type I) neovascular network.

This is a "Type I lesion", with a partially stabilized centre and a periphery that is still moderately active, suggesting persistence of activity and thus indicating a prolongation of treatment.

8 CLINICAL CASE NO. 4: ACTIVE TYPE I CNV (SUBEPITHELIAL OR OCCULT) – STILL ACTIVE

8.1 Clinical and biomicroscopic signs

A 68-year-old man presented with reduced vision, metamorphopsia and central scotoma in the right eye.

He is under treatment for exudative AMD for the past 20 months with anti-VEGF injections on a PRN after the loading phase.

- BCVA RE: 20/100

- BCVA LE: 20/40

Biomicroscopic examination revealed an extensive macular lesion of about two Disc Diameters (DD). Also, several hard drusen are seen at the posterior pole.

8.2 Traditional multimodal imaging

Autofluorescence (figure 42)

The image shows the presence of a large macular hypo-fluorescent lesion that is partially surrounded, mainly at the inferior border, by an intense hyper-fluorescent halo.

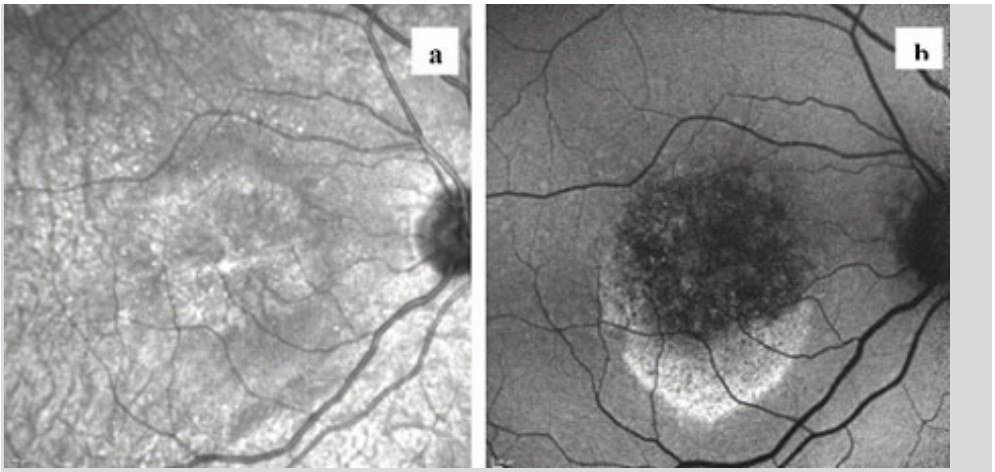

Figure 42: (a) Infrared. Extensive macular lesion of about 2 Disc Diameters (DD). Several hard drusen are also seen at the posterior pole, mainly at the border of the lesion. **(b) Autofluorescence.** The image shows the presence of

a large macular hypo-fluorescent lesion that is partially surrounded, mainly at the inferior border, by an intense hyper-fluorescent halo.

Fluorescein angiography, FA **(figure 43)**

In the early venous phase, a well-circumscribed hyper-fluorescent macular lesion is visible with irregular borders (staining), resembling a broad fibrovascular pigmented epithelium detachment (PED). Numerous hyper-fluorescent tiny spots are also seen, almost involving the entire posterior pole, due to the presence of hard drusen.

The late phase of FA shows marked hyper-fluorescence in the lesion area due to a staining effect, without appreciable signs of leakage.

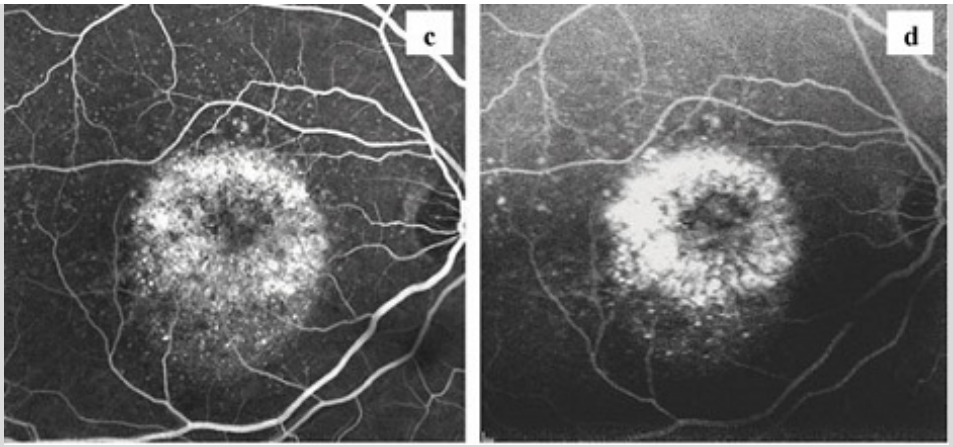

Figure 43: (a) Fluorescein angiography (arterio-venous phase). Well-circumscribed hyper-fluorescent macular lesion, with irregular borders (staining), resembling a wide fibrovascular PED. Numerous hyper-fluorescent tiny spots are also seen, involving almost the entire posterior pole, due to the presence of hard drusen. **(b) Fluorescein angiography (late phase).** Marked hyper-fluorescence in the lesion area due to a staining effect, without appreciable signs of fluorescein leakage.

Indocyanine Green Angiography, ICGA **(figure 44)**

In the early arterio-venous phase, a large Type I (subepithelial / occult) CNV is observed, forming a well-defined neovascular network within the PED. There are several large mature vessels radiating from the centre to the periphery of the lesion. The draining of the lesion appears to be present in the inferior-temporal quadrant.

In the late venous phase, the border of the lesion is more appreciable without clear evidence of a peripheral anastomotic arcade.

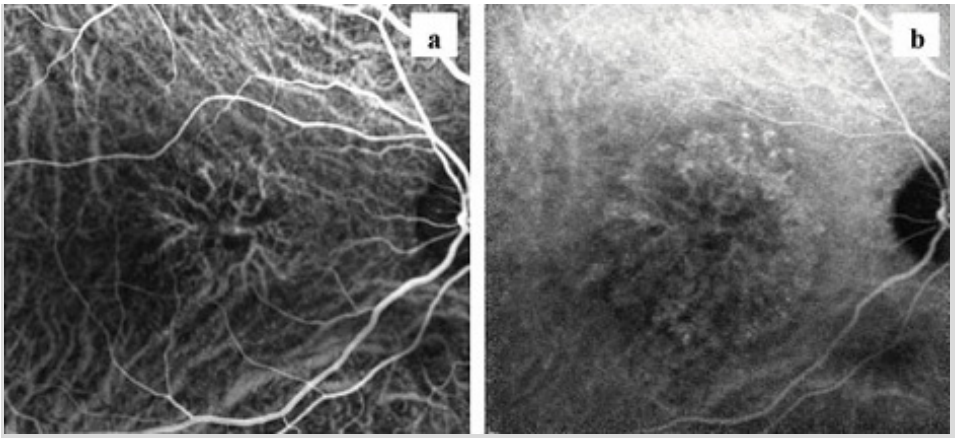

Figure 44: (a) ICG angiography (arterio-venous phase). A large Type I (subepithelial / occult) CNV is observed, forming a well-defined neovascular network within the PED. There are several large mature vessels radiating from the centre to the periphery of the lesion. The draining of the lesion appears to be mainly in the inferior-temporal quadrant of the choroid. **(b) ICG angiography (late phase).** In the late venous phase, the borders of the lesion are clearer with no clear evidence of a peripheral anastomotic arcade.

Optical Coherence Tomography, SD-OCT **(figure 45)**

The foveal depression is substantially maintained with very **limited subretinal fluid accumulation** (subfoveal hypo-reflective space). The outer retinal layers, especially the outer nuclear layer, are substantially thinned or not detectable in the whole 30° line scan. There are clear interruptions in the external limiting membrane and the ellipsoid zone swelling. The RPE appears to be atrophic or not distinguishable from the hyper-reflective fibrovascular lesion below. A large, thick, “dome-shaped” fibrovascular PED, involving almost the entire macular area, has resulted in an upward dislocation of the neurosensory retina. The Bruch’s membrane is detached from the RPE and is clearly visible. The PED has a heterogeneous hyper-reflective appearance, probably due to the concomitant presence of new vessels and scarring tissue.

The choroid is thinned, and, in some areas, only the large choroidal vessels are seen.

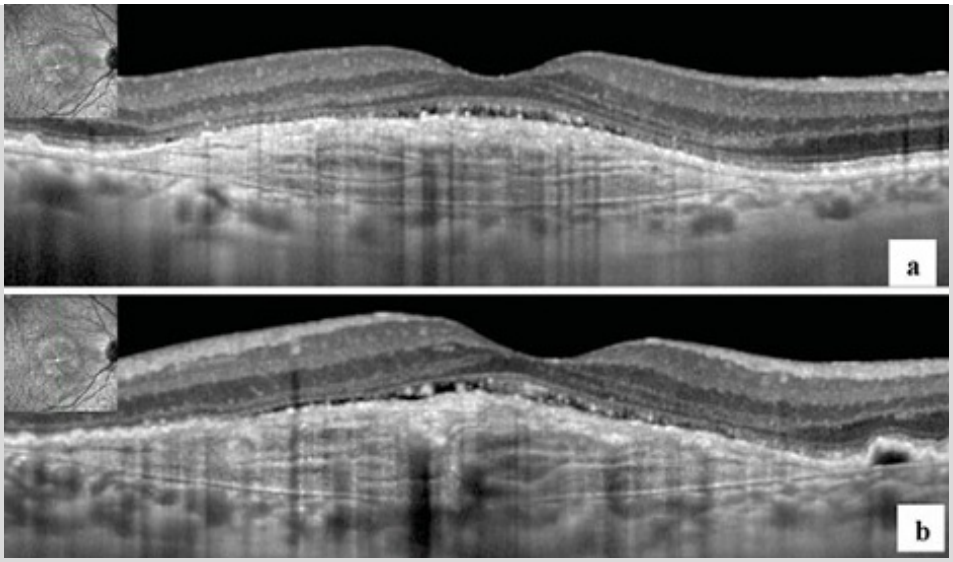

Figure 45: SD-OCT. (a) The foveal depression is substantially maintained with *limited subretinal fluid accumulation* (subfoveal hypo-reflective space). The outer retinal layers are substantially thinned or not detectable in the whole 30° linear scan. There are appreciable interruptions in the ELM and EZ swelling. **(b)** A large, thick, "dome-shaped" fibrovascular PED, involving almost the entire macular area, which has resulted in an upward dislocation of the neurosensory retina. The Bruch's membrane is detached from RPE and is clearly visible.The PED has a heterogeneous hyper-reflective appearance, probably due to the concomitant presence of new vessels and scarring tissue. The choroid is thinned, and, in some areas, only the large choroidal vessels are seen.

Suggested multimodal imaging diagnosis:

Extensive Type I neovascular lesion with very limited activity, suggesting a persistence or recurrence.

There is a need for prolonging the treatment.

8.3 OCT-Angiography

The OCT angiogram is evaluated with multiple 30 µm transverse C-scans, starting 30 µm above the RPE and ending at the choroidal-scleral interface. The 30-µm-step outer retinal/choroidal analysis allows the complete imaging of the entire lesion by highlighting different decorrelation signals, but only if they belong to coplanar structures.

Above the RPE (figure 46)

In the 30 µm thickness C-scan, there is no evidence of a clear decorrelation signal that could be attributed to choroidal neovascularization.

The hyper-intense signal is due to a “pseudo-image” of the retinal vessels caused by the reflectivity of the RPE or by the proximity of some intensely perfused structures (choriocapillaris).

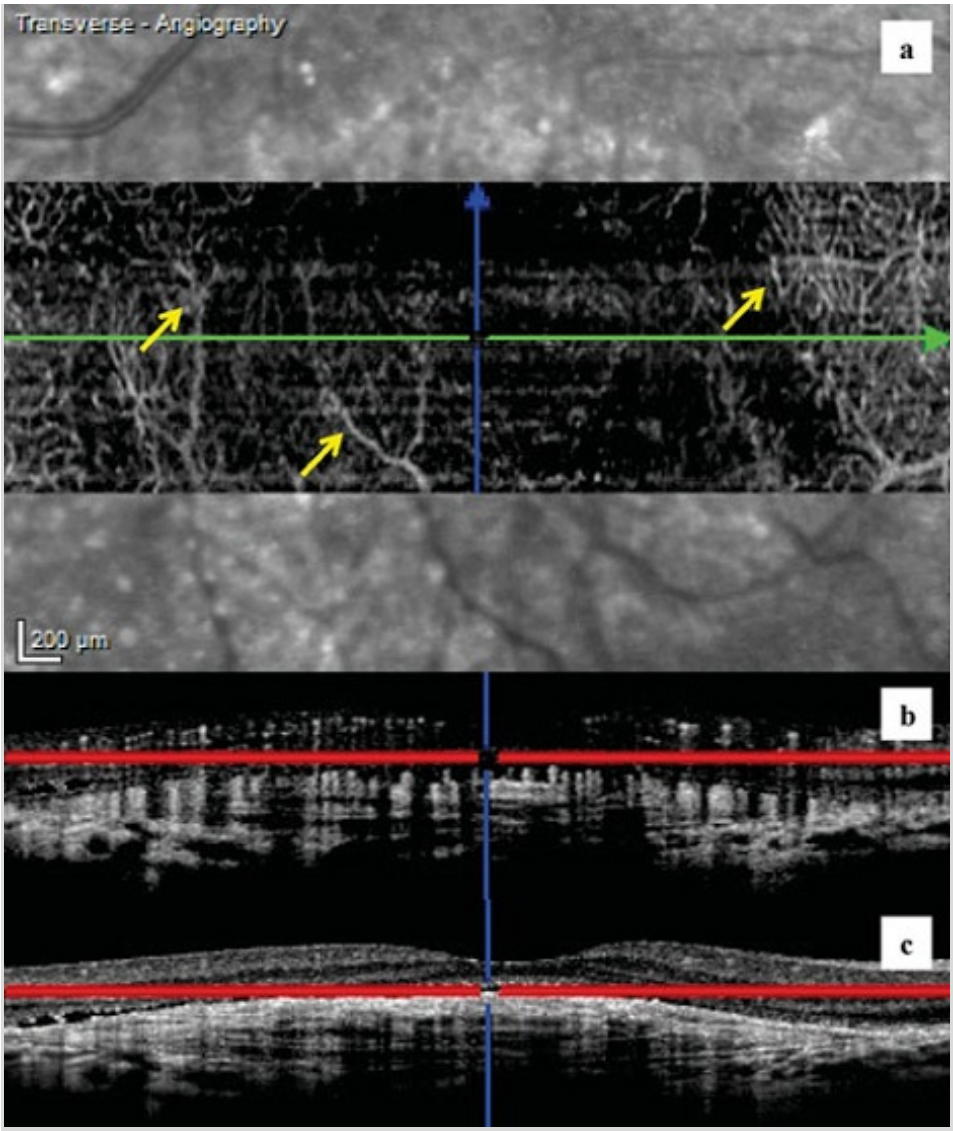

Figure 46: (a) OCT-A C-scan (30 µm above the RPE). No evidence of a clear decorrelation signal that could be attributed to CNV. The hyper-intense signal is due to a “pseudo-image” of the retinal vessels (*yellow arrows*) caused by the reflectivity of the RPE or by the proximity of some intensely perfused structures (choriocapillaris). **(b) OCT-Angio B-scan (30 µm above the RPE).** A clear decorrelation signal is appreciable from both retinal and choroidal vasculature. A pathologic hyper-intense signal is also present below the scanned area. **(c) Conventional OCT B-scan (30 µm above the RPE).** The conventional OCT is useful to identify the exact location of the lesion (above the RPE) and the presence of subretinal fluid accumulation.

At the back surface of the RPE (figure 47)

The next C-scan section is therefore placed inside the PED. Here a “spoked wheel”-shaped CNV is clearly seen.

The centre of the lesion is mainly filled by large mature vessels that branch into numerous tiny ones toward the periphery.

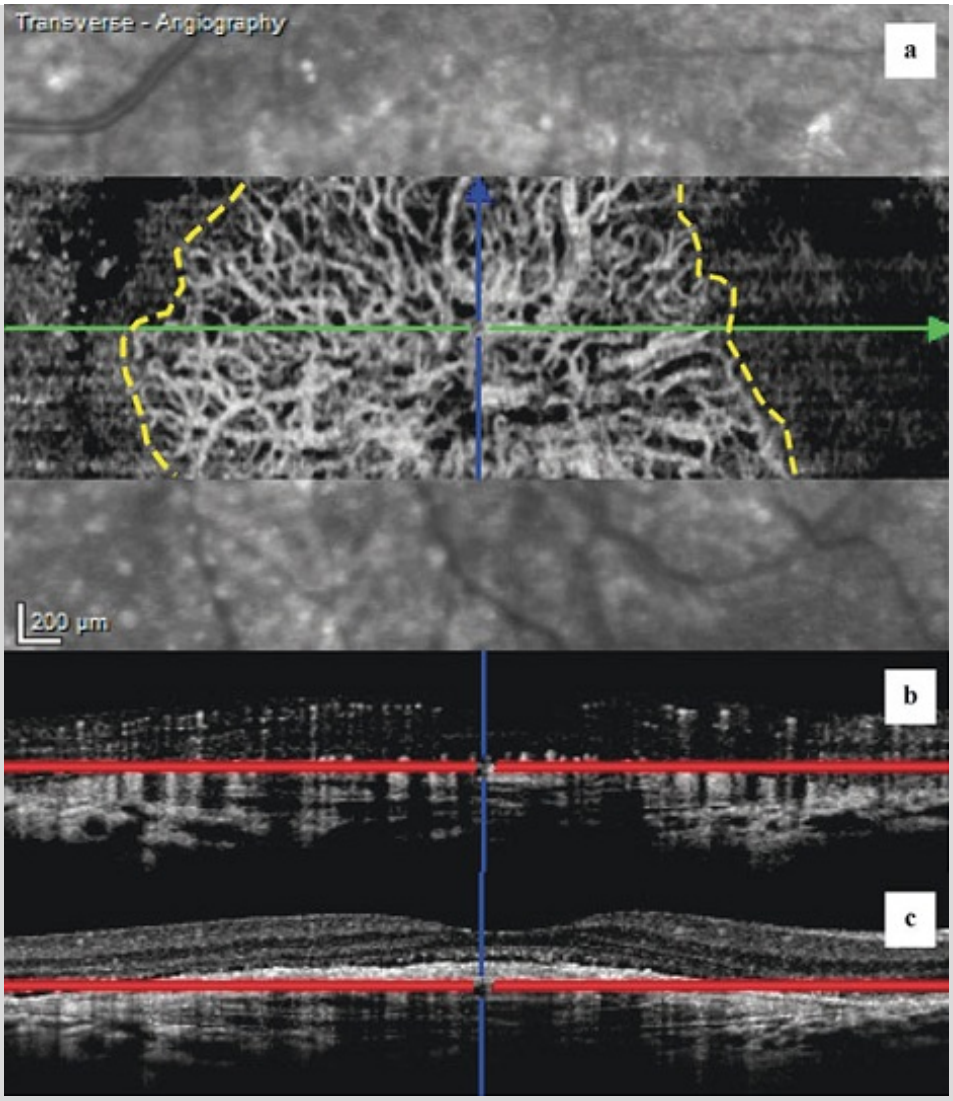

Figure 47: (a) OCT-A C-scan (back surface of the RPE). The 30 µm C-scan section is positioned at the back surface of the RPE and therefore inside the PED. Here, a “spoked wheel”-shaped CNV (*yellow dashed lines*) is clearly seen. The centre of the lesion is mainly filled by large mature vessels that branch into numerous tiny ones toward the periphery. **(b) OCT-Angio B-scan (back surface of the RPE).** The OCT-Angio B-scan shows the position of the C-scan (*red lines*), in this case at the back surface of the RPE. (**c) Conventional OCT B-scan (back surface of the RPE).** The conventional OCT B-scan shows the position of the C-scan *(red lines)*, in this case at the back surface of the RPE.

Deeper inside the PED (figure 48)

The following C-scan shows almost the entire horizontal extent of the neovascular network. It is finely anastomosed, with numerous tiny branching vessels radiating from the centre to the periphery and forming some peripheral vascular arcades.

This could be **an index of persistence of activity** in the lesion.

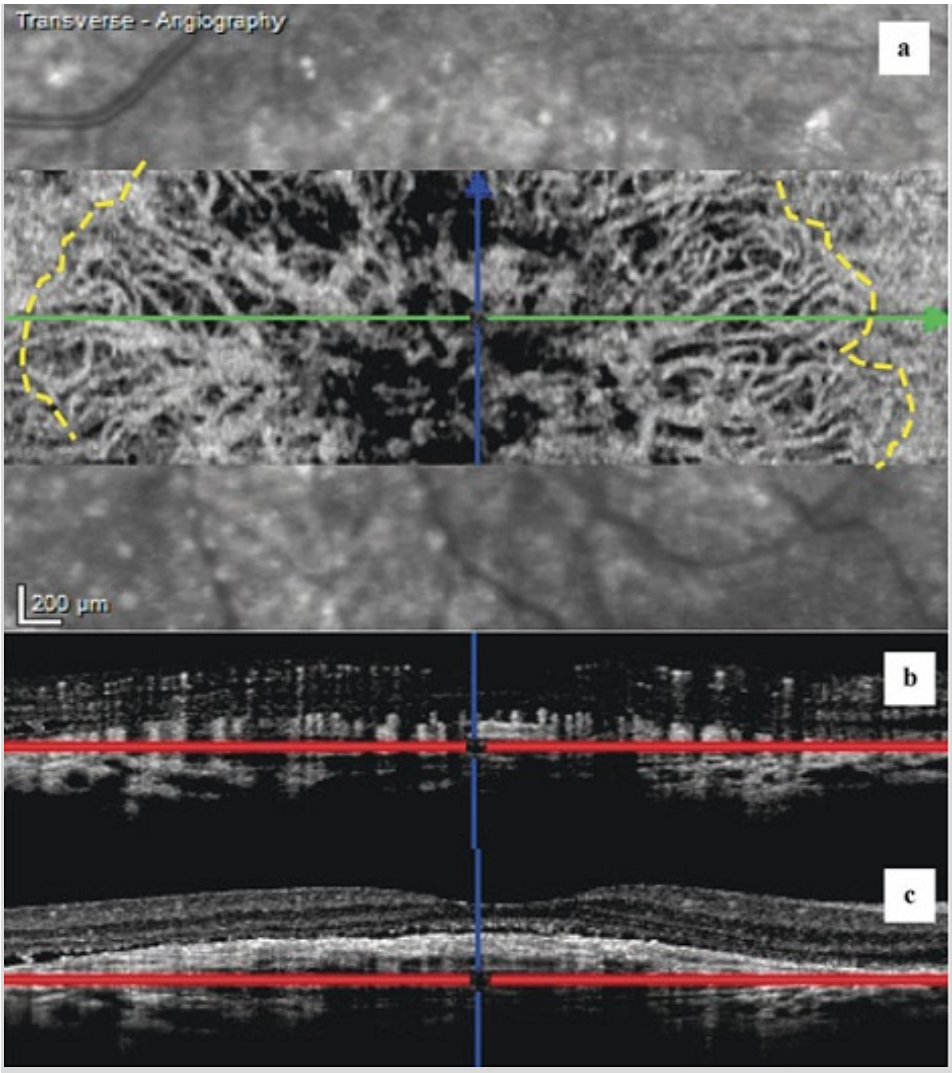

Figure 48: (a) OCT-A C-scan (above the Bruch's membrane). The 30-µm C-scan section is positioned deeper inside the PED. It almost shows the entire **horizontal extent of the neovascular network** (*yellow dashed lines*). It is finely anastomosed, with numerous tiny branching vessels, radiating from the centre to the periphery and forming some peripheral vascular arcades. **(b) OCT-Angio B-scan (above the Bruch's membrane).** The OCT-Angio B-scan shows the position of the C-scan (*red lines*), in this case deeper inside the PED above the Bruch's membrane. **(c) Conventional OCT B-scan (above the Bruch's membrane).** The conventional OCT B-scan shows the position of the C-scan (*red lines*), in this case deeper inside the PED above the Bruch's membrane.

Below the Bruch's membrane (figure 49)

Directly inside the choroid, we appreciate a diffuse hyper-intense signal, probably due to the remnants of the choriocapillaris and the Sattler's layer with a high hypo-intense central area.

This is probably caused by some large confluent choroidal draining vessels immediately below the lesion.

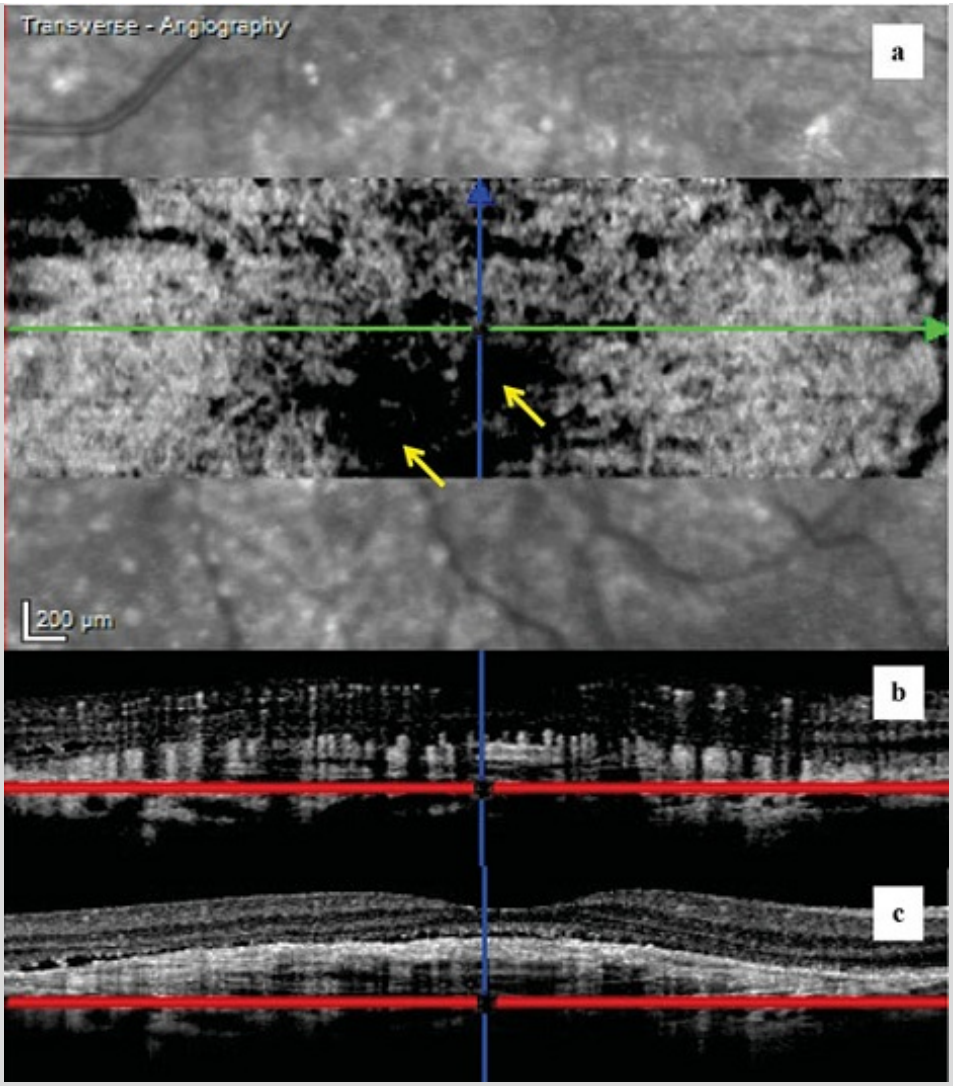

Figure 49: (a) OCT-A C-scan (below the Bruch's membrane). The 30 µm C-scan section is positioned below the Bruch's membrane, directly inside the choroid. A diffuse hyper-intense signal is appreciable due to the remnants of **the choriocapillaris** and the **Sattler's layer**. It shows a high hypo-intense central area probably caused by some large confluent choroidal draining vessels immediately below the lesion (*yellow arrows*). **(b) OCT-Angio B-scan (below the Bruch's membrane).** The OCT-Angio B-scan shows the position of the C-scan (*red lines*), in this case deep inside the choroid below the Bruch's membrane. **(c) Conventional OCT B-scan (below the Bruch's membrane).** The conventional OCT B-scan shows the position of the C-scan (*red lines*), in this case deep inside the choroid below the Bruch's membrane.

Suggested OCT-A diagnosis:

Extensive Type I mature neovascular lesion, with limited activity or recurrence mainly at the periphery.

Indication for prolonging the treatment.

8.4 Synthesis

The compliation of the different results is shown in **figure 50.**

ICGA shows a large Type I (subepithelial / occult) CNV in the early arterio-venous phase, forming a **well-defined neovascular network** (*dashed yellow line*) within the **PED**.

There are several **large mature vessels** (*yellow arrows*) radiating from the centre to the periphery of the lesion. Tiny vessels are not visible at the borders.

On **OCT-A**, a **"spiked wheel"-shaped CNV** (*green dashed lines*) is clearly seen. The large mature vessels in the centre of the lesion are not visible, because it is much deeper.

The centre of the lesion is mainly filled by **large mature vessels** (*green arrows*) that **branch** into **numerous tiny ones** towards the periphery. Anastomoses are rare with limited peripheral arcades. There is a mild hypo-intense perilesional halo (*yellow arrows*).

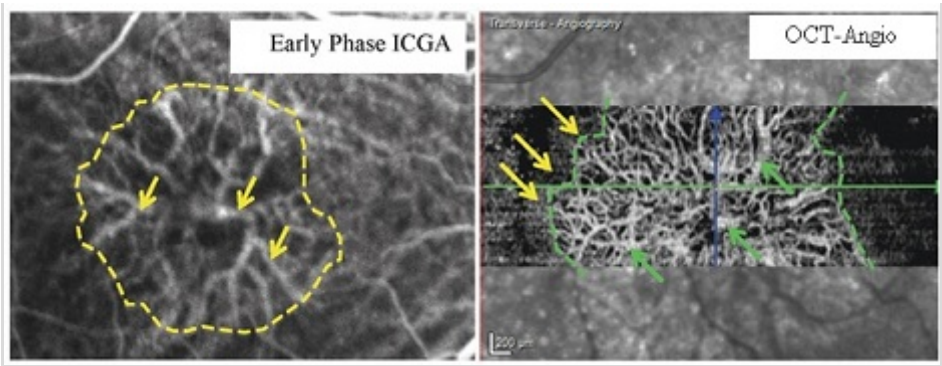

Figure 50: The ICGA (left) and the OCT-Angiography (right) clearly show a CNV Type I (subepithelial / occult).

Both ICGA (left) and OCT-Angiography (right) clearly show a Type I (subepithelial / occult) neovascular network.

This is a "Type I lesion", with a large, extensive, subepithelial or occult neovascular network. The concomitant presence of large mature vessels in the centre, and tiny well-perfused ones at the borders of the lesion (with peripheral arcades and anastomoses) suggests an old lesion, still active at the borders, and therefore indicating an additional intravitreal treatment.

9 CLINICAL CASE NO. 5: ACTIVE TYPE I CNV (SUBEPITHELIAL OR OCCULT) – QUIESCENT / RECURRENT

9.1 Clinical and biomicroscopic signs

A 75-year-old man with exudative AMD in the right eye (RE) was treated with anti-VEGF injections using a PRN scheme. He is now being followed up on a monthly basis.

- BCVA RE: 20/100
- BCVA LE: 20/25

Biomicroscopic examination revealed an extensive lesion of about three Disc Diameters (DD), extending beyond the borders of the macular area.

9.2 Traditional multimodal imaging

Autofluorescence (figure 51)

The image shows the presence of a large macular hypo-fluorescent lesion (due to substantial loss of macular pigment), surrounded by an intense oval shaped hyper-fluorescent halo.

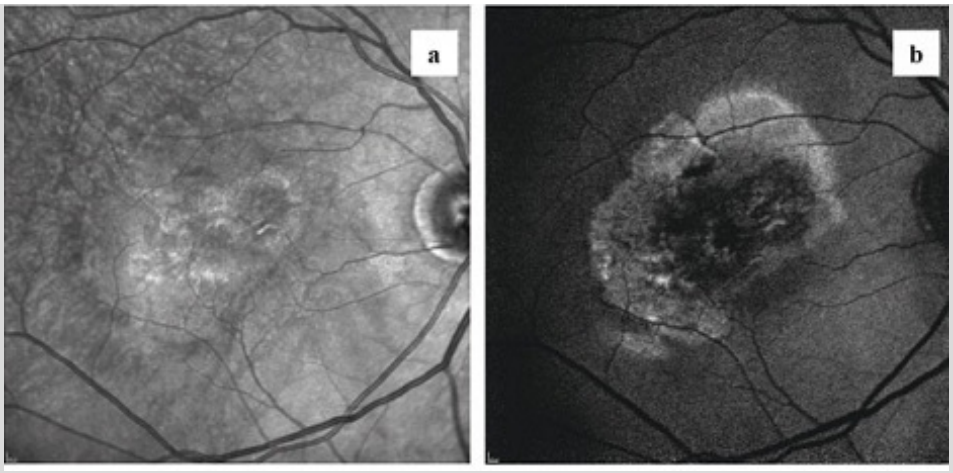

Figure 51: (a) Infrared. Extensive lesion of about three Disc Diameters, extending beyond the borders of the macular area. **(b) Autofluorescence.** Large macular hypo-fluorescent lesion (due to a substantial loss of macular pigment), surrounded by an intense oval shaped hyper-fluorescent halo.

Fluorescein angiography, FA **(figure 52)**

The early arterio-venous phase shows a large hyper-fluorescent macular with well-defined borders. The lesion appears to be composed of two major hyper-fluorescent components, separated by a sickle-shaped hypo-fluorescent area. Numerous hyper-/hypo-fluorescent pinpoints are also seen, involving the entire macular area.

The late phase of FA shows a marked hyperfluorescence of the two components of the lesion. Due to a staining effect; there are no clear signs of a fluorescein leakage.

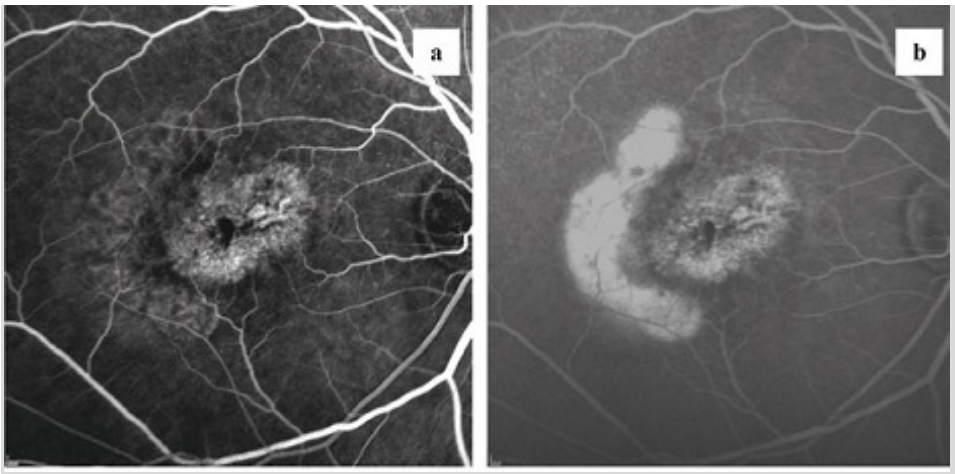

Figure 52: (a) Fluorescein angiography (arterio-venous phase). Larger hyper-fluorescent macular lesion with well-defined borders. The lesion appears to be composed of two major hyper-fluorescent components, separated by a sickle-shaped hypo-fluorescent area. Numerous hyper-/hypo-fluorescent *pinpoints* are also seen, involving the entire macular area. **(b) Fluorescein angiography (late phase).** Marked hyper-fluorescence of the two components of the lesion due to a staining effect. There are no clear signs of a fluorescein leakage.

Indocyanine Green Angiography, ICGA **(figure 53)**

In the early arterio-venous phase, a large Type I (subepithelial / occult) CNV is observed forming a well-defined neovascular network. There are several large mature vessels radiating from the centre to the periphery of the CNV. The draining of the lesion appears to be prevalent into the superior-temporal quadrant of the choroid.

In the late venous phase, the borders of the CNV are more visible. Temporal to the lesion, a sickle-shaped area of hypo-fluorescence is seen, probably due to RPE-outer choroid impairment.

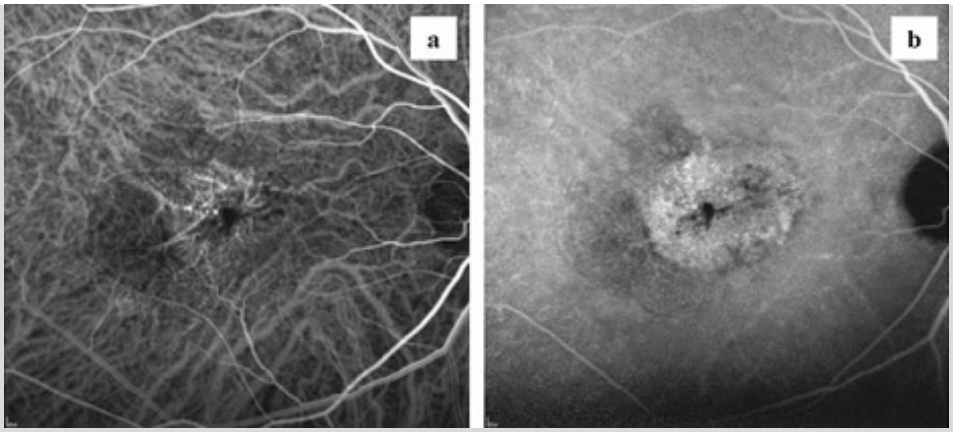

Figure 53: (a) ICG angiography (arterio-venous phase). A large **Type I** (subepithelial / occult) CNV is observed that forms a well-defined neovascular network. There are several large mature vessels radiating from the centre to the periphery of the CNV. The draining of the lesion appears to be prevalent into the superior temporal quadrant of the choroid. **(b) ICG angiography (late phase).** The borders of the CNV are more appreciable. Temporally to the lesion, a sickle-shaped area of hypo-fluorescence is seen, probably due to RPE-outer choroid impairment.

Optical Coherence Tomography, SD-OCT **(figure 54)**

The foveal depression is partially maintained without subretinal fluid accumulation. The outer retinal layers, especially the outer nuclear layer, are substantially thinned near the borders of the wide, fibrovascular PED. There are appreciable interruptions in the external limiting membrane and the ellipsoid zone. In some areas, the RPE appears atrophic or not distinguishable from the hyper reflective fibro vascular lesion below.

A large, “dome-shaped” *fibrovascular PED,* almost involving the entire macular area, has resulted in an upward dislocation of the neurosensory retina. The PED has a heterogeneous hyper-reflective appearance, probably due to the concomitant presence of new vessels and scar tissue.

The choroid is significantly thinned, and in some areas only the large choroidal vessels (Haller’s layer) are visible.

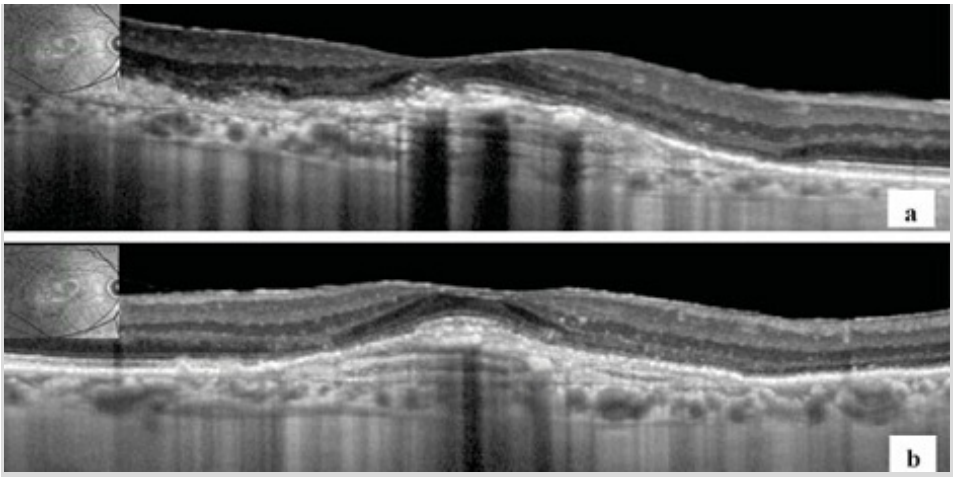

Figure 54: SD-OCT. The foveal depression is partially maintained without subretinal fluid accumulation. The outer retinal layers, especially the outer nuclear layer, are substantially thinned near the borders of the wide, flat, fibrovascular PED. There are appreciable interruptions in the ELM and the EZ. In some areas, the RPE appears atrophic or not distinguishable from the hyper-reflective fibrovascular lesion below. A large, "dome-shaped" fibrovascular PED, almost involving the entire macular area, has resulted in an upward dislocation of the neurosensory retina. The PED has a heterogeneous hyper-reflective appearance, probably due to the concomitant presence of new vessels and scar tissue.The choroid is significantly thinned and in some areas, only the large choroidal vessels (Haller's layer) are seen.

Suggested multimodal imaging diagnosis:

Extensive quiescent Type I neovascular lesion with a possible recurrence.

Re-treatment is not indicated, but a close follow up is required.

9.3 OCT-Angiography

The OCT angiogram is evaluated with multiple 30 µm C-scans, shaped on the Bruch's membrane profile. It starts 30 µm above the RPE and ends at the choroid-scleral interface. The 30-µm-step outer retinal/choroidal analysis allows complete imaging of the entire lesion by highlighting different decorrelation signals, but only if they belong to coplanar structures.

Above the RPE (figure 55)

In the 30 µm thickness C-scan, just above the RPE, there is no evidence of a clear decorrelation signal that could be attributed to choroidal neovascularization.

Some hyper-intense signals are due to "pseudo-images" of the retinal vessels, caused by the reflectivity of the RPE or by the proximity of some intensely perfused structures (choriocapillaris).

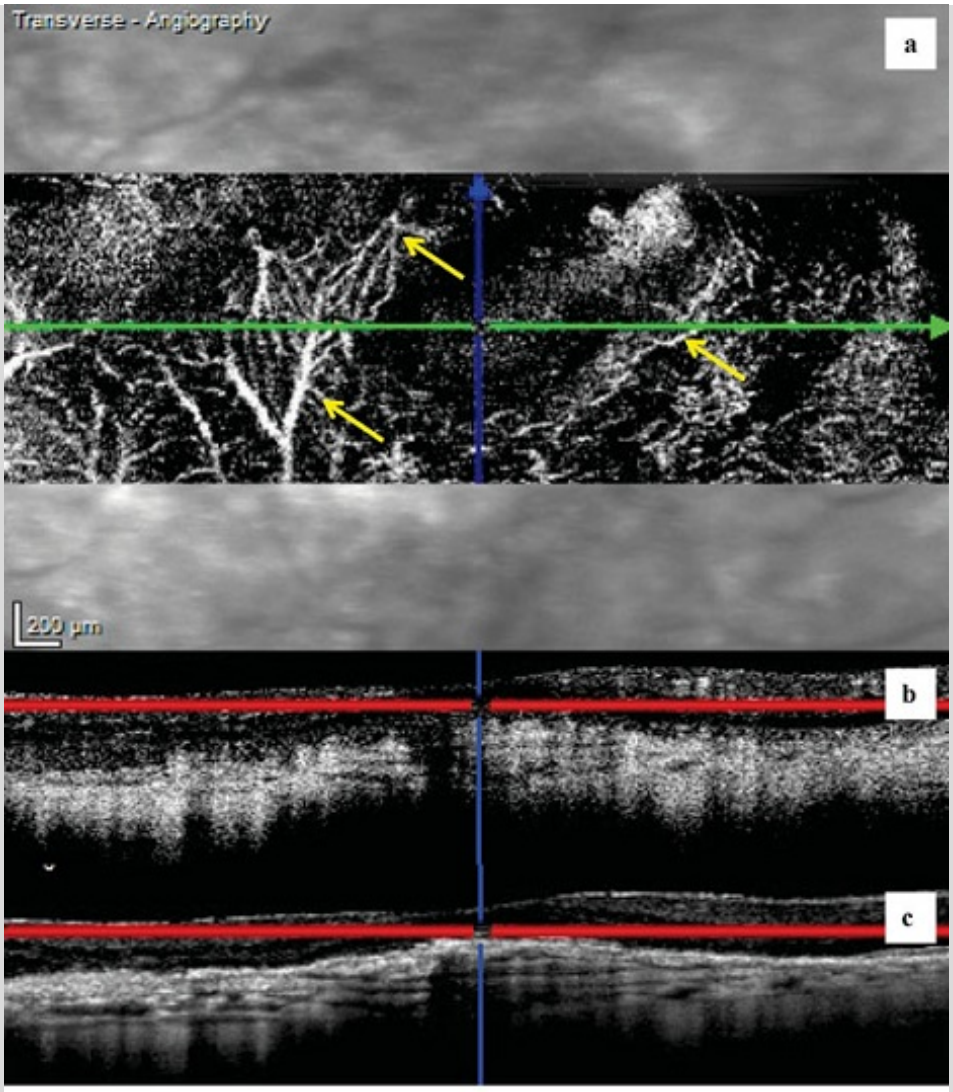

Figure 55: (a) OCT-A C-scan (30 µm above the RPE). No evidence of a clear decorrelation signal that could be attributed to CNV. The hyper-intense signal is due to "pseudo-images" of retinal vessels (*yellow arrows*) caused by the reflectivity of the RPE or by the proximity of some intensely perfused structures (choriocapillaris). **(b) OCT-Angio B-scan (30 µm above the RPE).** An evident decorrelation signal is appreciable from both retinal and choroidal vasculature. A pathologic hyper-intense signal is also present below the scanned area, in between the RPE and the Bruch's membrane. **(c) Conventional OCT B-scan (30 µm above the RPE).** The conventional OCT is useful to identify the exact location of the lesion (*red lines*) above the RPE.

At the back surface of the RPE (figure 56)

The next C-scan section is placed at the back surface of the RPE, and therefore inside the PED.

Some tiny vessels are seen forming a *poorly defined* neovascular network.

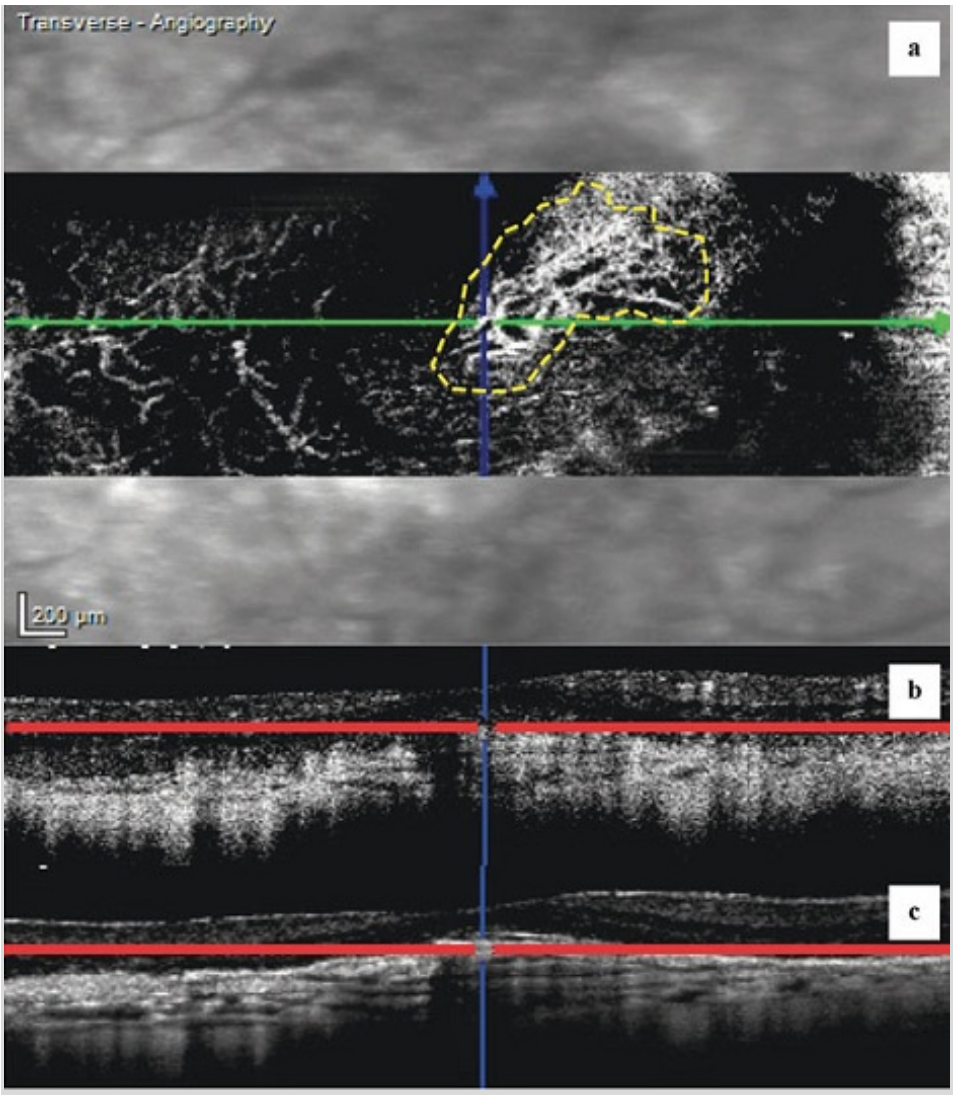

Figure 56: (a) OCT-A C-scan (back surface of the RPE). The 30 µm C-scan section is positioned at the back surface of the RPE, and therefore inside the PED. Some tiny vessels are seen, forming a poorly defined neovascular network (*yellow dashed line*). **(b) OCT-Angio B-scan (back surface of the RPE).** The OCT-Angio B-scan shows the position of the C-scan (*red lines*), in this case at the back surface of the RPE. (**c) Conventional OCT B-scan (back surface of the RPE).** The conventional OCT B-scan shows the position of the C-scan (*red lines*), in this case at the back surface of the RPE.

Deeper inside the PED (figure 57)

The following C-scan, deeper inside the PED, shows a *well-circumscribed CNV*. The centre of the lesion is mainly filled by large “mature“ vessels that branch into numerous tiny ones towards the periphery. No peripheral arcades are seen.

This appearance suggests a quiescent CNV. Nevertheless, this is still doubtful due to the numerous tiny vessels, suggesting that a close follow up is required.

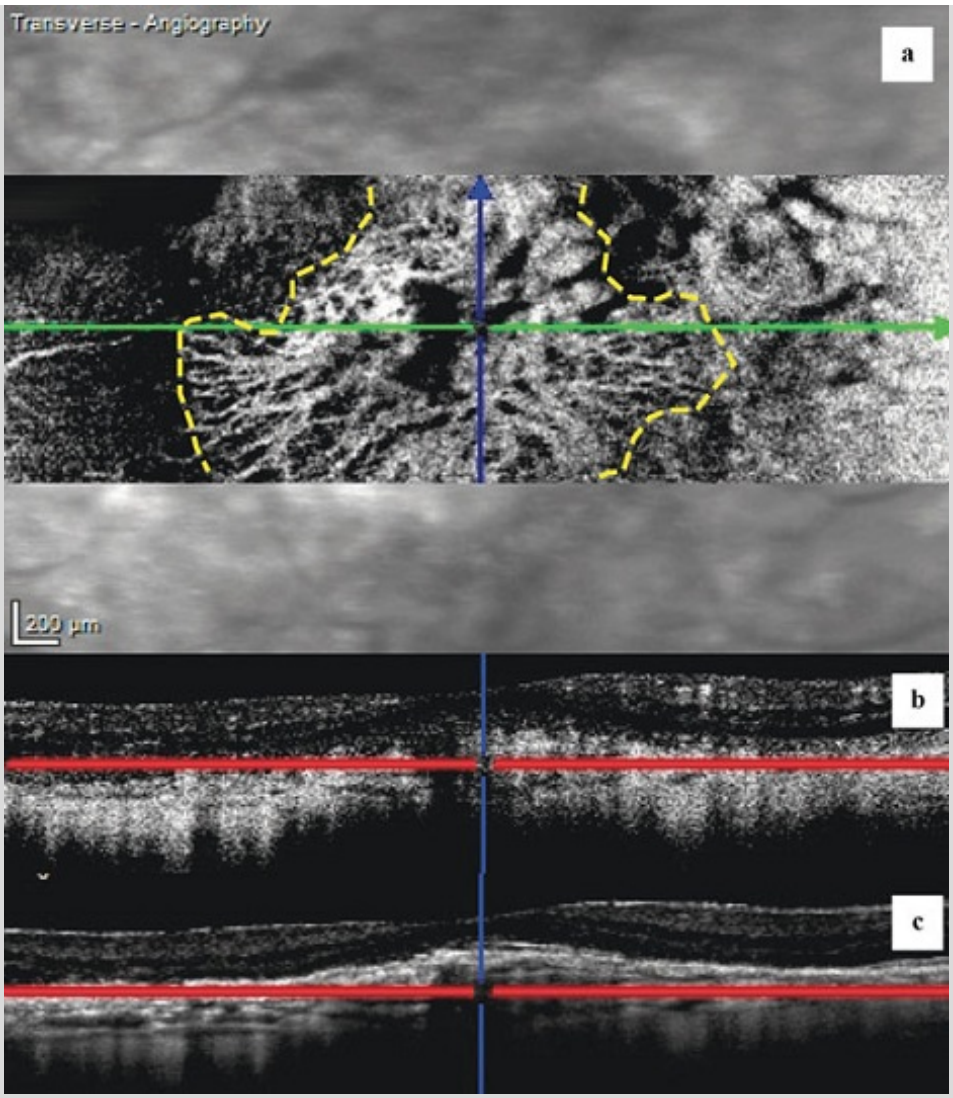

Figure 57: (a) OCT-A C-scan (above the Bruch’s membrane). The 30 µm C-scan section is positioned deeper inside the PED. It shows a well-circumscribed CNV (*yellow dashed line*). The centre of the lesion is mainly filled by large "mature" vessels that branch into numerous tiny ones towards the periphery with the *typical pattern of a dead tree*. No peripheral arcades are seen. **(b) OCT-Angio B-scan (above the Bruch’s membrane).** The OCT-Angio B-scan shows the position of the C-scan (*red lines*), in this case deeper inside the PED above the Bruch’s membrane. **(c) Conventional OCT B-scan (above the Bruch’s membrane).** The conventional OCT B-scan shows the position of the C-scan (*red lines*), in this case deeper inside the PED (above the Bruch’s mem-brane), and the absence of fluid accumulation.

Below the Bruch's membrane (figure 58)

Below the Bruch's membrane directly inside the choroid, we appreciate a diffuse hyper-intense signal, probably caused by remnants of the choriocapillaris and the Sattler's layer. There are high hypo-intense central structures due to large choroidal draining vessels immediately below the lesion.

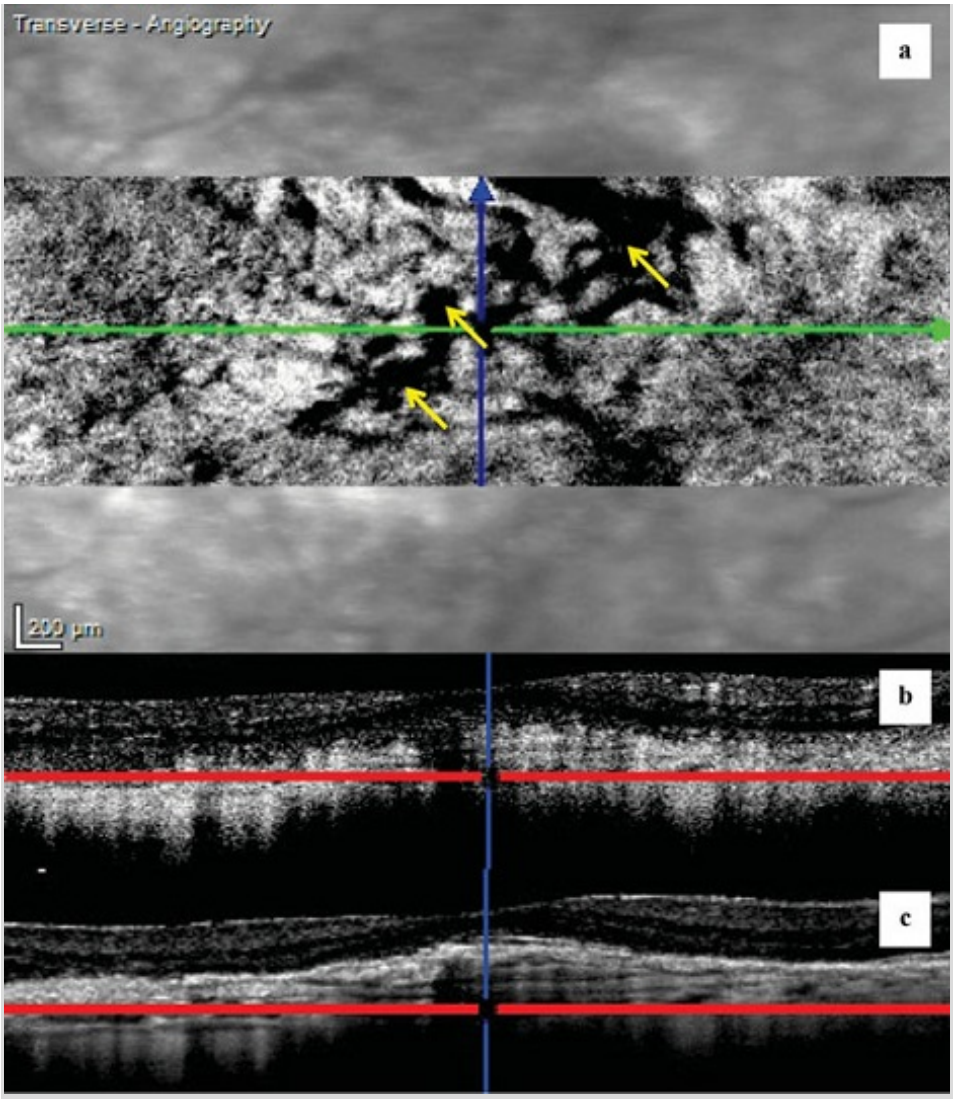

Figure 58: (a) OCT-A C-scan (below the Bruch's membrane). The 30-µm C-scan section is positioned below the Bruch's membrane, directly inside the choroid. A diffuse hyper-intense signal is appreciable, probably caused by remnants of the choriocapillaris and the Sattler's layer. There are high hypo-intense tubular structures (*yellow arrows*) due to large choroidal draining vessels immediately below the lesion. **(b) OCT-Angio B-scan (below the Bruch's membrane).** The OCT-Angio B-scan shows the position of the C-scan (*red lines*), in this case deep inside the choroid below the Bruch's membrane. **(c) Conventional OCT B-scan (below the Bruch's membrane).** The conventional OCT B-scan shows the position of the C-scan (*red lines*), in this case below the Bruch's membrane, and the absence of fluid accumulation.

Suggested OCT-A diagnosis:

Extensive Type I "mature" neovascular lesion without clear signs of activity.

No indication for re-treatment, but this is still doubtful; therefore, a close follow up is required.

9.4 Synthesis

The compliation of the different results is shown in **figure 59.**

ICGA shows a large Type I (subepithelial / occult) CNV (*dashed yellow line*).

There are several **large mature vessels** (*red arrows*) radiating from the centre to the periphery of the **CNV**.

There are no visible tiny vessels at the periphery.

OCT-A shows a well-circumscribed CNV (*green dashed line*) at this level. The centre of the lesion is mainly filled with **large mature vessels** (*red arrows*).

They are branching into numerous **tiny anastomosed ones** (*yellow arrows*), but without a well-defined arcade and having a “dead-tree“ pattern.

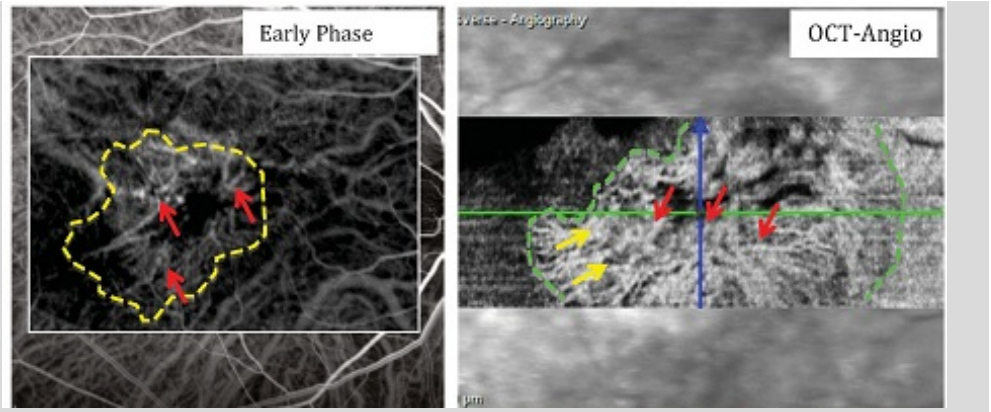

Figure 59: The ICGA (left) and the OCT-Angiography (right) clearly show a CNV Type I (subepithelial / occult).

Both ICGA and OCT-Angiography clearly show a Type I (subepithelial / occult) neovascular network.

This is a “Type I lesion”, with a large, extensive, and subepithelial or occult neovascular network. There is a concomitant presence of large mature vessels in the centre and tiny ones at the borders of the lesion, having a "dead-tree" pattern but without a well-defined arcade.This appearance suggests a quiescent CNV. But this is still doubtful due to the numerous tiny vessels. Therefore, a close follow up is recommended.

10 CLINICAL CASE NO. 6: ACTIVE TYPE I CNV – QUIESCENT

10.1 Clinical and biomicroscopic signs

An 89-year-old woman was treated with anti-VEGF injections for eAMD. She is now being followed up on a monthly basis.

- BCVA RE: 20/100

- BCVA LE: 20/40

Biomicroscopic examination: macular lesion of about one Disc Diameter (DD). There are also several hard drusen at the posterior pole, mainly at the border of the lesion.

10.2 Traditional multimodal imaging

Autofluorescence (figure 60)

The image shows an irregular hypo-fluorescent lesion due to macular pigment impairment in the fovea, partially surrounded by a slightly hyper-fluorescent halo.

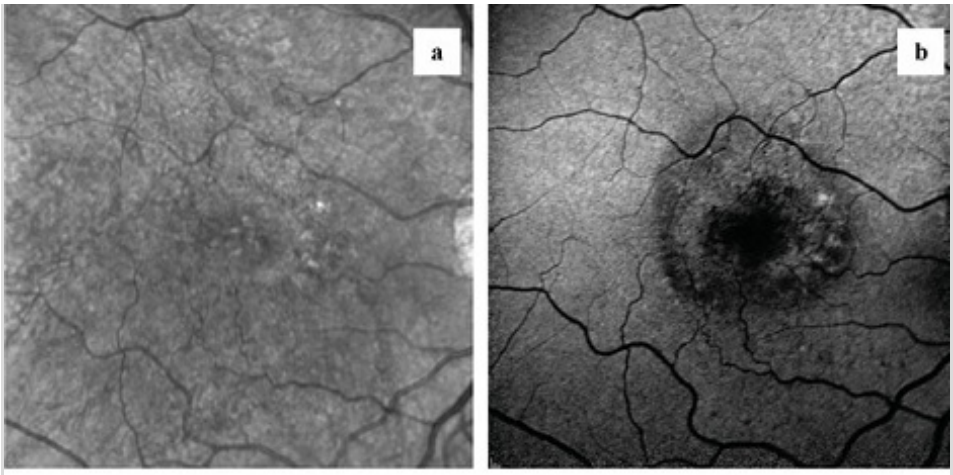

Figure 60: (a) Infrared. Macular lesion of about one Disc Diameter (DD). There are also several hard drusen at the posterior pole, mainly at the border of the lesion. **(b) Autofluorescence.** The image shows an irregular hypo-fluorescent lesion in the fovea, partially surrounded by a slightly hyper-fluorescent halo.

Fluorescein angiography, FA **(figure 61)**

FA in the early venous phase shows a poorly-circumscribed hyper-fluorescent macular lesion with irregular borders and pinpoints. Numerous hyper-fluorescent tiny spots are also seen involving almost the entire macular area; these are due to the presence of hard drusen.

In the late phase of FA, the hyper-fluorescent area (staining effect) does not increase or show appreciable signs of fluorescein leakage.

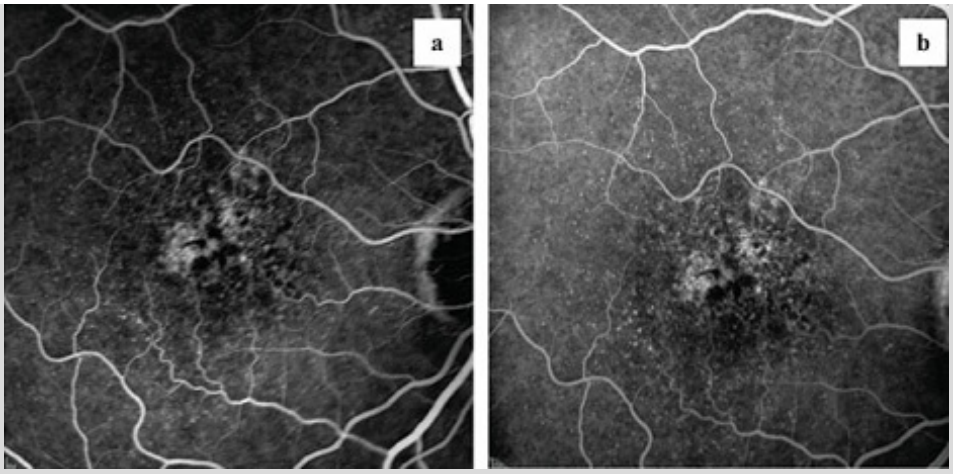

Figure 61: (a) Fluorescein angiography (arterio-venous phase). Poorly circumscribed hyper-fluorescent macular lesion with irregular borders and pinpoints. Numerous hyper-fluorescent tiny spots are seen almost involving the entire macular area; these spots are due to the presence of hard drusen. **(b) Fluorescein angiography (late phase).** The hyper-fluorescent area (staining effect) does not increase or show appreciable signs of fluorescein leakage.

Indocyanine Green Angiography, ICGA **(figure 62)**

In the early venous phase, a Type I (subepithelial / occult) CNV is observed. There are several large mature vessels radiating from the centre to the periphery of the lesion. The draining of the lesion appears to be mainly in the superior-temporal quadrant of the choroid.

In the late venous phase, the borders of the lesion are more visible, and a perilesional area of RPE-outer choroid impairment is also seen.

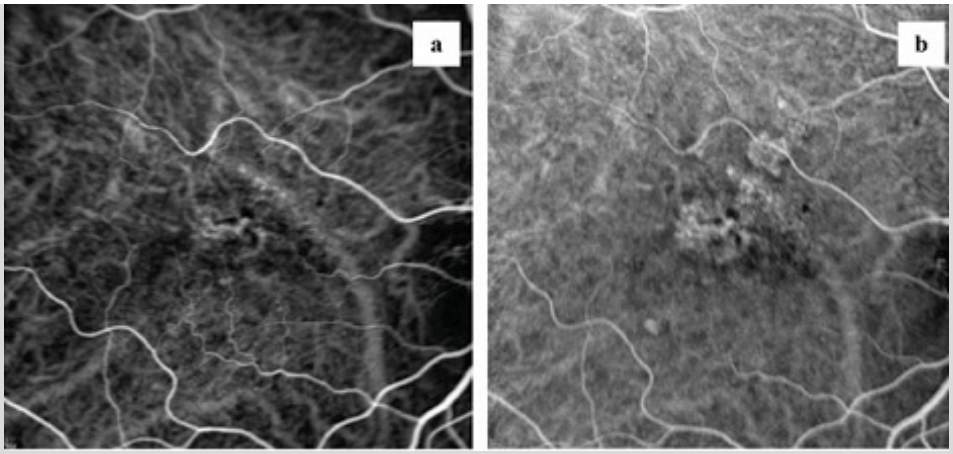

Figure 62: (a) ICG angiography (arterio-venous phase). A Type I (subepithelial / occult) CNV is observed from the early venous phase. There are several large mature vessels radiating from the centre to the periphery of the lesion. The draining of the lesion appears to be mainly in the supero-temporal quadrant of the choroid. **(b) ICG angiography (late phase).** The

border of the lesion is more visible. A perilesional area of RPE-outer choroid impairment is also seen.

Optical Coherence Tomography, SD-OCT **(figure 63)**

The foveal depression is partially maintained without sub-/intraretinal fluid accumulation. There are focal interruptions in the ellipsoid zone.

A “dome-shaped” fibrovascular PED, involving almost the entire macular area, has resulted in an upward dislocation of the neurosensory retina.

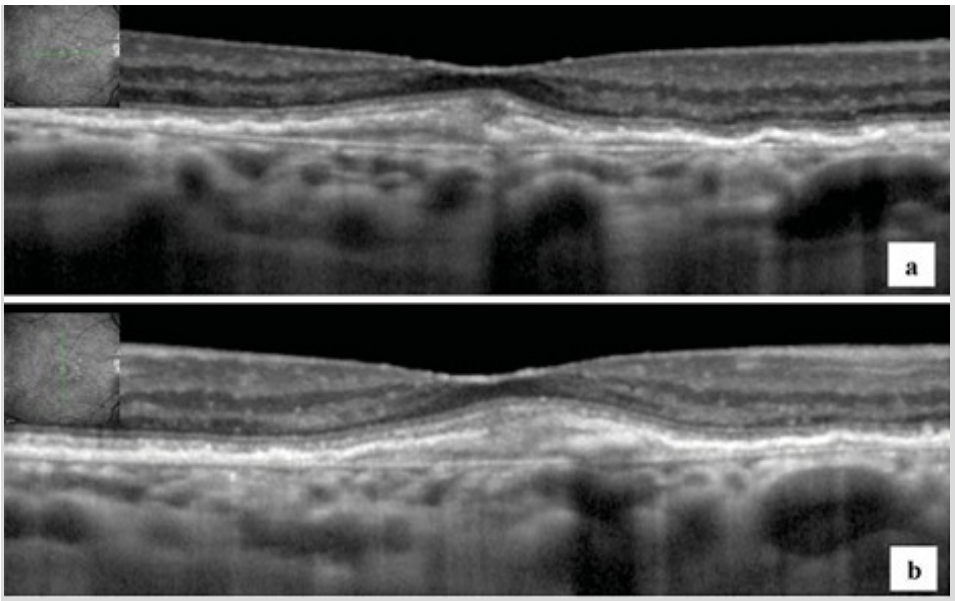

Figure 63: SD-OCT. The foveal depression is partially maintained without sub-/intraretinal fluid accumulation. There are focal interruptions in the EZ. A “dome-shaped” fibrovascular PED almost involving the entire macular area has resulted in an upward dislocation of the neurosensory retina.

Suggested multimodal imaging diagnosis:

Quiescent Type I neovascular lesion.

10.3 OCT-Angiography

The OCT angiogram is evaluated with multiple transverse 30 µm C-scans, starting 30 µm above the RPE and ending at the choroidal-scleral interface. The 30-µm-step outer retinal / choroidal analysis allows complete imaging of the entire lesion by highlighting different decorrelation signals, but only if they belong to coplanar structures.

Just above the RPE (figure 64)

In the 30 µm thickness C-scan, just above the RPE, there is no evidence of a clear decorrelation signal that could be attributed to choroidal neovascularization.

The hyper-intense signal is due to “pseudo-images” of the retinal vessels, caused by the reflectivity of the RPE or the proximity of some intensely perfused structures (choriocapillaris).

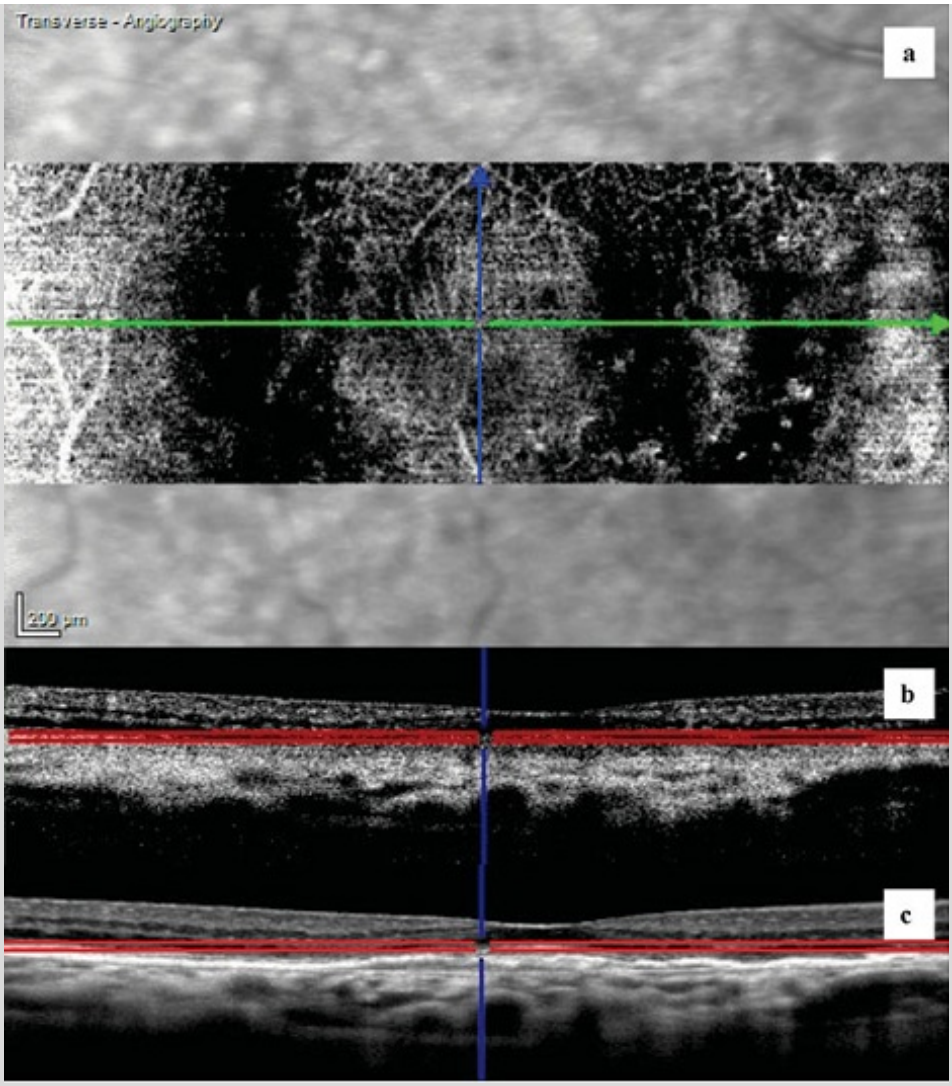

Figure 64: (a) OCT-A C-scan (30 µm above the RPE). No evidence of a clear decorrelation signal that could be attributed to CNV. The hyper-intense signal is due to “pseudo-images” of the retinal vessels, caused by the reflectivity of the RPE or the proximity of some intensely perfused structures (choriocapillaris). **(b) OCT-Angio B-scan (30 µm above the RPE).** An evident decorrelation signal is appreciable from both retinal and choroidal vasculature. A pathologic hyper-intense signal is also present below the scanned area. **(c) Conventional OCT B-scan (30 µm above the RPE).** The conventional OCT is useful to identify the exact location of the lesion above the RPE (*red lines*).

At the back surface of the RPE (figure 65)

The next C-scan section is placed at the back surface of the RPE and therefore inside the PED.

Several mid-diameter vessels can be reckognized that seem to have a radial distribution.

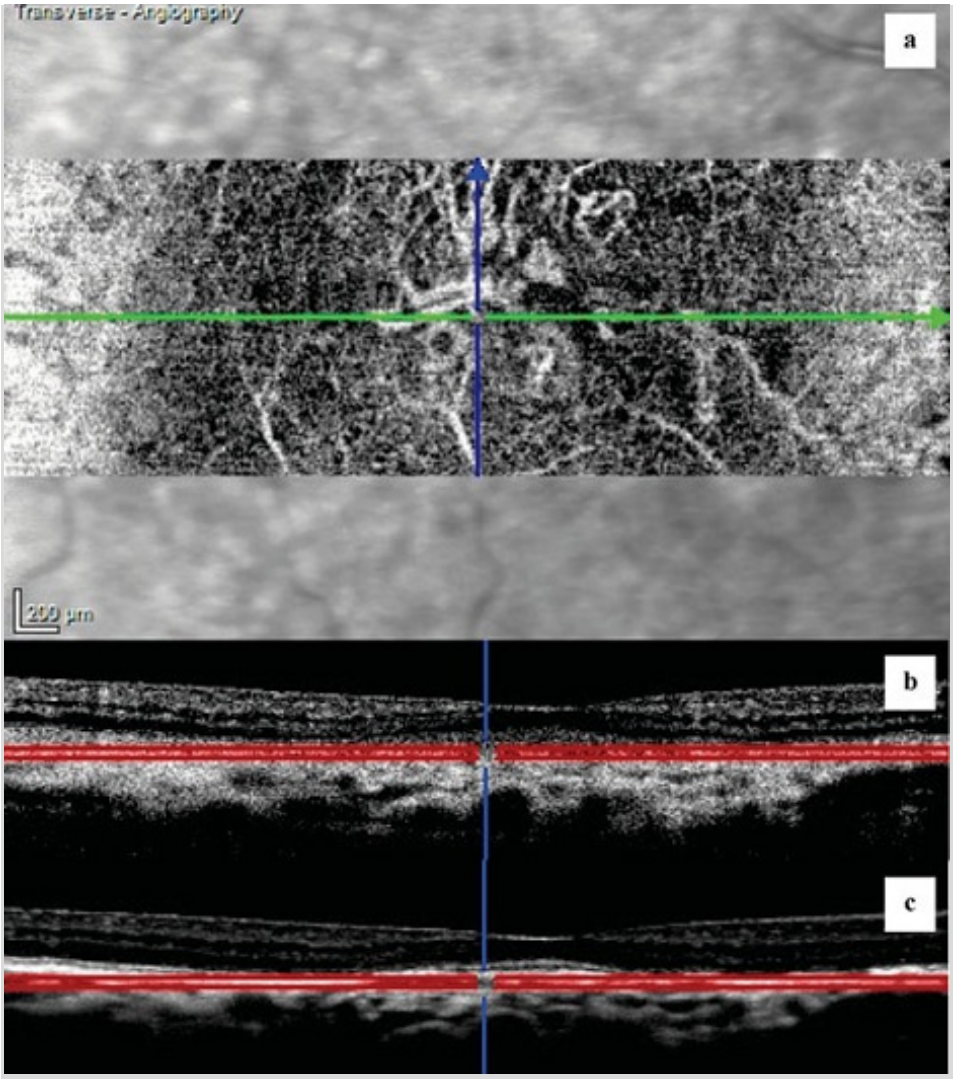

Figure 65: (a) OCT-A C-scan (back surface of the RPE). The 30 µm C-scan section is positioned at the back surface of the RPE and therefore inside the PED. *Several mid-diameter vessels* that seem to have a radial distribution can be reckognized. **(b) OCT-Angio B-scan (back surface of the RPE).** The OCT-Angio B-scan shows the position of the C-scan (*red lines*), in this case at the back surface of the RPE. (**c) Conventional OCT B-scan (back surface of the RPE).** The conventional OCT B-scan shows the position of the C-scan (*red lines*), in this case at the back surface of the RPE.

Deeper inside the PED (figure 66)

The following C-scan deeper inside the PED shows a “spiked wheel”-shaped CNV. The centre of the lesion is mainly composed of large mature vessels. Several mid-diameter vessels that seem to have a radial distribution are also visible, branching into some smaller ones towards the periphery.

The number of anastomoses is limited and the vessel’s termini have a relative “dead-tree” appearance.

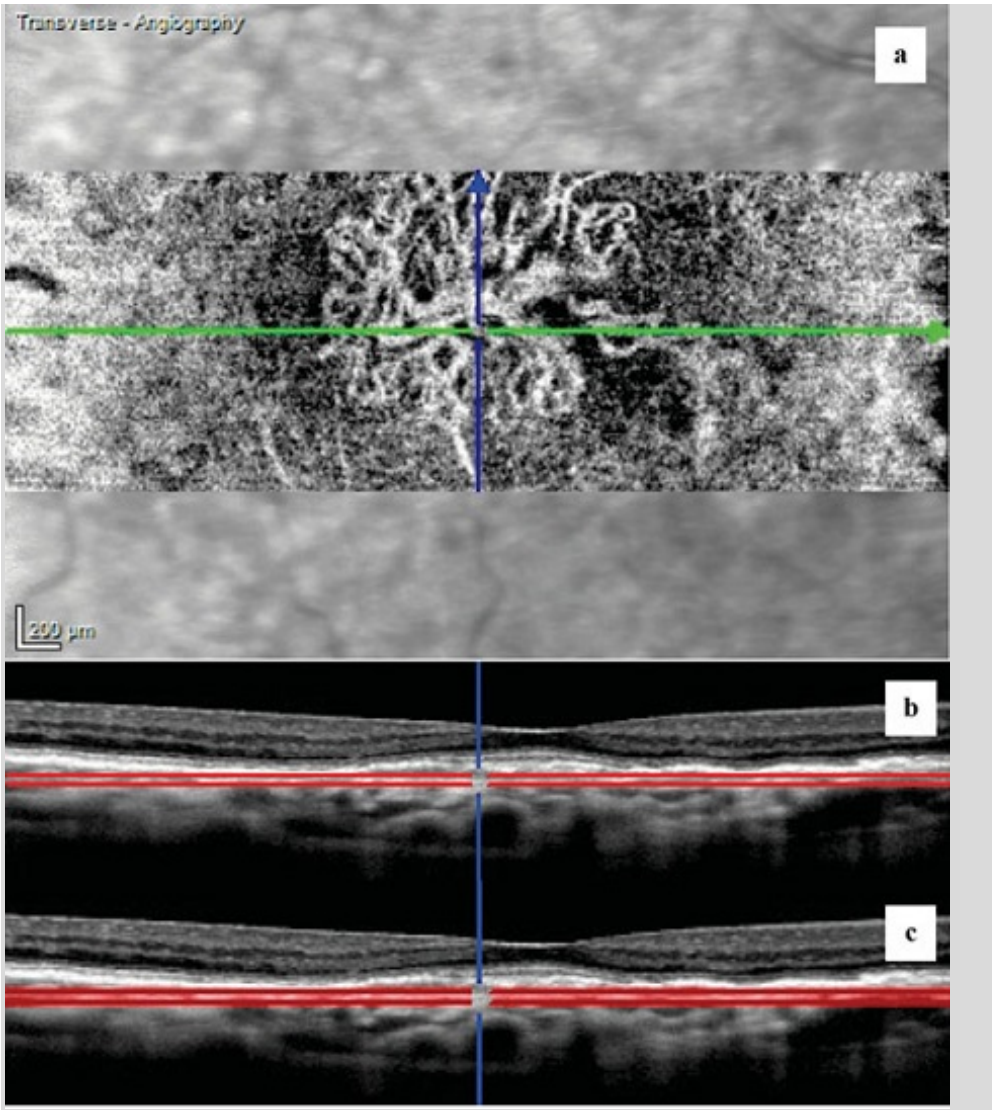

Figure 66: (a) OCT-A C-scan (above the Bruch’s membrane). The 30 µm C-scan section is positioned *deeper inside the PED*. It shows a “spiked-wheel”-shaped CNV. The centre of the lesion is mainly composed of large mature vessels that branch into some smaller ones towards the periphery. The number of anastomoses is limited and the vessel’s termini have a relative “dead-tree” appearance. **(b) OCT-Angio B-scan (above the Bruch’s membrane).** The OCT-Angio B-scan shows the position of the C-scan (*red lines*), in this case deeper inside the PED above the Bruch’s membrane. There is no fluid. **(c) Conventional OCT B-scan (above the Bruch’s membrane).** The conventional OCT B-scan shows the position of the C-scan (*red lines*), in this case deeper inside the PED above the Bruch’s membrane.There is no fluid accumulation.

Below the Bruch’s membrane (figure 67)

Below the Bruch's membrane directly inside the choroid, we appreciate a diffuse hyper-intense signal, probably due to remnants of the choriocapillaris and the Sattler's layer. There are also several high hypo-intense tubular structures because of large choroidal vessels draining, just below the lesion.

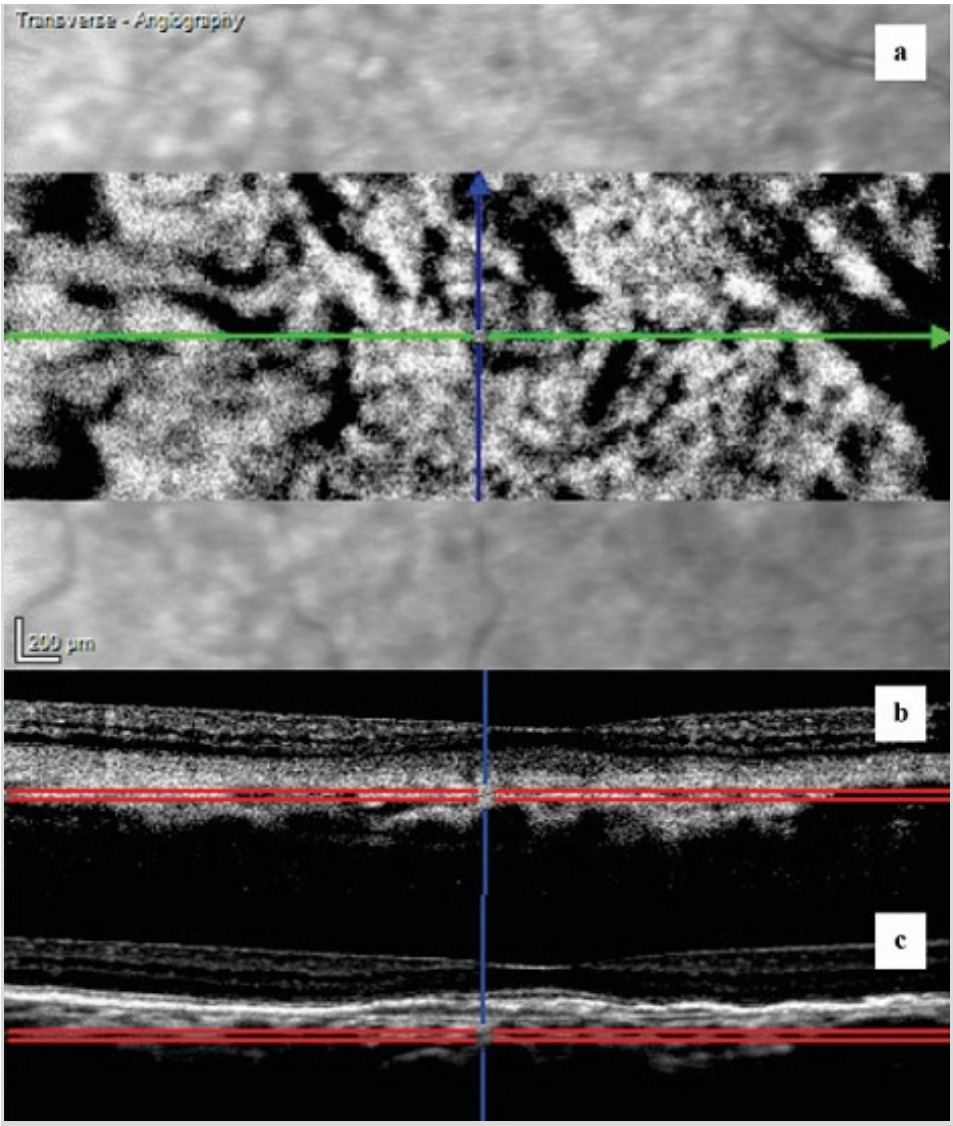

Figure 67: (a) OCT-A C-scan (below the Bruch's membrane). The 30 µm C-scan section is positioned below the Bruch's membrane, directly inside the choroid. A diffuse hyper-intense signal is evident, probably due to the remnants of the choriocapillaris and the Sattler's layer. There are also several high hypo-intense tubular structures bcause of the large choroidal vessels draining, just below the lesion. **(b) OCT-Angio B-scan (below the Bruch's membrane).** The OCT-Angio B-scan shows the position of the C-scan (*red lines*), in this case deep inside the choroid below the Bruch's membrane. **(c) Conventional OCT B-scan (below the Bruch's membrane).** The conventional OCT B-scan shows the position of the C-scan (*red lines*), in this case deep inside the choroid below the Bruch's membrane.

Suggested OCT-A diagnosis:

Type I mature neovascular lesion with no clear signs of activity.

No indication for prolongation of treatment.

10.4 Synthesis

The compliation of the different results is shown in **figure 68.**

ICGA reveals a hyper fluorescent neovascular lesion (*yellow dashed line*).

This network is mainly composed of several poorly-defined **large "mature" vessels** (*red arrows*).

These vessels are radiating from the centre to the periphery of the lesion.

OCT-A shows a **"spiked wheel"-shaped CNV** (*yellow dashed line*).

The centre of the lesion is mainly composed of **large mature vessels (***red arrows*) that **branch** into some smaller ones towards the periphery (*green arrows*).

The number of anastomoses is limited and the vessel's termini have a relatively **"dead-tree" appearance**.

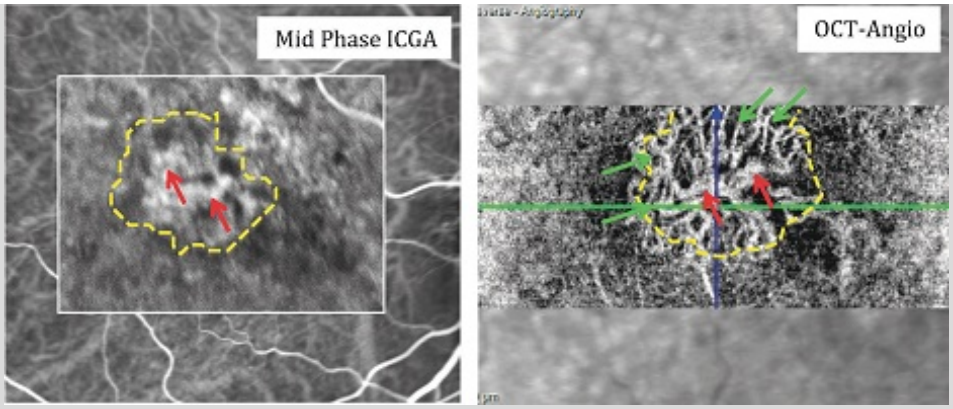

Figure 68: The ICGA (left) and the OCT-Angiography (right) clearly show a CNV Type I (subepithelial / occult).

Both ICGA and OCT-Angiography clearly show a Type I (subepithelial / occult) neovascular network.

This is a "Type I lesion", with a large, extensive, and subepithelial or occult neovascular network. The evidence of large mature vessels in the centre, radiating into smaller ones towards the periphery, poorly anastomosed, without peripheral arcades, and having a "dead tree" appearance, suggests a quiescent neovascular lesion. It does not appear to be necessary to prolong the treatment.

11 Clinical Case No. 7: Type 1 CNV (SUBEPITHELIAL OR OCCULT) – STILL ACTIVE

11.1 Clinical and biomicroscopic signs

A 70-year-old woman presented with gradual loss of vision and metamorphopsia in her left eye.

- BCVA RE: 20/25
- BCVA LE: 20/63

Biomicroscopic examination revealed a macular lesion of about two Disc Diameters (DD) with numerous drusen, involving a large part of the posterior pole.

11.2 Traditional multimodal imaging

Autofluorescence (figure 69)

The image shows the presence of a central hypo-fluorescent lesion (due to substantial impairment of macular pigment) in the macula, surrounded by an intense, oval shaped, hyper-fluorescent halo.

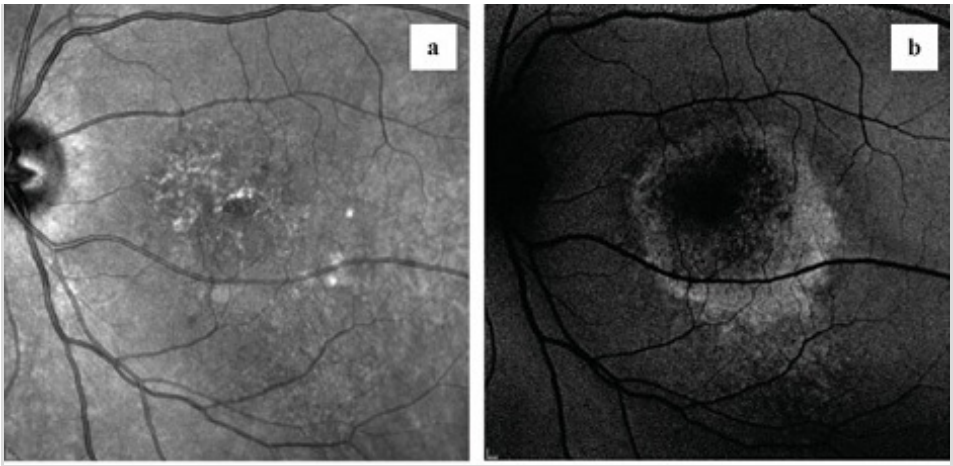

Figure 69: (a) Infrared. Macular lesion of about two Disc Diameters (DD) with numerous drusen involving a large part of the posterior pole. **(b) Autofluorescence.** Central macular hypo-fluorescent lesion (due to substantial impairment of macular pigment), surrounded by an intense, oval shaped, hyper-fluorescent halo.

Fluorescein angiography, FA **(figure 70)**

The early arterio-venous phase shows a hyper fluorescent macular lesion with pinpoints. An irregular hypo-fluorescent area surrounds and partially masks the lesion.

In the late phase of FA, the hyper-fluorescent area tends to enlarge. Fluorescein leakage appears especially at the borders of the CNV.

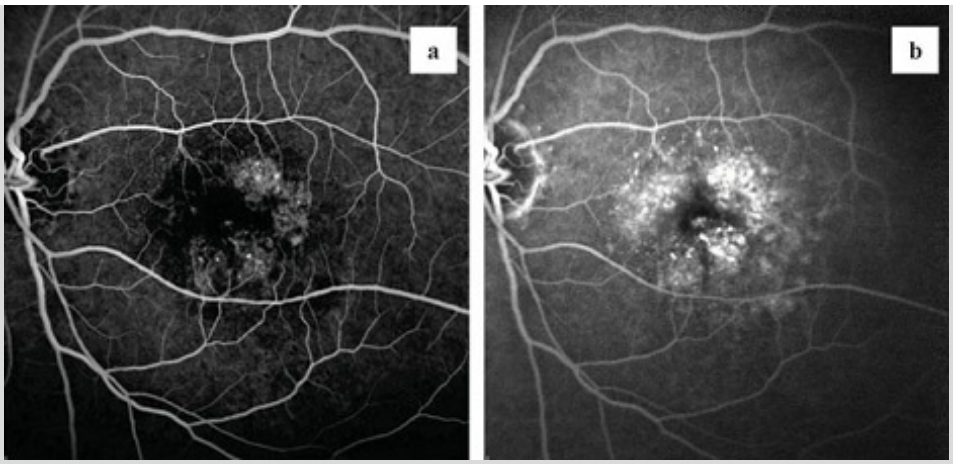

Figure 70: (a) Fluorescein angiography (arterio-venous phase). Hyper-fluorescent macular lesion with pinpoints. An irregular hypo-fluorescent area surrounds and partially masks the lesion. **(b) Fluorescein angiography (late phase).** The hyper-fluorescent area tends to enlarge, and fluorescein leakage appears mainly at the borders of the CNV.

Indocyanine Green Angiography, ICGA **(figure 71)**

From the early arterio-venous phase, a Type I (subepithelial / occult) CNV is visible, forming a well-defined neovascular network. There are several large mature vessels radiating from the centre to the periphery of the CNV.

In the late venous phase, the borders of the CNV are more visible. The entire hyper-fluorescent area is surrounded by a hypo-fluorescent halo, due to the well-demarcated PED.

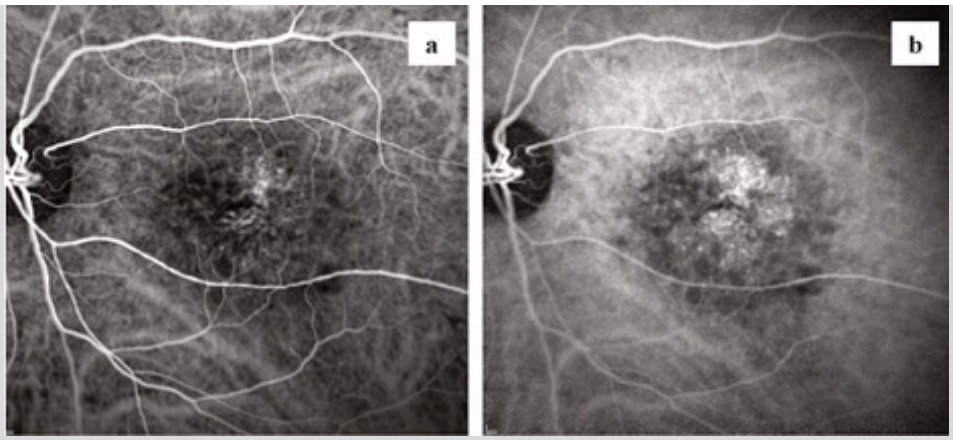

Figure 71: (a) ICG angiography (arterio-venous phase). A Type I (subepithelial / occult) CNV is observed from the early arterio-venous phase, forming a well-defined neovascular network. There are several large mature vessels radiating from the centre to the periphery of the CNV. **(b) ICG angiography (late phase).** The borders of the CNV are more visible. The

entire hyper-fluorescent area is surrounded by a hypo-fluorescent halo, due to the well-demarcated fibrovascular PED.

Optical Coherence Tomography, SD-OCT **(figure 72)**

The foveal depression is partially maintained with limited subretinal fluid accumulation.The outer retinal layers (especially the outer nuclear layer) are substantially thinned near the borders of the wide, fibrovascular PED. There are focal interruptions in the ELM and the EZ swelling.

A fibrovascular PED, involving almost the entire macular area, has resulted in an upward dislocation of the neurosensory retina. The PED has a heterogeneous hyper-reflective appearance, probably due to the concomitant presence of new vessels and scar tissue.

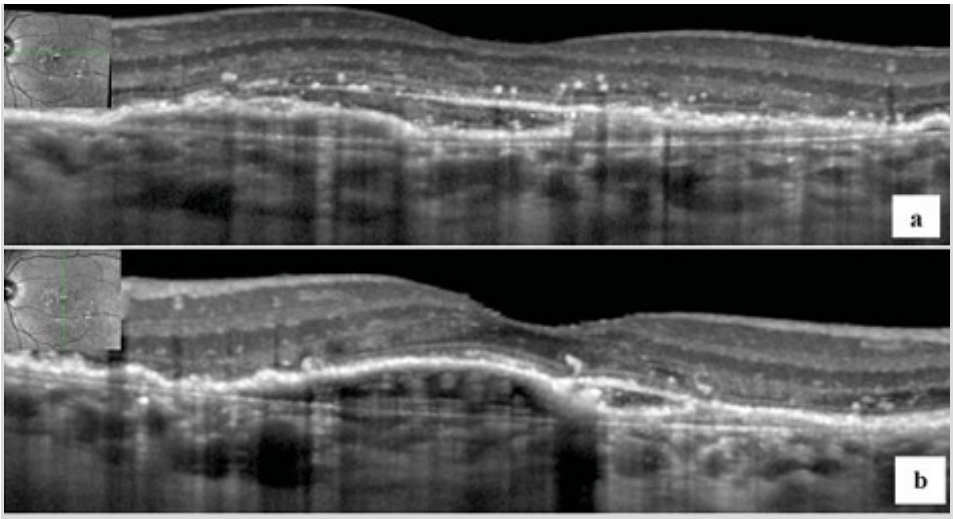

Figure 72: SD-OCT. The foveal depression is partially maintained with limited subretinal fluid accumulation. The outer retinal layers (especially the outer nuclear layer) are substantially thinned near the borders of the wide, fibrovascular PED. There are focal interruptions in the ELM and EZ swelling. A fibrovascular PED, involving almost the entire macular area, has resulted in an upward dislocation of the neurosensory retina. The PED has a heterogeneous hyper-reflective appearance, probably due to the concomitant presence of new vessels and scar tissue.

Suggested multimodal imaging diagnosis:

Quiescent Type I neovascular lesion.

11.3 OCT-Angiography

The OCT angiogram is evaluated with multiple 30 µm thickness transverse C-scans, starting 30 µm above the RPE and ending at the choroidal-scleral interface. The 30 µm-step outer retinal / choroidal analysis allows complete imaging of the entire lesion by highlighting different decorrelation signals, but only if they belong to coplanar structures.

Just above the RPE (figure 73)

In the 30 µm-thickness C-scan, just above the RPE, there is no evidence of a clear decorrelation signal that could be attributed to choroidal neovascularization.

Some hyper-intense signals are due to “pseudo-images” of the retinal vessels, caused by the reflectivity of the RPE or by the proximity of some intensively perfused structures (choriocapillaris).

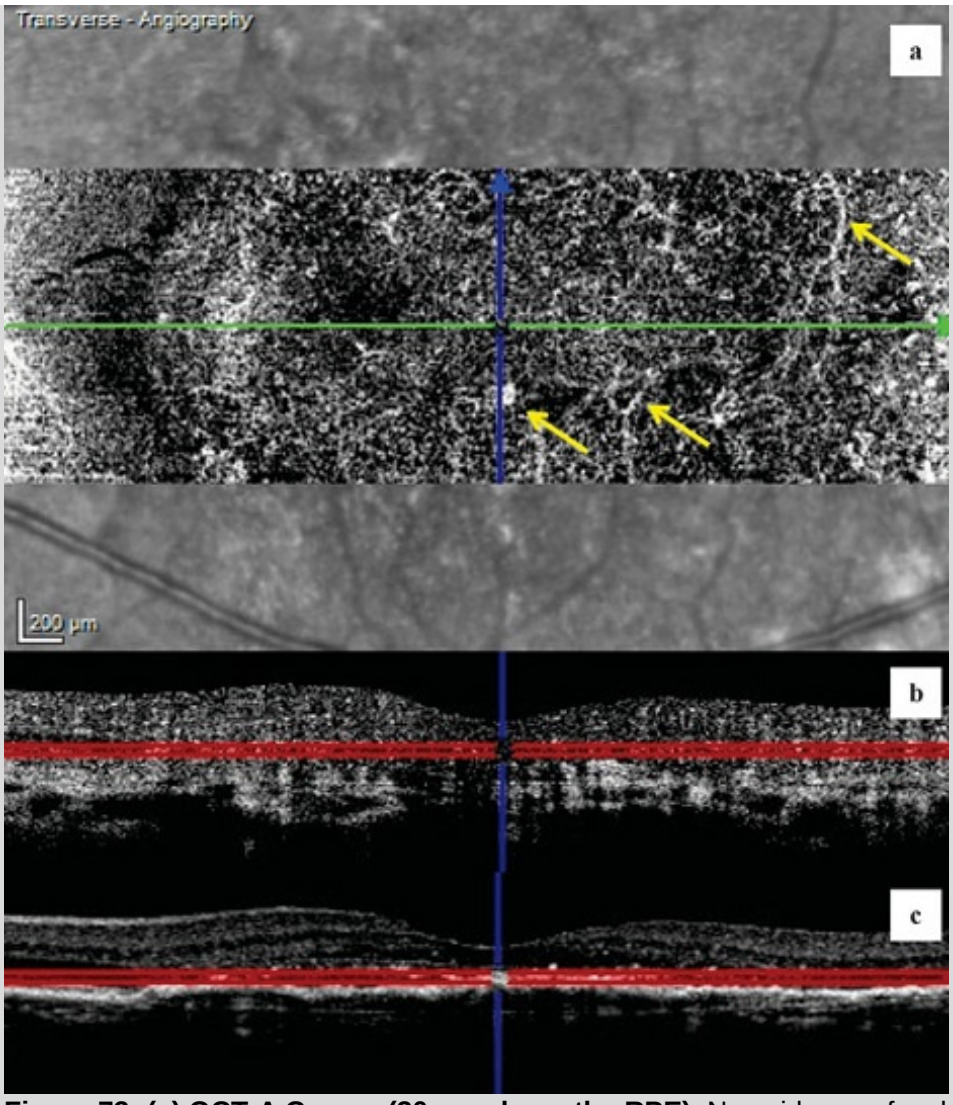

Figure 73: (a) OCT-A C-scan (30 µm above the RPE). No evidence of a clear decorrelation signal that could be attributed to the CNV. The hyper-intense signal is due to “pseudo-images” of retinal vessels (*yellow arrows*), caused by the reflectivity of the RPE or by the proximity of some intensely perfused structures (choriocapillaris). **(b) OCT-Angio B-scan (30 µm above the RPE).** An evident decorrelation signal is appreciable from both retinal and choroidal vasculature. A pathologic hyper-intense signal is also present below the scanned area (*red lines*). **(c) Conventional OCT B-scan (30 µm above the RPE).** The conventional OCT is useful to identify the exact location of the lesion above the RPE (*red lines*) and the presence of subretinal fluid accumulation.

At the back surface of the RPE (figure 74)

The next C-scan section is placed at the back surface of the RPE and therefore inside the PED.

Several large mature vessels are seen forming a well-defined neovascular network.

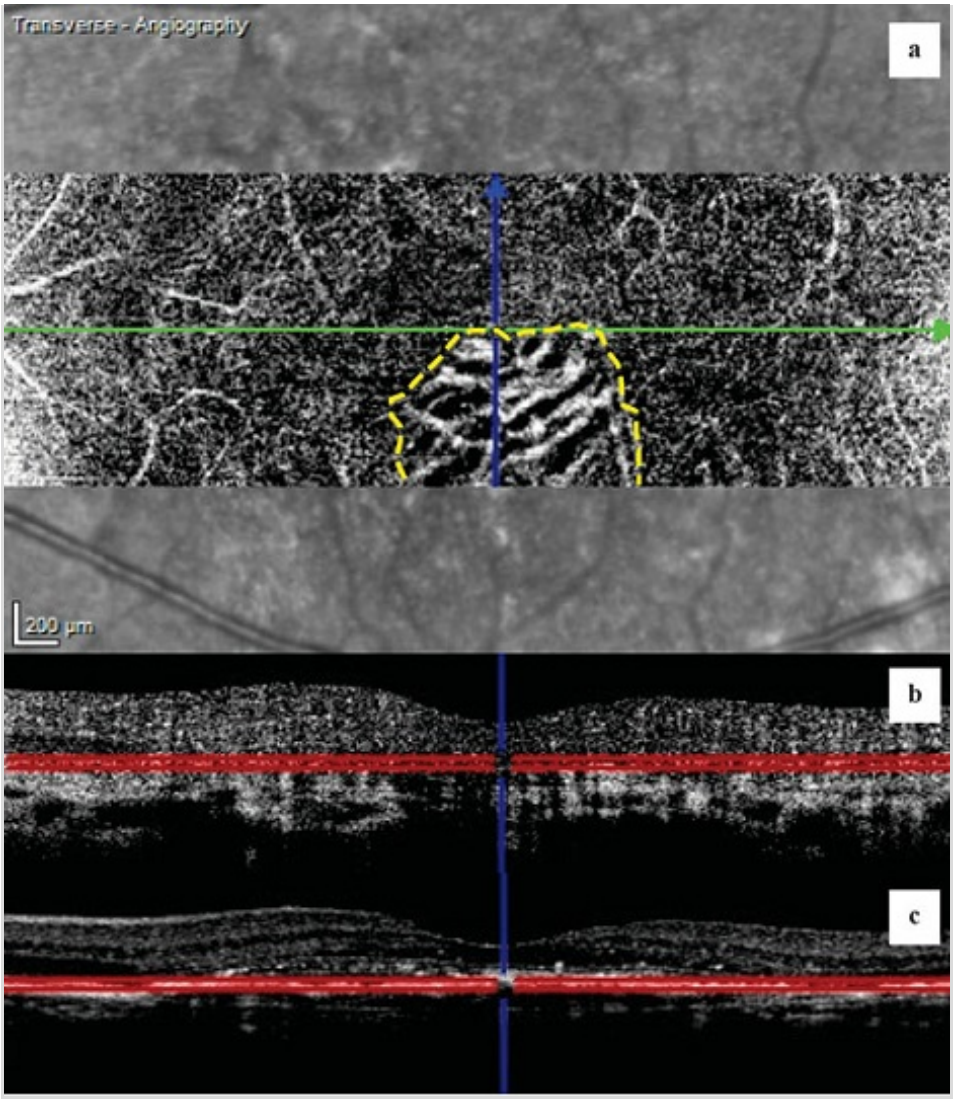

Figure 74: (a) OCT-A C-scan (back surface of the RPE). The 30 µm C-scan section is positioned at the back surface of the RPE and therefore inside the PED. Some large "mature" vessels are seen forming a well-defined neovascular network (*yellow dashed line*). **(b) OCT-Angio B-scan (back surface of the RPE).** The OCT-Angio B-scan shows the position of the C-scan (*red lines*), in this case at the back surface of the RPE. (**c) Conventional OCT B-scan (back surface of the RPE).** The conventional OCT B-scan shows the position of the C-scan (*red lines*), in this case at the back surface of the RPE.

Deeper inside the PED (figure 75)

The following C-scan, deeper inside the PED, almost shows the entire CNV, which has a typical “sea-fan” shape.

There is a wide network of large mature vessels in the centre, but they branch into numerous tiny ones toward the periphery. These small, peripheral vessels are anastomosed and sometimes form a partial peripheral arcade at the border of the lesion.

This appearance could **be an index of persistent activity** of the CNV.

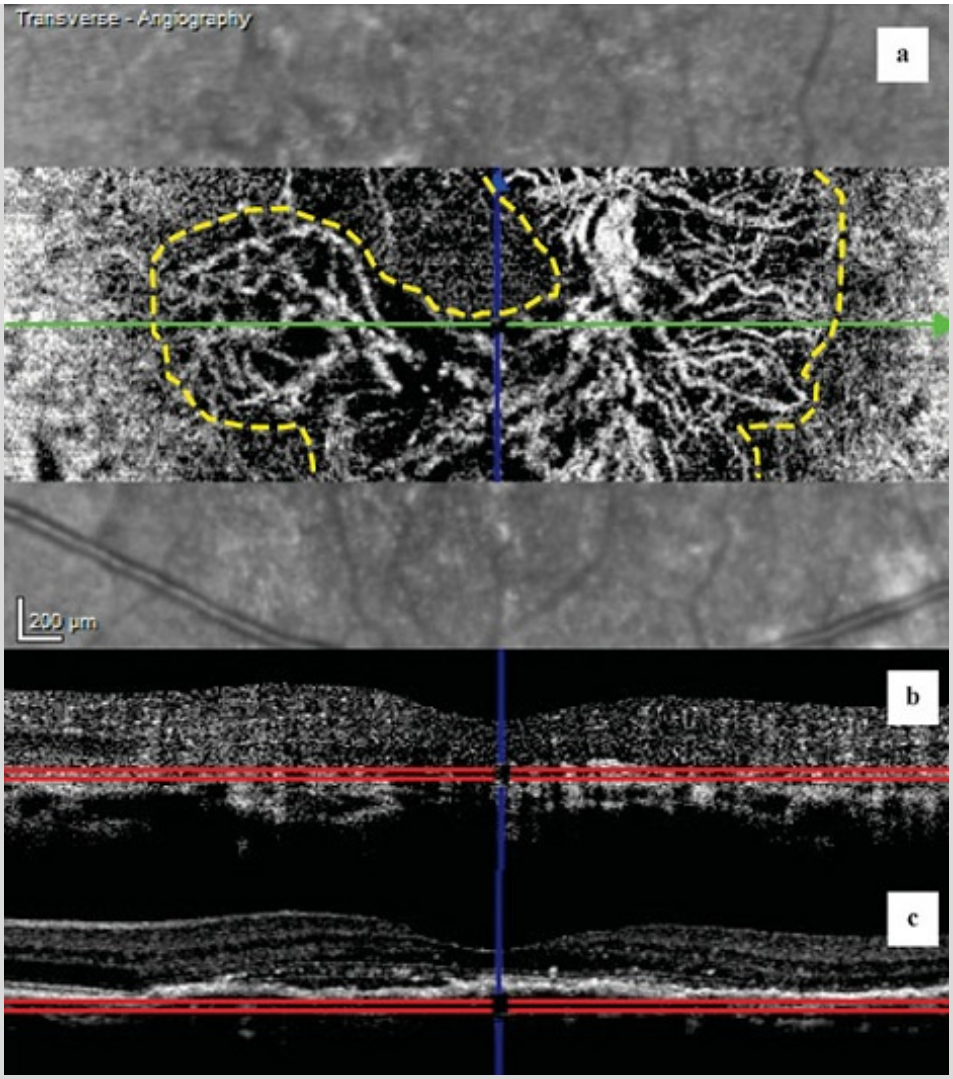

Figure 75: (a) OCT-A C-scan (above the Bruch’s membrane). The 30 µm C-scan section is positioned deeper inside the PED. It shows almost the entire CNV *(yellow dashed line*) which has a typical “sea-fan” shape. There is a wide network of large “mature“ vessels that branch into numerous tiny ones towards the periphery. These small, peripheral vessels are anastomosed and sometimes form a partial peripheral arcade at the border of the lesion. **(b) OCT-Angio B-scan (above the Bruch’s membrane).** The OCT-Angio B-scan shows the position of the C-scan (*red lines*), in this case deeper inside the PED above the Bruch’s membrane. **(c) Conventional OCT B-scan (above the Bruch’s membrane).** The conventional OCT B-scan shows the position of the C-scan (*red lines*), in this case deeper inside the PED above the Bruch’s membrane.

Below the Bruch’s membrane (figure 76)

Below the Bruch's membrane, directly inside the choroid, we appreciate a diffuse hyper-intense signal that is probably caused by remnants of the choriocapillaris and the Sattler's layer.

There are high hypo-intense linear structures due to the large choroidal draining vessels immediately below the lesion.

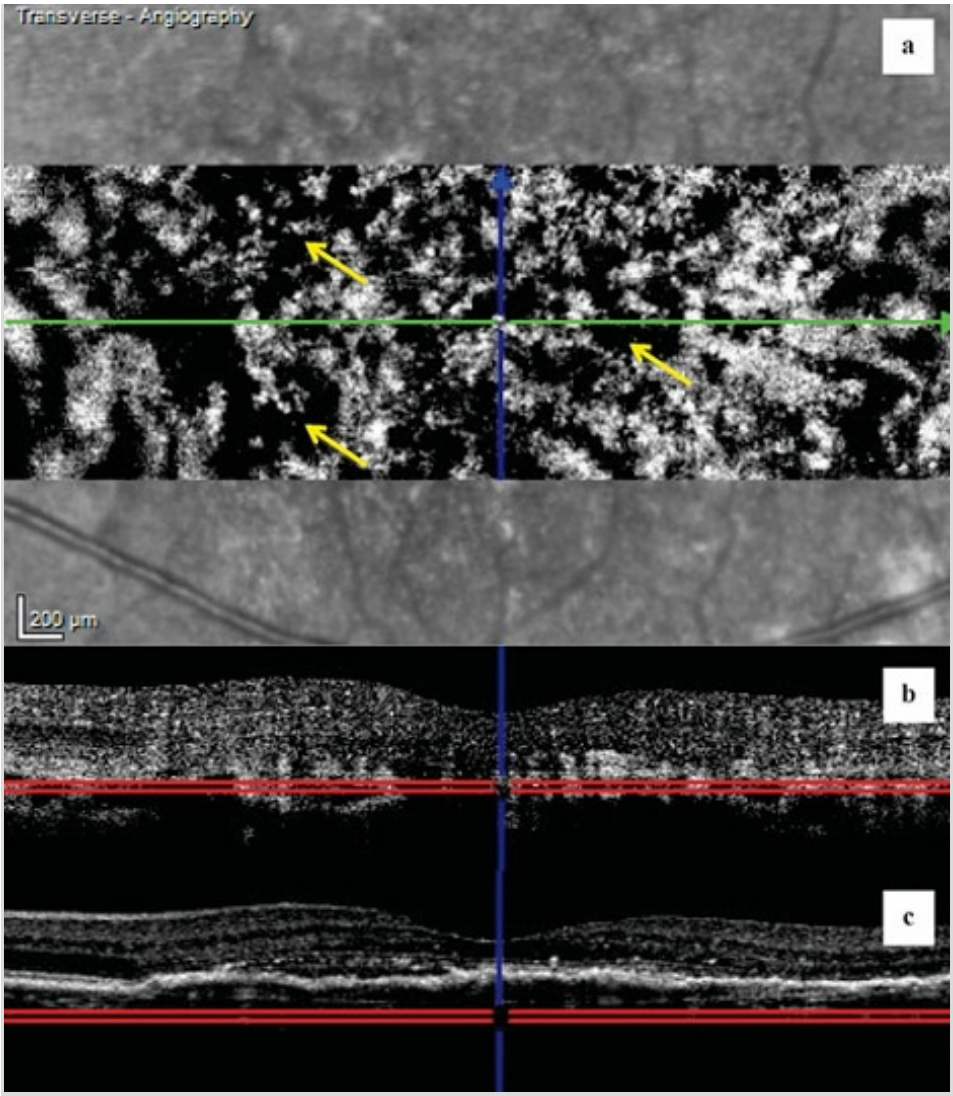

Figure 76: (a) OCT-A C-scan (below the Bruch's membrane). The 30 µm C-scan section is positioned below the Bruch's membrane, directly inside the choroid. A diffuse hyper-intense signal is appreciable, probably caused by remnants of the choriocapillaris and the Sattler's layer. There are high hypo-intense central structures due to the large choroidal vessels draining immediately below the lesion. **(b) OCT-Angio B-scan (below the Bruch's membrane).** The OCT-Angio B-scan shows the position of the C-scan (*red lines*), in this case deep inside the choroid below the Bruch's membrane. **(c) Conventional OCT B-scan (below the Bruch's membrane).** The conventional OCT B-scan shows the position of the C-scan (*red lines*), in this case deep inside the choroid below the Bruch's membrane.

Suggested OCT-A diagnosis:

Type I mature neovascular lesion with no clear signs of activity.

No indication for prolongation of treatment.

11.4 Synthesis

The compliation of the different results is shown in **figure 77.**

ICGA shows a broad Type I (subepithelial / occult) CNV from the early arterial-venous phase, forming a **well-defined neovascular network**.

There are **several large mature vessels** (*red arrows*) with a radial distribution that originates in the centre of the lesion.

OCT-A shows almost the **entire CNV** (*yellow dashed line*), which has a **typical "sea-fan" shape**.

There is a wide network of **large "mature" vessels** (*red arrows*) that **branch** into **numerous tiny ones** towards the periphery.

These small, peripheral vessels are **anastomosed** and sometimes form a partial **peripheral arcade** (*green arrows*) at the border of the lesion. This appearance could be an index of activity of the CNV

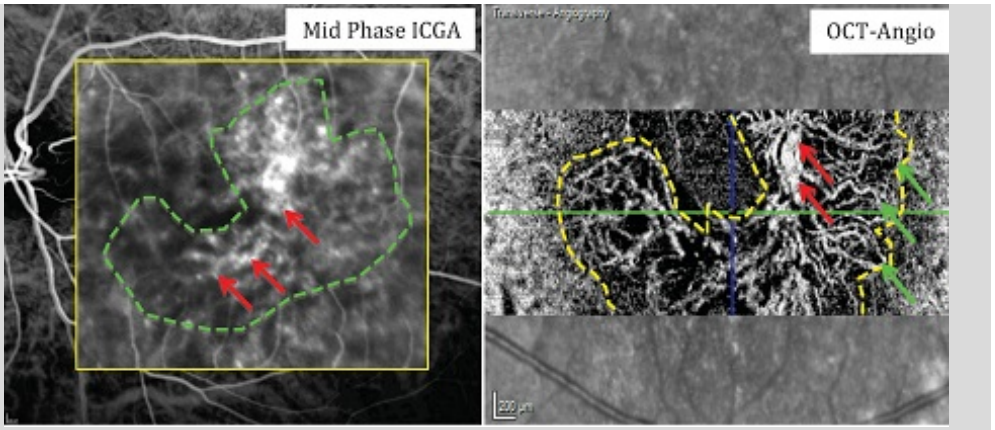

Figure 77: The ICGA (left) and the OCT-Angiography (right) clearly show a CNV Type I (subepithelial / occult).

Both ICGA and OCT-Angiography clearly show a Type I (subepithelial / occult) neovascular network.

This is a "Type I lesion", with a large, extensive, and subepithelial (or occult) neovascular network. The evidence of numerous tiny vessels that are anastomosed, with partial peripheral arcades and having a typical "sea fan" appearance suggests a still active neovascular lesion.

Therefore, the prolongation of intra-vitreal treatment is indicated.

12 CLINICAL CASE NO. 8: ATROPHIC AMD

12.1 Clinical and biomicroscopic signs

A 71-year-old man presented with an established diagnosis of atrophic AMD.

- BCVA RE: 20/80
- BCVA LE: 20/400

Biomicroscopic examination revealed an atrophic lesion of about 2/3 Disc Diameters (DD) in the macula. Several hard drusen were seen at the posterior pole, mainly in the border of the lesion.

12.2 Traditional multimodal imaging

Autofluorescence (figure 78)

The image shows a large hypo-fluorescent lesion due to loss of macular pigment that is surrounded by a marked hyper-fluorescent halo.

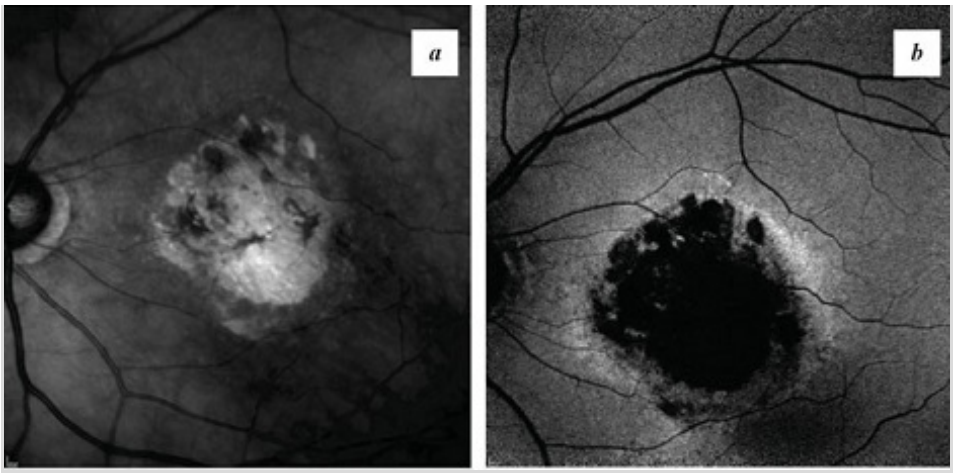

Figure 78: (a) Infrared. Atrophic lesion of about 2/3 Disc Diameters (DD) in the macula. Several hard drusen are also seen in the posterior pole, mainly at the border of the lesion. **(b) Autofluorescence.** The image shows a large hypo-fluorescent lesion due to loss of macular pigment that is surrounded by a marked hyper-fluorescent halo.

Fluorescein angiography, FA **(figure 79)**

The early arterio-venous phase shows a well-circumscribed and hyper-fluorescent macular lesion, with pinpoints. There are also some hypo-fluorescent areas inside the lesion (possible RPE hyperplasia).

In the late phase of FA, the hyper-fluorescent area does not increase (staining effect) or show appreciable signs of fluorescein leakage.

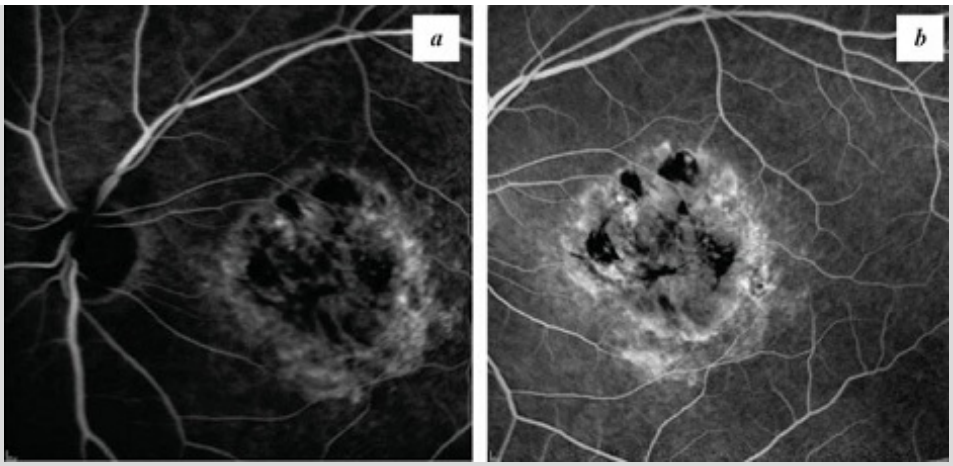

Figure 79: (a) Fluorescein angiography (arterio-venous phase). Well-circumscribed hyper-fluorescent macular lesion with pinpoints. There are also some hypo-fluorescent areas inside the lesion (RPE hyperplasia). **(b) Fluorescein angiography (late phase).** The hyper-fluorescent area does not increase (staining effect) or show appreciable signs of fluorescein leakage.

Indocyanine Green Angiography, ICGA **(figure 80)**

In the early venous phase, a large window defect is seen in the macular area allowing a clear visualization of the large choroidal vessels.

In the late phase, the large geographic atrophy in the macular area remains the main finding. There is no evidence of a choroidal neovascular network.

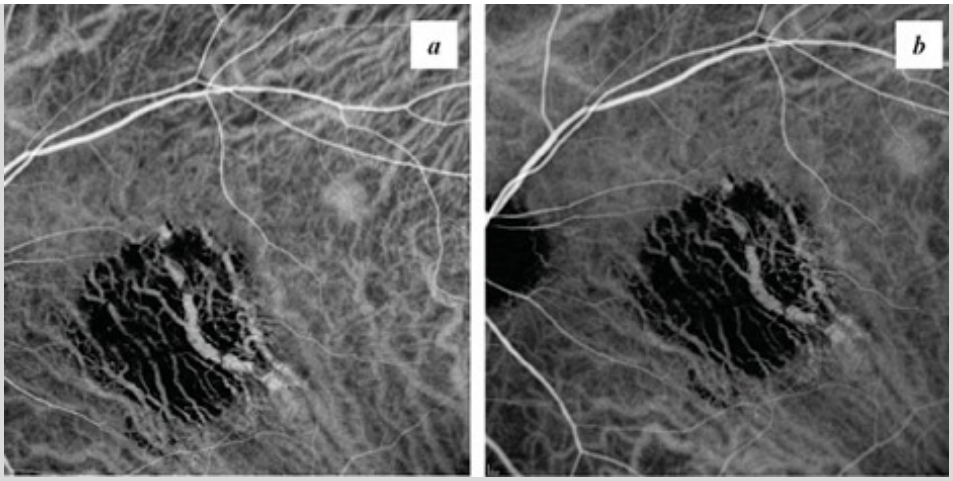

Figure 80: (a) ICG angiography (arterio-venous phase). A large window defect is seen in the macular area allowing clear visualization of the large choroidal vessels. **(b) ICG angiography (late phase).** In the late phase, the large geographic atrophy in the macular area remains the main finding. No evidence of choroidal neovascular network.

Optical Coherence Tomography, SD-OCT **(figure 81)**

The foveal depression is substantially impaired without sub/intra-retinal fluid accumulation. There is a diffuse outer retinal atrophy in the macular area, involving almost all the layers from the inner nuclear layer to the photoreceptors.

The RPE is not seen in the subfoveal area. Areas of focal thickening at the border of the atrophy appear, probably due to RPE hyperplasia. The choroid is significantly thinned in the macular area, and only some large choroidal vessels can be seen.

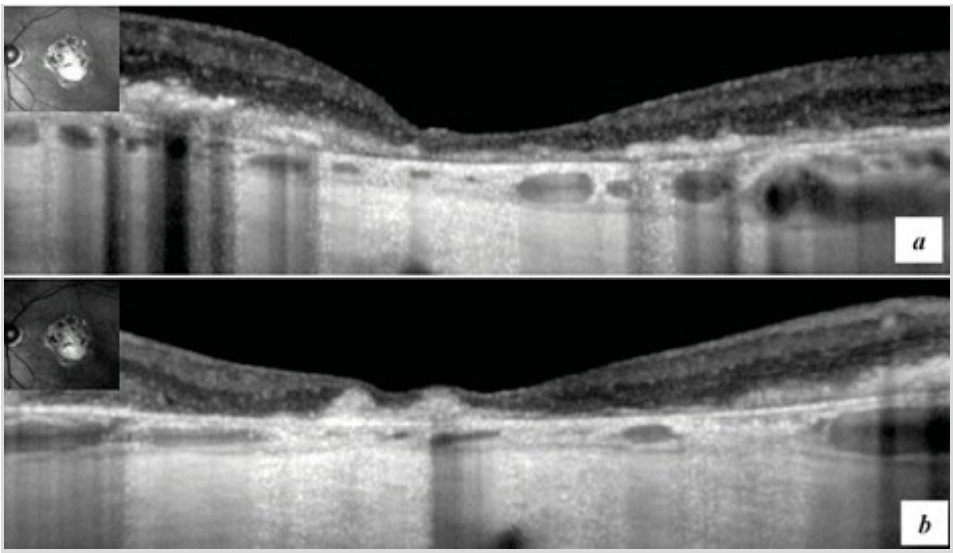

Figure 81: SD-OCT. The foveal depression is substantially impaired without sub-/intraretinal fluid accumulation. There is a diffuse outer retinal atrophy in the macular area, involving almost all the layers from the inner nuclear layer to the photoreceptors. The RPE is not visible in the subfoveal area. Areas of focal thickening at the border of the atrophy appear, probably due to RPE hyperplasia. The choroid is significantly thinned in the macular area and only some large choroidal vessels are appreciable.

Suggested multimodal imaging diagnosis:

Atrophic AMD without evidence of CNV.

No indication for treatment with intra-vitreous injections.

12.3 OCT-Angiography

The OCT-A analysis of the large atrophic area starts from the inner retinal layers in order to show the area of superficial capillary plexus perfusion.

The outer retinal layers and the choroid are evaluated with multiple 30 µm thickness C-scans, shaped on the Bruch's membrane profile, starting 30 µm above the RPE and ending at the choroidal-scleral interface. The 30 µm-step outer retinal/choroidal analysis allows complete imaging of the entire atrophic lesion by highlighting different decorrelation signals, but only if they belong to coplanar structures.

At the level of the ganglion cells layer E (figure 82)

The first OCT-A image is a 30 µm thickness C-scan, shaped on the IML profile and taken at the level of the ganglion cells layer, where the superficial capillary plexus (SCP) is normally located.

In this case, a significantly enlarged perifoveal arcade is evident due to the extensive retinal impairment, caused by severe geographic atrophy. The SCP appears almost fully preserved and normally perfused.

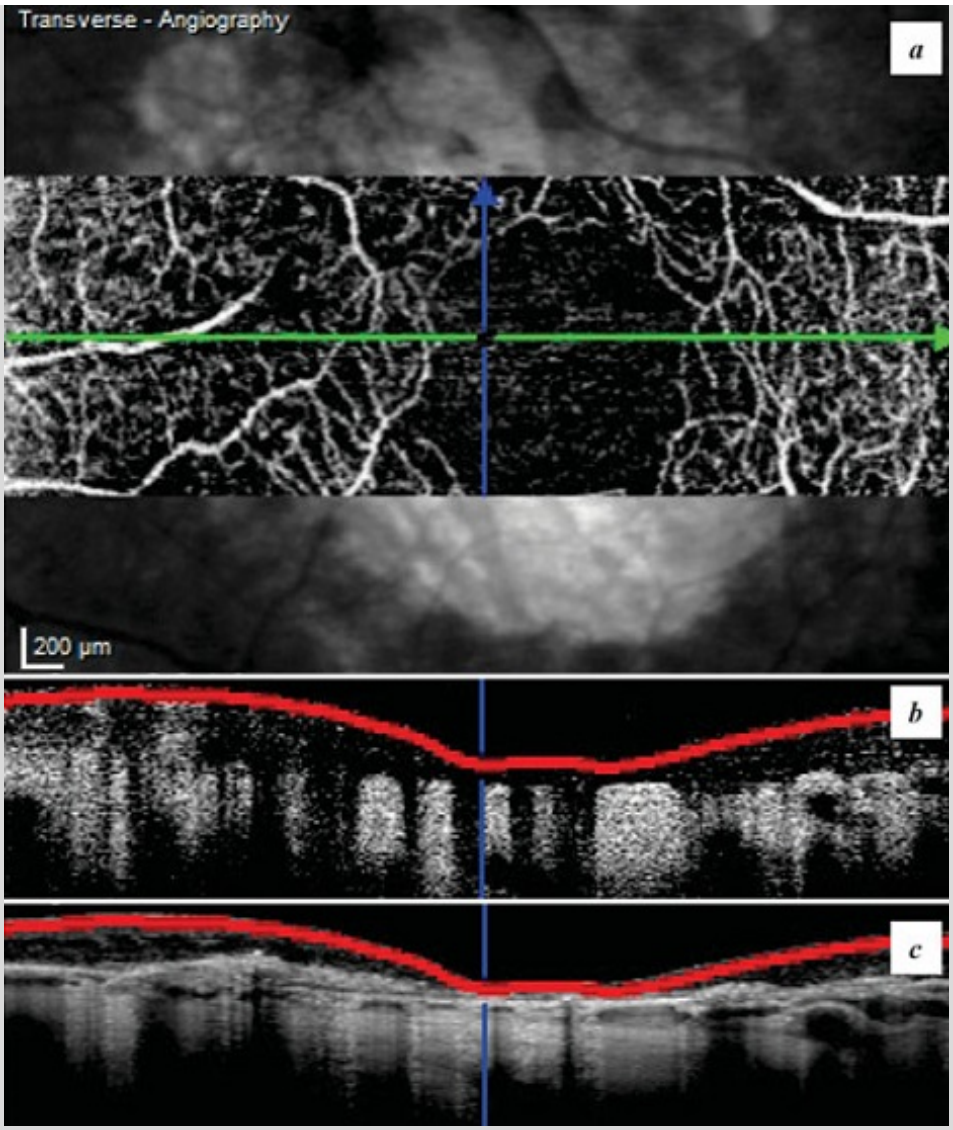

Figure 82: (a) OCT-A C-scan (at the level of the ganglion cells layer). 30-µm-thickness C-scan shaped on the ILM profile and taken at the level of the ganglion cells layer, where the superficial capillary plexus (SCP) is normally located. In this case, a *significantly enlarged perifoveal arcade* is seen due to the extensive retinal impairment caused by severe geographic atrophy. The SCP appears to be almost fully preserved and normally perfused. **(b) OCT-Angio B-scan (at the level of the ganglion cells layer).** An evident decorrelation signal is appreciable from both retinal and choroidal vasculature. **(c) Conventional OCT B-scan (at the level of the ganglion cells layer).** The conventional OCT is useful to identify the ocation of the C-scan section.

Just above the RPE (figure 83)

In the 30 µm thickness C-scan just above the RPE there is no evidence of a clear decorrelation signal that could be attributed to Type II choroidal neovascularization.

The hyper-intense signal is due to “pseudo-images” of the retinal vessels, caused by the reflectivity of the RPE or by the proximity of some intensively perfused structures (remnants of choriocapillaris resp. Sattler’s layer).

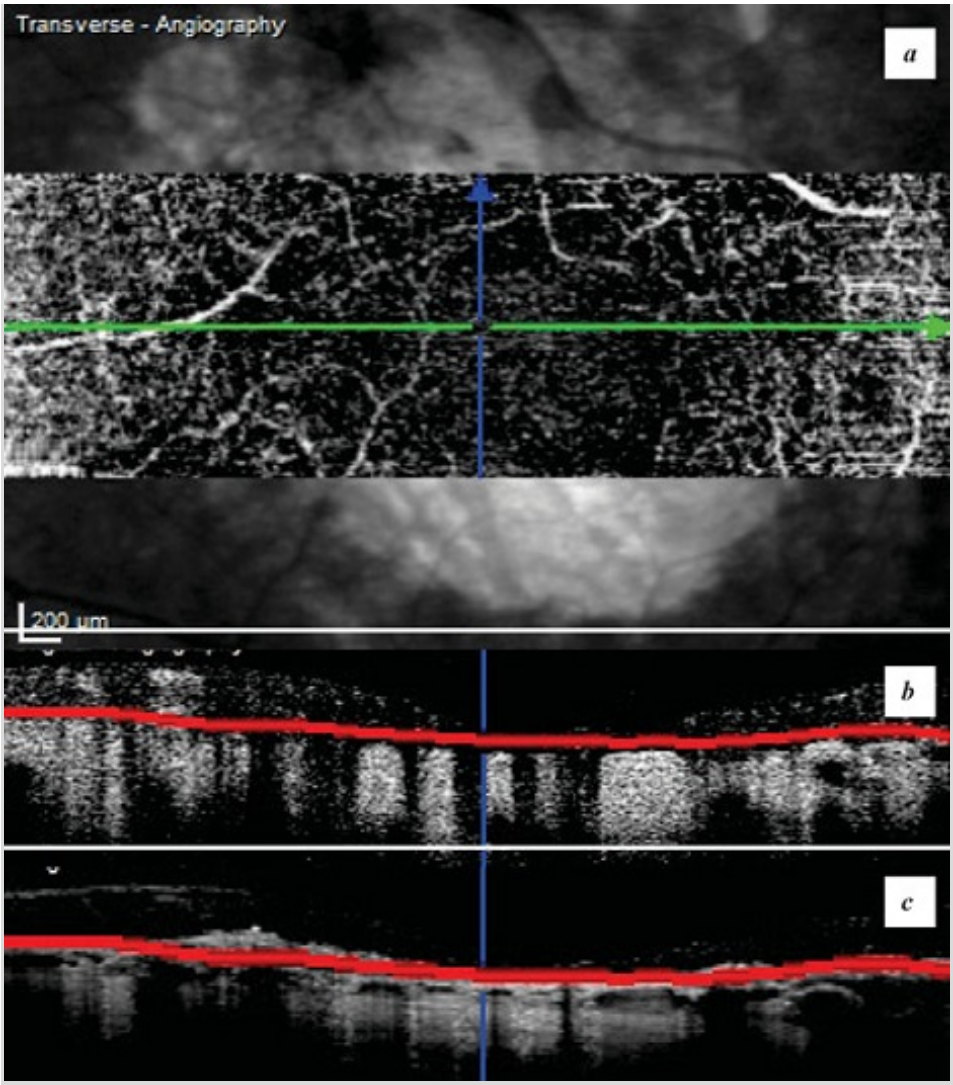

Figure 83: (a) OCT-A C-scan (30 µm above the RPE in the foveal area). There is no evidence of a clear decorrelation signal that could be attributed to Type II choroidal neovascularization. The hyper-intense signal is due to “pseudo-images” of the retinal vessels, caused by the reflectivity of the RPE or by the proximity of some intensively perfused structures (remnants of choriocapillaris resp. Sattler’s layer). **(b) OCT-Angio B-scan (30 µm above the RPE in the foveal area).** An evident decorrelation signal is appreciable from both retinal and choroidal vasculature. **(c) Conventional OCT B-scan (30 µm above the RPE in the foveal area).** The conventional OCT is useful to identify the exact location of the C-scan section (*red lines*).

At the back surface of the RPE (figure 84)

The next C-scan section is placed at the back surface of the remnants of the RPE, below the Bruch's membrane.

The clear visualization of some mid-diameter vessels (Sattler's Layer) and large choroidal vessels (Haller's Layer) is due to the diffuse atrophy of choriocapillaris.

There is no evidence of any decorrelation signal that could be attributed to a neovascular network.

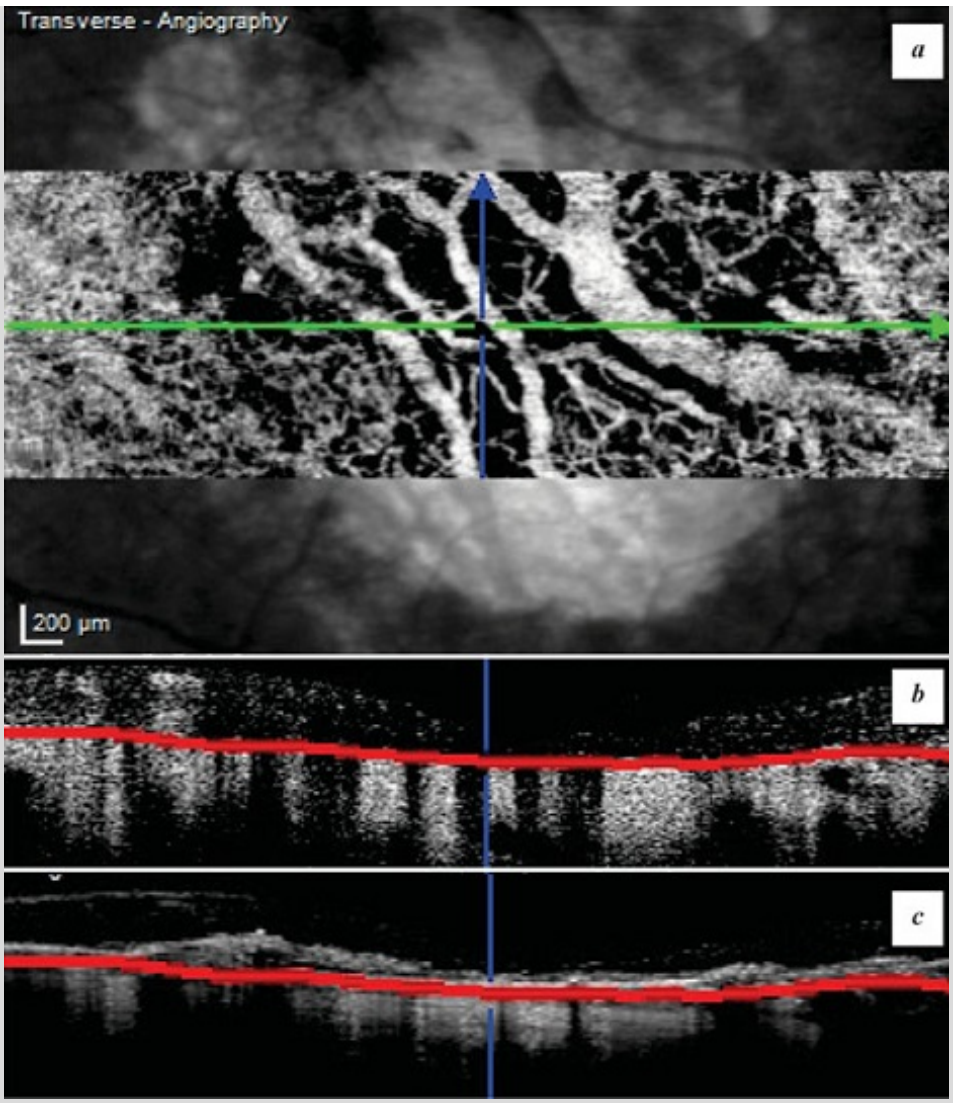

Figure 84: (a) OCT-A C-scan (back surface of the RPE). The next C-scan section is placed at the back surface of the remnants of the RPE, below the Bruch's membrane. There is a clear visualization of some mid-diameter vessels (Sattler's Layer) and large choroidal vessels (Haller's Layer) due to diffuse atrophy of choriocapillaris. There is no evidence of any decorrelation signal that could be attributed to a neovascular network. **(b) OCT-Angio B-scan (back surface of the RPE).** The OCT-Angio B-scan shows the position of the C-scan (*red lines*), in this case at the back surface of the RPE. (**c) Conventional OCT B-scan (back surface of the RPE).** The conventional OCT B-scan shows the position of the C-scan (*red lines*), in this case at the back surface of the RPE.

Deep inside the choroid (figure 85)

Deep inside the choroid, we appreciate a diffuse hyper-intense signal of the large choroidal vessels that is caused by the atrophy of all choroidal vascular layers above.

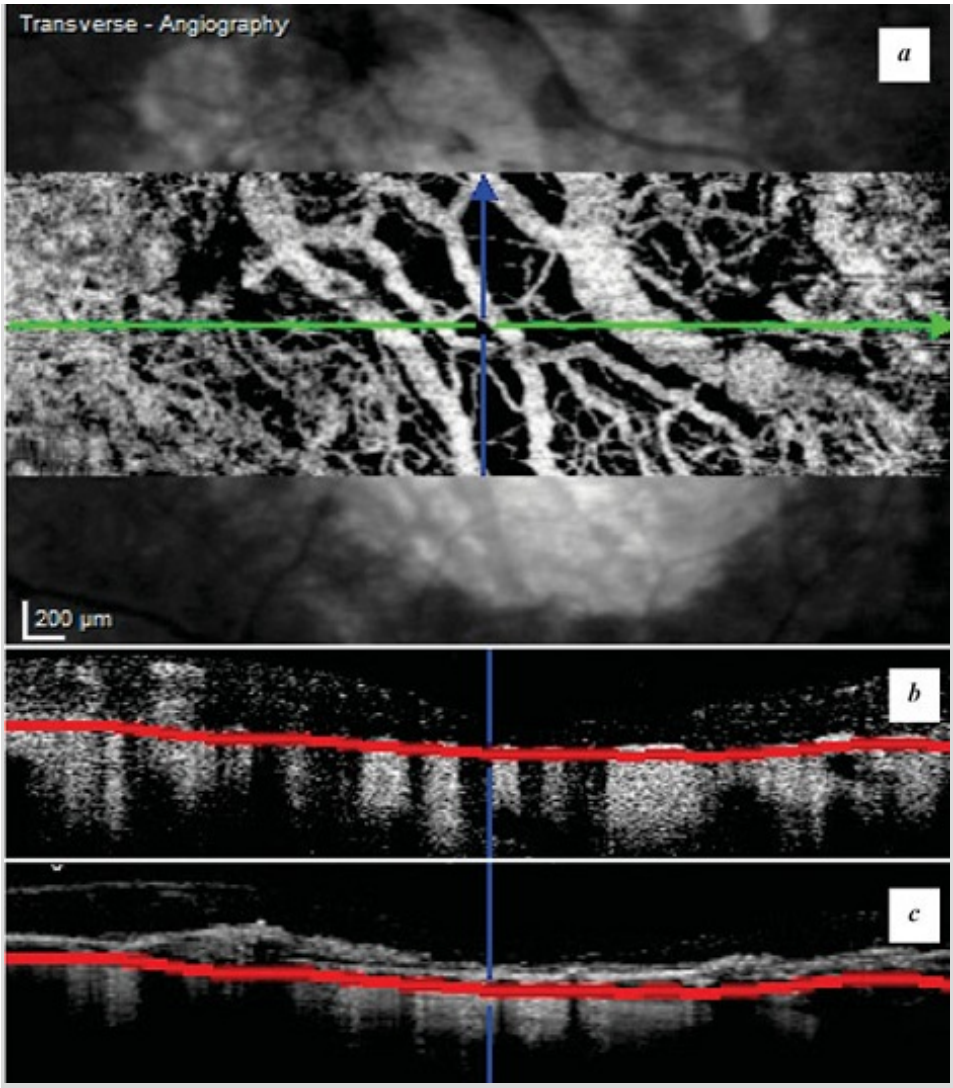

Figure 85: (a) OCT-A C-scan (below the Bruch's membrane). Deep inside the choroid, we appreciate a diffuse hyper-intense signal of the large choroidal vessels that is caused by atrophy of all choroidal vascular layers above. **(b) OCT-Angio B-scan (below the Bruch's membrane).** The OCT-Angio B-scan shows the position of the C-scan (*red lines*), in this case deep inside the choroid. This scan is characterized by a hyper-intense decorrelation signal coming from the large choroidal vessels. **(c) Conventional OCT B-scan (below the Bruch's membrane).** The conventional OCT B-scan shows the position of the C-scan (*red lines*), in this case deep inside the choroid.

Suggested OCT-A diagnosis:

Atrophic AMD without any evidence for choroidal neovascularization.

No indication for treatment with intra-vitreous injections.

12.4 Synthesis

The compliation of the different results is shown in **figure 86.**

ICGA shows a **large window defect** in the macular area (*yellow dashed line*).

This will allow a clear visualization of the **large choroidal vessels** (*red arrows*).

No evidence of choroidal neovascular network is seen.

OCT-A shows some **mid-diameter vessels** (Sattler's Layer – *green arrows*) and **large choroidal vessels** (Haller's Layer – *red arrows*).

This is due to the **diffuse atrophy of the choriocapillaris**.

There is no evidence of any decorrelation signal that could be attributed to a neovascular network.

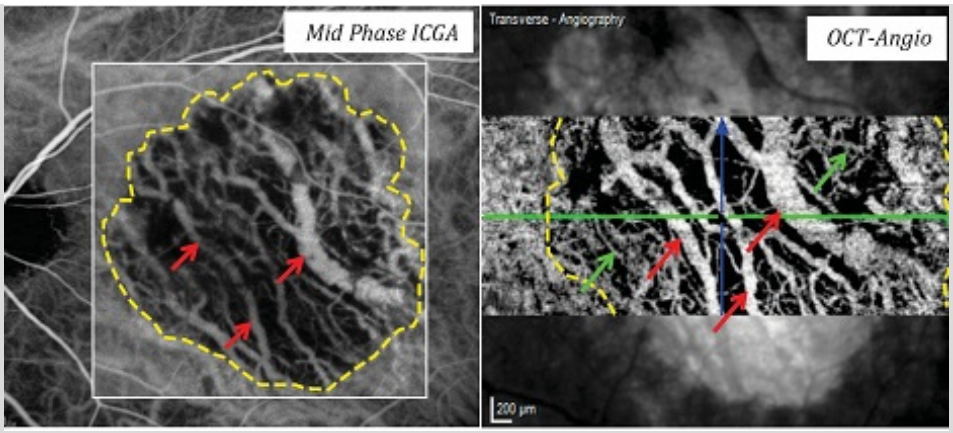

Figure 86: The ICGA (left) and the OCT-Angiography (right) clearly show a **large area of geographic atrophy in the macula**, without any evidence of **choroidal neovascularization**.

Both ICGA and OCT-Angiography clearly show a severe chorioretinal atrophy in the macula, with clear visualization of deep choroidal vascular structures.

There is no evidence of a neovascular network at the centre or at the borders of the lesion. Therefore, this is a typical case of atrophic AMD without any neovascular complications.

There is no indication for treatment with intra-vitreous injections.

13 CONCLUSION

OCT-Angiography (OCT-A) is a new and promising imaging modality that allows the visualization of both the retinal and choroidal vascular layers as well as a neovascularization in the macular region.

OCT-Angiography generates a high contrast between circulating blood cells and static tissues and a “decorrelation“ signal, which enables visualization in three dimensions (3D) of choroidal and retinal vessels without any dye injection.

The specific advantage of OCT-A over traditional fluorescein angiography is that it provides a three-dimensional, deep, and functional information on blood flow in the vessels and, in particular, in the case of new vessels.

Certainly, fluorescein angiography retains some advantages: evaluating the walls of the smallest vessels and capillaries, their permeability (normal or abnormal), recognizing diffusion phenomena, analyzing the circulatory dynamics (delays or the absence of perfusion), the concept of ischemia (localized or widespread) and, even better, obtaining images of the entire posterior pole resp. up to the periphery.

All these capabilities of dye angiography are precious, often very useful for the initial diagnosis and indeed irreplaceable in cases of doubtful diagnosis!

However, dye angiography only provides two-dimensional images (2D), which superimpose all vascular perfused layers in the retina and the choroid.

OCT-Angiography, on the contrary, can be easily performed without any intravenous injection. It benefits the patient, based on frequent evaluations and a guided regimen that is best suited to each case.

OCT-Angiography also provides functional information on blood flow in addition to the morphological or structural details provided by standard OCT, because both examinations are simultaneously performed.

The interpretation of OCT-A (associated with Standard OCT-scans), performed on simultaneous B-scan and C-scan images, obviously requires some learning time but several “activity criteria“ of new vessels are already under study and statistical validation.

This new development and remarkable imaging progress will thus allow a fast and easy diagnosis.

Therapeutic decisions are enabled without any delay during post treatment follow-up. These are likely to become more frequent, effective and very well tolerated.